RESOLVING INFLAMMATION AFTER STROKE

Through

MODULATION OF FORMYL PEPTIDE RECEPTOR 2/THE LIPOXIN RECEPTOR

~

THESIS by MISS HELEN KATHERINE SMITH

DEPARTMENT of MEDICINE, IMPERIAL COLLEGE LONDON

Submitted as a requirement of the degree of Doctor of Philosophy

Declaration of originality

I declare that the all the work within this thesis has been conducted and consolidated by me, Miss H K Smith. This statement refers to the literature review and illustrations of the introduction; the laboratory work recorded in the results section; the analysis of the discussion, and the wording throughout. Where the science of others is used as a basis or explanation for my own work, it is appropriately referenced.

Copyright

Abstract

Stroke kills 15 million people a year and causes disabilities in many more millions who survive. Most strokes are caused by a blood clot, yet only seven percent of patients qualify for early pharmacological clot removal. Damage is frequently exacerbated even as blood reperfuses an ischaemic brain region, through a concomitant inflammatory response to the damaged tissue. Following the continual failure in clinical trials of drugs intended to tackle both initial excitotoxic cell death and pro-inflammatory mechanisms during ischaemia/reperfusion (I/R), this thesis is premised on enhancing 'pro-resolving' anti-inflammatory pathways.

Formyl Peptide Receptor 2/the lipoxin receptor (FPR2/ALX; mouse orthologue Fpr2/3) and two of its ligands, Lipoxin A4 (LXA_4) and Annexin A1 (AnxA1), are part of an endogenous anti-inflammatory system. They actively resolve inflammation through a reduction in characteristic leukocyte-endothelial (L-E) interactions, while promoting the production of anti-inflammatory cytokines and non-phlogistic phagocytosis of leukocytes already within tissue. Chapters 3-5 of this thesis describe the development of mouse model of global cerebral I/R (5 min ischaemia/40 min or 2 h reperfusion) through which L-E interactions are assessed using intravital microscopy. Substantial reductions in L-E interactions following treatment with FPR2/ALX ligands (AnxA1 N-terminal peptide $AnxA1_{Ac2-26}$ and LXA_4 analogue 15-epi-LXA_4) are demonstrated along with variations in cytokine levels (MCP-1, IL-6 and IL-10) after 2 h of reperfusion. The reductions are shown to be variable with respect to the duration of reperfusion, concentration of 15-epi-LXA_4 and the time of treatment administration. In addition, the effects are abrogated by co-treatment with FPR antagonists, which independently cause a highly pronounced acute inflammatory response in the model. Chapters 6 and 7 provide further investigation into the role of FPRs in stroke and inflammation, through chemotaxis studies on human monocytes (from stroke patients and healthy controls) and through use of an FPR1-target MRI contrast agent in mice following lipopolysaccaride-induced inflammation.

Overall, the data provide evidence that Fpr2/3 ligands are able to reduce inflammation following cerebral I/R, that an FPR2/ALX-targeted drug may therefore be effective in human stroke, and that its optimal use is likely to be administration time, dose and FPR2/ALX ligand-dependent.

Contents

List of figures

List of tables

List of abbreviations

aCSF, artificial cerebrospinal fluid 58
ANG II, angiotensin II type 1
AnxA1, Annexin A1
ATP, adenosine triphosphate
Aα, arachidonic acid
Aβ1–42, amyloid β42
Boc2, N-t-butoxycarbonyl-Phe-Leu-Phe-Leu-Phe
CAM, cell adhesion molecule
CCA, common carotid artery
cm, centimetres
COX, cyclooxygenase
CT, computer tomography
DMSO, dimethyl sulfoxide
Dα, docosahexaenoic acid
EDTA, ethylenediaminotetraacetic acid
Eα, eicosapentaenoic acid
FPR, formyl peptide receptor (human)
Fpr, formyl peptide receptor (mouse)
g, grams
h, hours
HTAB, hexadacyl trimethylammonium bromide
i.p., intraperitoneal
i.v., intravenous
I/R, ischaemia/reperfusion
ICAM-1, intercellular adhesion molecule-1
IL, interleukin
IL-1, Interleukin-1
IL-10, interleukin-10
IL-6, interleukin-6
IL-8, interleukin-8
IVM, intravital fluorescence video microscopy
JAM, juntional adhesion molecules
kg, kilograms
l, litres
L-E, leukocyte-endothelial
LOX, lipoxygenase
LPS, lipopolysaccharide
LXA4, lipoxin A4
M, molar
MCA, middle cerebral arteries
MCAO, middle cerebral artery occlusion
MCP-1, monocyte chemoattractant protein-1
min, minutes
ml, mililitres
mm, milimetres
MMP, matrix metalloproteinase
MN, mononuclear
MNc, monocyte
MPO, myeloperoxidase
MRI, magnetic resonance imaging
NADPH, nicotinamide adenine dinucleotide phosphate (reduced)
NIRF, near-infrared fluorescence imaging
nM, nanomolar
NMDA, N-methyl-D-aspartate
OCT, optimum cutting temperature
PARP, poly (ADP-ribose) polymerase
PBS, phosphate buffered saline
PE, polyethylene
PECAM-1, platelet-endothelial cell adhesion molecule-1
p-ERK, phospho-ERK
PET, positron emission tomography
PFA, paraformaldehyde
pg, picograms
PG, prostaglandin
PGI2, prostacyclin
PMN, polymorphonuclear
PSGL-1, P-selectin glycoprotein ligand-1
RBC, red blood cell
ROS, reactive oxygen species
RPMI, Roswell Park Memorial Institute
SAA, serum amyloid A
sec, seconds
SLeX, sialyl LewisX
T, tesla
TGFβ, transforming growth factor-β
TIA, transient ischaemic attack
TLR, toll-like receptor
TMB, tetramethylbenzidine
TNFα, tumour necrosis factor-α
TPA, tissue Plasminogen Activator
TXA2, thromboxane
VE-cadherin, vascular endothelial-cadherin
ZO-1, zona-occludin-1
µl, microlitres
µm, micrometres
µM, micromolar

Acknowledgements

Thanks to Doctor Felicity Gavins, my principal supervisor, for her continued guidance, encouragement and enthusiasm. I intend to pursue a career in research and feel confident in doing so thanks to the high level of training I have received throughout my PhD.

Thanks to the other members of the microcirculation group over the three years I have been a part of it, for the supportive atmosphere and friendship, particularly through long hours with the intravital microscope in our windowless little room.

Thank you to Dr Graeme Stasiuk, for the collaborative effort towards preparing an FPR-targeted MRI contrast agent, and to Marzena Wylezinska-Arridge and Jordi Tremoleda for their technical knowledge and assistance with the MRI machines.

Thanks to Colin Rantle, the neuroscience laboratory manager, whose knowledge, competence and good nature are highly appreciated, and to the staff of the animal units at Hammersmith Campus, for taking care of the mice.

Supervisors

DOCTOR FELICITY GAVINS and PROFESSOR DORIAN HASKARD

Chapter One

Introduction

1.1 Stroke

1.1.1 Epidemiology, aetiology, classification

Stroke is one of the largest causes of death in the UK, second to only heart disease and cancer. Worldwide, incidence is increasing in ageing populations subjected to metabolic syndrome, obesity and smoking (Hankey 1999, Boden-Albala and Sacco 2000). Stroke now claims 15 million lives each year—70,000 of those in the UK (Donnan, Fisher et al. 2008, ONS 2008). Moreover, these 15 million represent only 24 percent of stroke cases. The subsequent cost is felt widely: patients who survive (76 percent) often suffer some extent of disability and require palliative care; direct annual expenditure on stroke in the UK is estimated to be £4 billion (5.5 percent of the total UK expenditure on health care), and the cumulative costs (which includes 'indirect' care: specialist care and income support) to be close to £9 billion (Saka, McGuire et al. 2009).

Stroke is the cessation or reduction of blood flow to the brain (Figure 1), causing cell death and consequently diverse loss of function in the patient (Donnan, Fisher et al. 2008). Considerable tissue damage is initiated minutes after stroke onset (see section 1.1.2.1) and an ischaemic core is produced which will become the focus of (currently) irreversible cell damage. The core is encapsulated by a region of cells whose survival is dependent on multiple factors (Rohl, Ostergaard et al. 2001)—this region is the penumbra and can potentially be recovered pharmacologically to some extent in the hours following stroke, during a critical reperfusion period (see section 1.1.2).

Disturbance in the cerebral vasculature can arise from an ischaemic or haemorrhagic episode and may affect the brain in a focal or global manner (Adams, Bendixen et al. 1993). In incidences of focal ischaemic stroke (the most common form of cerebrovascular accident, accounting for approximately 68 percent of cases, see (ONS 2008), the cerebral blood supply is obstructed locally by occlusion of major vessels or arteriole ends/small vessels, often as a result of an embolus from the heart, a thrombus or trauma (Adams, Bendixen et al. 1993). Global ischaemic stroke (12 percent of cases) involves loss of blood supply to the entire brain and is usually subsequent to cardiac arrest (Landau 1992, Adams, Bendixen et al. 1993) or trauma, whereas haemorrhagic stroke (20 percent of cases) is usually the result of a burst aneurysm and/or trauma (Landau 1992).

Brain imaging of stroke patients is usually carried out within 24 h of stroke onset (Latchaw, Alberts et al. 2009) in order to determine stroke aetiology (ischaemic or haemorrhagic); the location and

severity of the infarct, and the possibility of a second stroke (or transient ischaemic attack; TIA). The most commonly used imaging modalities are computed tomography (CT) and magnetic resonance imaging (MRI). CT scans are frequently used where a patient may benefit from a clot-dispersing treatment (ideally scanning within 3 h), or to diagnose a stroke as ischaemic or haemorrhagic. MRI is used more frequently over a longer period, where detailed severity/positional information is required.

Extensive resources are funnelled into patient management in stroke units and other forms of rehabilitative care (Adams, del Zoppo et al. 2007, Conroy, DeJong et al. 2009), but often with little improvement on patient outcome. The demand for alternative, more flexible and clinically relevant therapies is clear from these figures, and reflected in the enormous body of work targeting the zenith of stroke research—a salvaged penumbra (Figure 1).

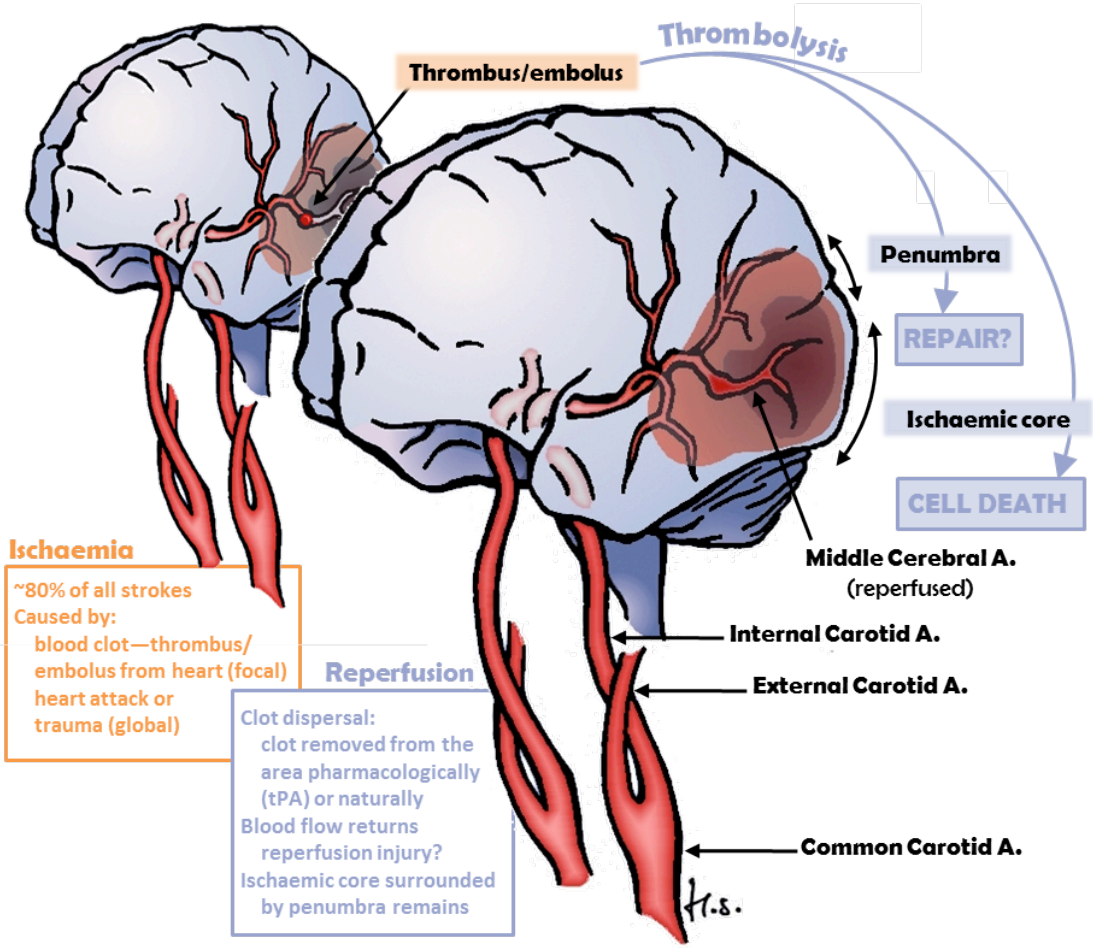

Figure 1. The brain during ischaemic stroke and following reperfusion (Smith Unpublished). A thrombus or embolus from the heart blocks a major blood vessel supplying the brain. Following clot removal, blood returns to the ischaemic region and parenchymal cells form an ischaemic core (focus of ischaemia) and a surrounding penumbra (cells not committed to survival or death). tPA = tissue Plasminogen Activator.

1.1.2 The ischaemic cascade

The pathophysiological process of stroke involves temporally executed interactions between numerous cell types, including neurons themselves, glia, endothelia and cells of the immune system (Figure 2). This section (*The ischaemic cascade*) will describe the concerted involvement of these cell types in the progression of stroke—from initial excitotoxic cell death and subsequent reperfusion injury, to breakdown of the blood-brain barrier (BBB) and long term prognoses—as well as the animal models used to represent these processes.

1.1.2.1 Excitotoxic cell death

From the outset, reduced oxygen and variably reduced glucose supplies (with respect to proximity to the central ischaemic region in focal stroke) result in necrotic and/or apoptotic neuronal and glial cell death by a range of mechanisms.

Throughout this stage in stroke pathology, single-strand DNA breaks may cause rapid activation of nuclear protein poly (ADP-ribose) polymerase (PARP), reducing intracellular concentrations of its substrate (NAD^+), thereby slowing cellular mechanisms of energy production (Abdelkarim, Gertz et al. 2001, Li, Klaus et al. 2010). Decreased energy (adenosine triphosphate, ATP; 'energy') production disrupts tightly maintained neuronal ion channels (Mattson, Culmsee et al. 2000, Sims and Muyderman 2010), producing unmediated release of excitatory glutamate. This accumulates in the extracellular space and further stimulates glutamate receptors, ultimately causing immense calcium influx through *N*-methyl-D-aspartate (NMDA) receptors and voltage-dependent calcium channels. This early state has the potential to lead to necrotic or apoptotic cell death, and is referred to as *excitotoxicity* (Figure 2).

Initial hunts for stroke treatments were based on the premise that all structural deficits were fixed at this point—at the point of clot-removal; more recently, however, detailed brain scans have shown that an infarct can continue growing beyond 24 h after the stroke onset (reviewed in (Fisher 1997). This proved that delayed mechanisms must also significantly worsen the degree of tissue damage. It was subsequently discovered that influences on prolonged tissue survival are in fact linked to activity in blood vessels supplying the cerebrum during reperfusion, rather than the cerebral parenchyma itself. This aspect of stroke pathology is discussed in the next section (1.1.2.2).

1.1.2.2 Ischaemia/reperfusion injury

If the absence of oxygen and nutrients persists, cells will die. Reperfusion of an infarct with blood is therefore absolutely necessary for tissue survival, and usually occurs (by endogenous or pharmacological means) where stroke is not immediately fatal. With the ostensible benefits of a replenished blood supply, there is an inflammatory response which may cause extensive tissue damage—this known as *ischaemia/reperfusion (I/R) injury* (Figure 2).

Blood-borne leukocytes, platelets, glia and neurons participate in the physiological and morphological changes brought about by the release of cytokines (see section 1.2.1.1), cell adhesion molecule (CAM) expression (see section 1.2.1.2) and oxidative stress (see section 1.2.1.3) (Gavins, Yilmaz et al. 2007, Wang, Tang et al. 2007). Most pertinently during I/R, up-regulated CAM expression on cerebral post-capillary venules in and around the infarct establishes the evolution of these venule walls into sites of intense leukocyte-/platelet-endothelia interaction. The BBB formed by these endothelia becomes 'leaky', allowing an excess of leukocytes and plasma to penetrate the brain parenchyma—this leukocyte extravasation is the hallmark of inflammation and is illustrated in Figure 3 (p.31). Once within the injured brain tissue, leukocytes release reactive oxygen species (ROS) and in general deposit more cellular debris than can be mopped up by phagocytes in the impaired tissue. The discriminate phases required for leukocyte extravasation to occur are described in detail in section 1.2.1.

A 'no-reflow' phenomenon may cause failure of reperfusion completely in circumscribed areas. This is the clogging of capillaries caused by leukocyte adhesion (Figure 3I; p.31) (del Zoppo, Schmid-Schonbein et al. 1991, Caceres, Schleien et al. 1995). Incomplete reperfusion also related to the inflammatory response arises from cerebral oedema (through compromised microvascular endothelia and perivascular glia) and blood cell sludging (Bottiger, Krumnikl et al. 1997).

Throughout the inflammatory response, a concomitant battery of anti-inflammatory agents is deployed, including eicosanoids (Ye, Wu et al. 2010) and glucocorticoid-linked mechanisms (Lim and Pervaiz 2007). Each of these (described in detailed in section 1.3.2) provides an endogenous safeguard against excess inflammation.

1.1.2.3 Blood-brain barrier breakdown

The BBB is the tightly regulated interface between the central nervous system (CNS) and its blood supply. Specifically, the BBB is comprised of the endothelial cells of vasculature within the CNS and their superlative intercellular junctions which restrict paracellular transport into the parenchyma.

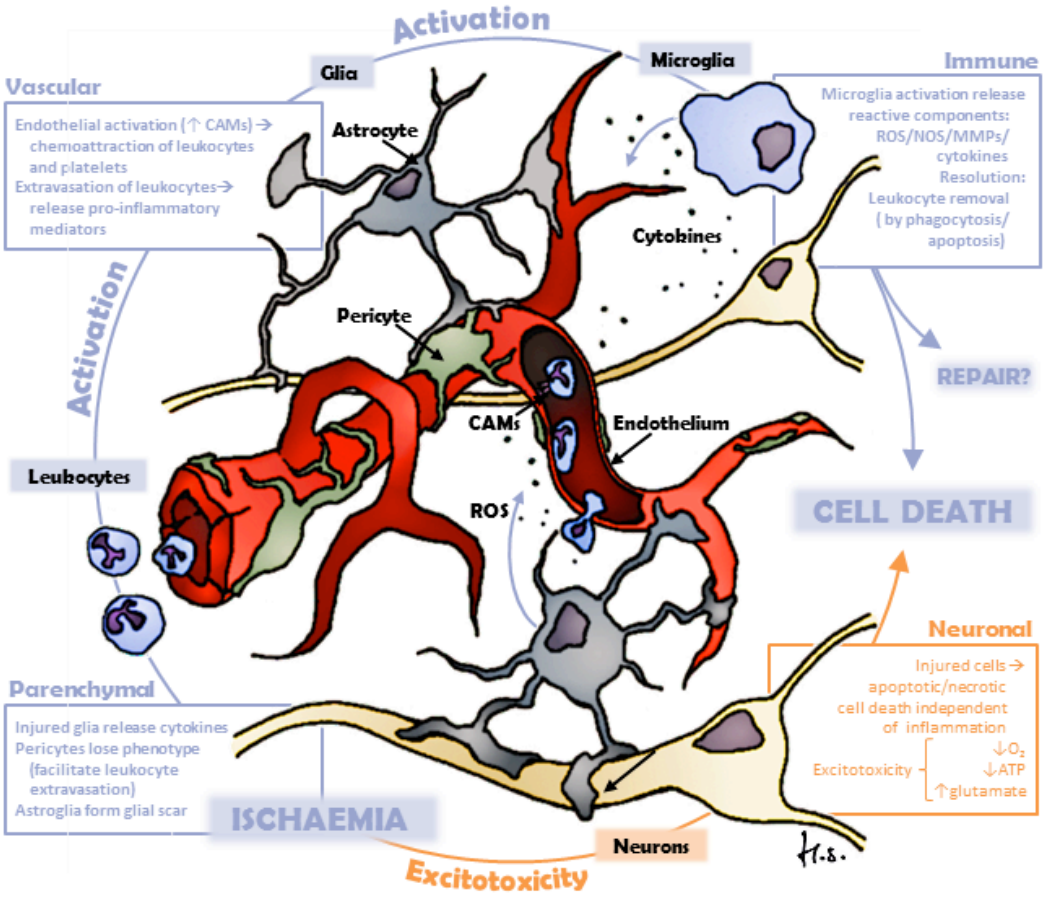

Figure 2. Concerted cellular and molecular activity in the brain during stroke (Smith Unpublished). Ischaemia results in several routes of cell/tissue damage: excitotoxicity (acute cell damage/death due to sudden decrease in oxygen supply); activation of pro-inflammatory pathways (acute but prolonged and due to release of pro-inflammatory cytokines from microglia and injured neurons, followed by increased cell adhesion molecule (CAM) expression and extravasation of leukocytes); release of oxidative component such as reactive oxygen species (ROS) and matrix metalloproteinases (MMPs) from injured parenchymal cells and leukocytes, and the formation of glia scars (astrocyte activity).

Under healthy conditions, the integrity of the BBB is maintained by a series of adherens junctions and tight junctions (Hawkins and Davis 2005). Adherens junctions are ubiquitous in vasculature and predominantly composed of intercellular vascular endothelial (VE)-cadherin interactions. It is primarily tight junctions that deliver low permeability specifically throughout cerebral endothelium. Several protein components which connect endothelial cells constitute tight junctions: membrane-bound junctional adhesion molecules (JAMs), occludins and claudins, are held in place by cytoplasmic proteins zona-occludin-1 (ZO-1), AF-6 and 7H6 (Rubin and Staddon 1999).

Breakdown of the barrier during stroke is associated with increased vascular permeability. This effect is biphasic (occurring at first several hours after ischaemic onset, second 1-2 days following the first) and occurs in part through matrix metalloproteinases (MMPs) mediating tyrosine phosphorylation of occludin (Baskaya, Rao et al. 1997). Despite implicit pro-inflammatory consequences of BBB breakdown in stroke, a notable benefit is that a leaky BBB—largely impenetrable to pharmacological treatment in health—means lower doses and entirely different drug treatments may be considered (McCarty 2005) [1].

1.1.2.4 Long-term progression of pathology

The variation between individual human (non-experimental) experiences of ischaemic stroke is as such that prognoses range from the development of no discernible neurological deficits, to severe disability or death. This is due to the near-infinite possible infarct locations and volumes at a cellular level, and presents a unique research problem—one which, at least with respect to physical therapy, is simplified by the observation of outward similarities between stroke patients. A common factor in ischaemic stroke is that blood flow dynamics often result in emboli from the heart becoming lodged in or downstream of the middle cerebral arteries (MCA) (Bogousslavsky, Van Melle et al. 1988). These arteries arise bilaterally from the Circle of Willis and have branches

[1] The discovery of a link between stress and a 'leaky' BBB arose in part from observations made from soldiers in the Persian Gulf War. Pyridostigmine (an acetylcholinesterase inhibitor, principally used in the treatment of myasthenia gravis) was administered to soldiers prior to engaging in battle for its protective effects against organophosphate 'nerve agents'. In healthy controls, pyridostigmine is prevented from crossing the BBB by a quaternary ammonium group which limits side effects to those arising from the periphery (including abdominal pain, diarrhoea, polyuria, rhinorrhea, increased sweating and salivation). Surprisingly, in soldiers under conditions of war, CNS-related side effects (including headache, insomnia, drowsiness, nervousness, difficulties in performing calculations and focusing attention) were increased threefold—to an extent where central effects predominated over the peripheral. It was concluded that in these recipients effects were due to BBB disruption in a stressful situation.

supplying the majority of the lateral surface of their respective hemispheres, sections of the frontal and temporal lobes (supplying Broca's area and Wernicke's area), and some deep branches supplying the basal ganglia. Causes of widely recognised symptoms of stroke can therefore be identified as the absence of normal functioning in these brain regions: frontal and temporal lobe damage in particular giving rise to some extent of unilateral paralysis and aphasia or alternative speech difficulties respectively.

Youth is an excellent indicator for good prognoses in stroke cases; death during the acute phase of middle MCA stroke is cited as 5-30 percent, depending of the age of the cohort (Kaste and Waltimo 1976, Sacquegna, De Carolis et al. 1984, ONS 2008). It is also observed that smoking—but not hypertension—can indicate a poor prognosis (Kaste and Waltimo 1976). A degree of hemiparesis and/or spasticity occurs in almost all strokes with the exception of TIAs (short-lived 'mini strokes' often with no immediate disruptive neurological effects)—the worst paralysis affecting those over the age of 65 (Granger, Hamilton et al. 1992) and improved physical outcomes seen in four percent of tissue plasminogen activator (tPA; see section 1.1.3.1) recipients (NINDS 1995). For all ages, as a stroke (minor or otherwise) increases the likelihood of a second stroke by up to 40 percent over a five year period (Sacquegna, De Carolis et al. 1984), a strong possibility of further attacks is the most generally applicable prognosis. The parameters for various clinical, lifestyle, radiological and biochemical aspects of MCA stroke outcome have now been collated to form a five-point prognostic score including the following risk factors: age (<50 corresponds to reduced risk and 80+ the greatest); National Institutes of Health Stroke Scale (NIHSS) score (<5 indicates lower risk and 15+ greater); infarct volume (as defined by diffuse-weighted imaging, DWI: <20 cm^3 indicates lower risk and 100 cm^3 greater); white blood cell count (above $8.5\times10^3/mm^3$ indicates poor outcome, below improved), and hyperglycaemia (where its presence indicates higher risk) (Vora, Shook et al. 2011).

1.1.2.5 Animal models of cerebral ischaemia/reperfusion

The complex cellular interplay through the course of stroke cannot yet sufficiently be replicated *in vitro*. Cell systems can be used productively to dissect molecular pathways (Ford 2008, Zhang, Li et al. 2008) and to provide supportive evidence for other research, but they are not sufficient bases for drug trials. As a result, investigations of potential therapeutic targets are largely conducted *in vivo*. Fewer than ten models of focal stroke exist in animals (Carmichael 2005), the most commonly used being middle cerebral artery occlusion (MCAO) model of focal stroke, due to its reproducibility and similarity to the human condition (Longa, Weinstein et al. 1989, Belayev, Busto et al. 1999). The MCAO technique involves passing a suture up the internal carotid artery until the

origin of the MCA is met (Ardehali and Rondouin 2003). Cerebral tissue that is not supplied solely by the MCA is fed by the Circle of Willis throughout an elected ischaemic period (frequently one hour), while the suture remains inserted. An infarct is produced, consistently and unilaterally, in the region of cortex supplied by the occluded MCA.

Nonhuman primates have vascular and neuronal brain structures (particularly white matter, see (Arai and Lo 2009) most similar to humans, making them a preferred model for stroke. In practice, rodents are the most common models used due to ethical, institutional and cost difficulties with primate models (Richard Green, Odergren et al. 2003), and the potential for genetic approaches. Rodent studies frequently use rats in preference to mice—the narrow apertures of the cerebrovasculature in mice render the rat model technically more amenable, but mice are used in genetic studies where knock-out/-in or related animals are required. Table 1 gives a non-exhaustive list of commonly practised cerebral I/R models. Reperfusion injury is an additional significant cause of tissue damage in stroke to be represented in models. This can be achieved using the MCAO model (by withdrawing the suture) or in a bilateral common carotid artery occlusion (BCCAO; global) model in which both carotid arteries are clamped or ligated then reopened (see *Methods*, section 2.2). Modelling the reperfusion phase is essential in order that associated cerebral inflammation may be studied, the details of which are covered in section 1.2.

Table 1. Advantages and disadvantages of commonly used models of cerebral ischaemia.

Type of Cerebral Ischaemia	Aetiology of I/R	Animal model	Advantages	Disadvantages
Global	Surgical obstruction of major vessels supplying brain (BCCAO/plus basilar artery/plus vertebral arteries); silk ligatures or aneurysm clips/removal of obstruction [1].	Rodents	Simple, highly replicable surgical procedure; simple reperfusion model with good long-term survival rate; use of genetically manipulated mice enables dissection of pathology-causing mechanisms [a].	Hypotension and/or hypoxia may be necessary to elicit complete ischaemia; collateral circulation results in varied inter-/intra-species outcomes; anaesthesia/additional measures/time scales may confound translation of data into human therapies [b]; pathophysiological mechanisms of lissencephalic rodent brain may differ from human brain [b]; animals used are frequently young and healthy, unlike frequent human cases of comorbidity [9; b].
	Cardiac arrest; cold potassium chloride [2, 3] or ventricular fibrillation [4]/Cardiopulmonary resuscitation; combinations of adrenaline, 100% oxygen, chest compressions and defibrillation.	Primates/ Dogs/Cats/ Rodents	Mimics induction of human global cerebral ischaemia commonly occurring following cardiac arrest; potassium chloride elicits clear, consistent infarcts in hippocampus and caudoputamen.	Labour intensive and expensive, particularly in larger animals and long term studies.
	Hypoxia ischaemia; ligation of one CCA followed by exposure to 8% oxygen/removal of ligature and return to normoxia [5].	Rodents	Simple, highly replicable surgical procedure; mimics hypoxia-ischaemia experienced in human foetal and neonatal stages.	Not broadly representative of global ischaemia.
	Neck tourniquet or cuff/removal of cuff [6].	Primates/ Dogs/Cats	To some extent, mimics human trauma-induced global ischaemia.	Venous congestion and vagal nerve compression lead to varied outcomes.
Focal	Obstruction of middle cerebral artery; intraluminal suture/monofilament advanced to junction of anterior and middle cerebral A./removal of obstruction.	Primates/ Dogs/Cats/ Rodents	To some extent, mimics human thromboembolic stroke; similar disease progression to human stroke; simple reperfusion model with good long-term survival rate.	Invasive surgery; variability in infarct size and physiological outcome, particularly in larger animals; produce infarct sizes far larger than clinically assessed human stroke [10; 11] perhaps encouraging research to focus on reducing infarct size rather than re-establishment of particular neuronal circuits.
	Macrosphere embolisation.	Rodents/ primates	Ischaemia over large area without craniotomy.	Risk of haemorrhage.
	Photochemical thromboembolisation; photochemical induction of common carotid A. thrombosis followed by mechanical release of thrombi [7].	Rodents	Requires only a small craniotomy and dura stays in tact.	Risk of microvascular injury.
Multifocal	Embolilsation; blood clots generated *in vitro* or 50-µm polyethylene microspheres injected intracranially from external carotid A. [8].	Rat	Mimics human intravascular pathophysiology of arterial thrombus generation from an atherosclerotic plaque.	Location of infarct not consistent.

[a] True wherever the use of murine model is possible.

[b] Disadvantage in the case of most models (some models do not require anaesthesia (Pulsinelli and Brierley 1979), presenting the most likely reasons for the failure of animal research carried forward to clinical trials.

[1] (Ishikawa, Sekizuka et al. 2007); [2] (Neigh, Karelina et al. 2009); [3] (Kofler, Otsuka et al. 2006); [4] (Radovsky, Safar et al. 1995); [5] (Kumari, Willing et al. 2010); [6] (Bacher, Kwon et al. 1998); [7] (Lozano, Abulafia et al. 2007); [8] (Mayzel-Oreg, Omae et al. 2004); [9] (Fischer, Arnold et al. 2006); [10] (Brott, Marler et al. 1989); [11] (Belayev, Busto et al. 1999).

1.1.3 Failings in current treatments for ischaemic stroke

'Time is brain' is a phrase used to good effect (having been 'borrowed' from Benjamin Franklin) by those aiming to quantify and emphasize the significance of temporal neuronal loss following stroke (Hill and Hachinski 1998, Saver 2006, Penn 2009). In patients experiencing a typical large vessel ischaemic attack, 1.9 million neurons are destroyed every minute (based on a 10 h ischaemic stroke in an average-sized brain, see Saver 2006). Time is therefore the presiding influence on any attempt to treat an ischaemic stroke. Despite this, an extended duration between stroke onset and diagnosis in hospital explains only part of the failure of prospective treatments. This section (*Failings in current treatments for ischaemic stroke*) discusses other aspects which have contributed to the lack of novel, effective stroke therapies, including current clinical treatment of stroke, clinical trials to date and their potential design flaws, as well as the shortfalls in experimental animal models of stroke.

1.1.3.1 Current stroke therapies

Research to date has observed and tried to compensate for several of the pathological processes described in the previous section (1.1.2), and over a thousand basic studies have reached clinical trial stage (clinicaltrials.gov 2011). Success with these has so far been non-existent, with the single exception of 'clot-busting' tPA (Davis and Donnan 2009). The reasons for these failures have been covered elsewhere in detail (Richard Green, Odergren et al. 2003, Holloway, Smith et al. 2011), but the crux seems to be that results obtained using animal models are not sufficiently representative of the clinic; that the necessary temporal restrictions on treatment administration in basic research do not practically lend themselves to the clinic, and that there is poor observation of inclusion criteria outlined following animal studies, once a drug has reached trial stage. The resounding message from each of these concerns is that new studies and therapies should be designed with flexibility in mind, in order to provide the greatest outcomes for the greatest number of patients.

Among the failures there have been a few successes: focal strokes are primarily the result of a blockage which terminates the blood supply to recipient cerebral tissue, therefore efforts to reverse initial ischaemia centre on thrombolysis using intravenous tPA or surgical angioplasty, stenting or thrombectomy (Smith, Sung et al. 2008). Thrombolytic tPA is effective through platelet disaggregation and catalysis of fibrin breakdown (Loscalzo and Vaughan 1987). It provides some efficacy only if administered during the short, 4.5 hour period after the onset of ischaemia (Davis

and Donnan 2009)—recently extended from 3 h (NINDS 1995, Chiu, Krieger et al. 1998). Use of tPA therefore relies on early recognition of stroke symptoms, the swift arrival of a patient at hospital and quick, accurate diagnosis of stroke aetiology (through brain scanning). Thrombolytic treatment of a haemorrhagic stroke misdiagnosed as ischaemic could be fatal or exacerbate a bleed. If these criteria are met, tPA has been shown to reduce mortality over 3 months by four percent, as well as long-term disability (NINDS 1995). Despite the benefits seen in some patients, tPA holds an associated increased risk of symptomatic intracerebral haemorrhage and can be neurotoxic if it enters the parenchyma through the leaky BBB (Wang, Tsirka et al. 1998, Flavin, Zhao et al. 2000). Efforts to combine treatment with anti-inflammatory agents intended to preserve BBB integrity may optimise this therapeutic route (Zhang, Zhang et al. 2003).

Increased risk of a subsequent stroke following a first means prophylactic treatments are advised such as low-dose subcutaneous heparin and antiplatelet agents such as aspirin and clopidogrel (Lees, Ford et al. 2008). In addition to prophylaxis, personalised pastoral and physical therapy are the focus during rehabilitation, which is a variably beneficial approach (Smith, Sung et al. 2008). (Interestingly, singing has produced positive effects in some, particularly aphasic, patients (Johansson 2011), possibly as a result of neuronal plasticity).

The predominant cause of non-fatal global cerebral ischaemia is cardiac arrest (Bottiger, Grabner et al. 1999). Mortality and neurological dysfunction arising during this post-resuscitation period are largely due to neuronal damage amassed during concomitant cerebral I/R (Schneider, Bottiger et al. 2009); while cardiac function may be restored, cerebral resuscitation is contingent upon aspects of the reperfusion period (see section 1.1.2). Neuroprotection afforded by induced hypothermia following cardiac arrest has been reported since the late 1950s (Williams and Spencer 1958), and convincing evidence upholding the therapeutic process has since escalated. Two major randomised clinical trials in 2002 (Bernard, Gray et al. 2002, HCASG 2002) described a significant decrease in mortality and increase in favourable neurological outcome in patients resuscitated then systemically cooled to 32-34 °C following ventricular fibrillation. From 2003, the use of mild therapeutic hypothermia has been recommended in comatose adult patients, post-cardiac arrest.

1.1.3.2 Clinical trials to date

Novel drugs designed to limit excitotoxic cell death and I/R injury have proved disappointing in clinical trials: humanised monoclonal antibodies targeting intercellular adhesion molecule-1 (ICAM-1) intended to reduce recruitment of leukocytes to endothelial walls during inflammation showed no benefit, indeed they may worsen patient outcome (EAST 2001); NMDA antagonists

aimed at reducing excitotoxicity failed in phase III clinical trials (Morris, Bullock et al. 1999); GABA-potentiators (Lyden, Shuaib et al. 2002), designed to block initial excitotoxic cell death and ximelagatran (a thrombin inhibitor aimed at secondary prevention) ultimately produced unacceptably high quantities of liver enzyme alanine aminotransferase (Olsson 2003). Interestingly, a trial using an antagonist (rhIL-1ra) for pro-inflammatory cytokine Interleukin-1 (IL-1) is in Phase III clinical trials (Emsley, Smith et al. 2005). In Phase II trials, clinical outcomes were improved in patients treated within 6 h of stroke onset.

The application of viable compounds in basic science uses animals with standardised lesions, receiving treatment at highly controlled time points and outcome monitoring at equally well-defined endpoints. Inferred shortfalls in the animal models themselves are discussed in section 1.1.3.3, yet it must be emphasized that clinical trial structure rarely observes the strict temporal aspects of preceding animal studies in which a treatment has proved effective. Whether this is down to intrinsic flaws in clinical trial design or simply the impractical nature of a regimented stroke therapy is unclear—it is probably a combination of these. The onus is therefore shared by basic science and the animal models it uses.

1.1.3.3 Shortfalls in animal models of stroke

Earlier studies that assess infarct volumes without reperfusion have had little capacity to measure the deleterious effects of inflammation or improved functional outcome (Alessandrini, Namura et al. 1999, Yepes, Sandkvist et al. 2000). In this respect animal models have now progressed, yet establishing a reproducible rodent model that faithfully replicates the human condition remains a contentious issue. Table 1 (p.23) lists advantages and shortfalls with respect to relevance and practicality.

Future experimental design should recognise the unpredictable nature of human stroke. Differential action of putative therapeutic peptides should be demonstrated not only according to dose, but to varying durations of I/R and the home-to-hospital journey—why have animal studies using well-studied potential treatments, on the brink clinical trials, not been more observant of the time between stroke onset and diagnosis in the clinic? Some experimental and clinical disparities will be difficult to eliminate: animals are deeply anaesthetised prior to receiving a stroke—of course this is not typically the case in humans. Studies using conscious animals have been used in previous decades (Jones, Morawetz et al. 1981), but are now likely to remain redundant due to ethical constraints. A principal failing of rodent models of focal cerebral I/R—the vast ischaemic extension over hemispheres not seen in nonfatal human stroke—would ideally be addressed.

Failure to focus specifically on the regeneration or re-wiring of infarcted neuronal circuits as well as the generic promotion of cell-survival may prove an obstacle to the production of successful treatment of stroke.

Possibly the largest culprit for data-skewing (one which may have been the most misleading in presenting potential pharmacological targets) is the poor control of body temperature during I/R and subsequent recovery, and the effect this has on blood flow. Incidental to some anaesthetics and treatments used in I/R studies is a decrease in body temperature. While mechanistically ambiguous, hypothermia has shown experimental *as well as* clinical success rates beyond all alternatives (Li, Omae et al. 1999, Boysen and Christensen 2001). It is crucial, therefore, that experimental design includes rigorous regulation of body temperature.

As discussed early in this chapter (see section 1.1.3.1), tPA is the only pharmacological treatment routinely used with stroke patients. This drug showed positive results pre-clinically in a 'quantal bioassay', as described by the Zivin group, who pioneered the use of tPA (Zivin and Waud 1992). This method of analysis invokes an 'all or nothing' assessment of efficacy, and demonstrated that tPA would work. Of interest is that this method has not produced positive results for any other purported stroke treatment entering clinical trials to date.

1.2 Inflammation

1.2.1 The leukocyte adhesion cascade

The hallmark of inflammation in both pathogen-induced and sterile (pathogen-free, e.g. I/R) immune responses is the instigation of the leukocyte adhesion cascade at the site(s) of injury. Under pathogenic conditions, this process is an effective means of ridding the site of invading organisms. This section (*The leukocyte adhesion cascade*) will cover the arrival of leukocytes at damaged endothelial walls; their subsequent rolling, adhesion and emigration through these walls into parenchyma; molecular components involved in this process and evidence which indicates leukocyte infiltration as a limiting factor in tissue damage. Figure 3 gives an overview of these aspects and of discriminate phases involved in the progression of the cascade.

1.2.1.1 Chemotaxis of leukocytes to sites of inflammation

The inflammatory process in I/R begins with the somatic dispersion of emergency signals from injured neurons, glia and vascular endothelia at the site of ischaemia. The result is the generation of molecular landing strips which guide leukocytes to sites of inflammation. As little as 5 min following ischaemia, microglia within the brain tissue and endothelial Weibel-Palade bodies (storage granules) release cytokines such as interleukin-1β (IL-1β), tumour necrosis factor-α (TNFα), monocyte chemoattractant protein-1 (MCP-1) and interleukin-8 (IL-8) (Saito, Suyama et al. 1996, Kostulas, Pelidou et al. 1999). *Cytokine* is a broad, collective term which indicates a small protein or peptide signalling molecule with a regulatory function around the body. In the inflammatory environment of cerebral I/R these are classed as either *interleukins* (e.g. IL-1β and TNFα above) or *chemokines* (e.g. IL-8—blurring the line between nomenclature and function—and MCP-1 above). Interleukins and chemokines are inflammatory mediators (interleukin literally meaning: 'occurring between leukocytes' (OED 2012)—a definition which has been overturned since the observation that they are released from many cell types). Chemokines, however, hold the more specific function of providing directional information for leukocytes in a process called *chemotaxis* (movement along a chemical gradient).

The precise concoction of pro-inflammatory cytokines deployed during I/R is variable, especially in the brain versus the periphery (Offner, Subramanian et al. 2006). In stroke, for example, interleukin-6 (IL-6) is elevated in acute phase stroke and high plasma concentrations (10+ pg/ml) correlate with poor prognoses (Waje-Andreassen, Krakenes et al. 2005). IL-1 has also long been

recognised as a crucial driver of inflammation following I/R (Yamasaki, Matsuura et al. 1995), and is being pursued as a therapeutic target (Denes, Pinteaux et al. 2011). In general, chemokines are expressed on or beneath endothelial walls under stress, as intravascular and parenchymal gradients of pro-inflammatory mediators (Utgaard, Jahnsen et al. 1998). This graded expression of chemokines—which enables leukocyte chemotaxis to sites of inflammation—is triggered by pro-inflammatory interleukins.

Neutrophils (polymorphonuclear, PMN cells) and monocytes (mononuclear, MN cells) are the predominant leukocyte subsets involved in the innate immune response (as opposed to lymphocytes in the adaptive response). Each has a distinct role in inflammation: neutrophils in the acute stages as frontline, oxidant-wielding defence against suspected pathogens, and monocytes through later stages with a mop and bucket (see section 1.2.1.3). To produce this biphasic influx of leukocytes, each cell type responds to different key chemokines: monocytes primarily to MCP-1 (Valente, Graves et al. 1988), among others such as macrophage inflammatory protein-1α (MIP-1α) and RANTES (reviewed in (Graves and Jiang 1995), and neutrophils to IL-8 (Kukulski, Ben Yebdri et al. 2009, Henkels, Frondorf et al. 2011).

Once in contact with G-protein-coupled receptors (GPCRs) on leukocytes (for review see (Murdoch and Finn 2000), chemokines are able to induce various changes in leukocyte conformation/activation state including: calcium flux (Schaff, Yamayoshi et al. 2008); respiratory bursts (the release of ROS, see section 1.2.1.3) (Elbim and Lizard 2009); neutrophil granule release (de Boer, Hack et al. 1993) and enhanced migratory potential which facilitates leukocyte rolling, slow rolling, adhesion, firm adhesion and ultimate emigration into the parenchyma, as discussed in the following section (1.2.1.2).

1.2.1.2 Rolling, adhesion, emigration of leukocytes

The chemotaxis of leukocytes to sites of inflammation is followed by leukocyte tethering onto highly activated endothelial walls. This process is mediated by a CAM subset known as the *selectins* (Ley and Gaehtgens 1991). Endothelial Weibel-Palade bodies release P-selectin enabling initial attachment of leukocytes. Similarly, α-granules (storage bodies in platelets, equivalent to Weibel-Palade bodies in endothelial cells) release P-selectin on platelet activation; this allows platelet-leukocyte interactions which enhance leukocyte capture (Barkalow, Goodman et al. 1996). L-selectins allow leukocyte-leukocyte interactions, enabling further neutrophil cell tethering. Endothelial-bound P-selectin and leukocyte-bound L-selectin transiently bind P-selectin glycoprotein ligand-1 (PSGL-1) and sialyl Lewis^X (SLe^X) (Somers, Tang et al. 2000). These

interactions produce Velcro-like attachments which, owing to momentum issued by the blood flow, allow leukocytes to roll disjointedly along vessel walls, assessing levels of tissue damage through local CAM expression (Barber, Foniok et al. 2004). This is phase is defined as *leukocyte rolling*, and is followed by a period of *slow rolling*.

As leukocytes roll on endothelial selectins, signals are transduced that enable the extracellular extension of a second family of CAMs known as *integrins* (heterophilic, heterodimeric proteins consisting of various α and β subunits). This is a partial activation which allows reversible binding of integrin ectodomains, particularly $\alpha_L\beta_2$ integrins (Yago, Shao et al. 2010), to ICAM-1; this is sufficient to reduce the rolling speed of leukocytes (Dunne, Ballantyne et al. 2000). ICAM-1 is a member of the final known family of CAMs involved in the recruitment of leukocytes to injured tissue—the *immunoglobulins*.

The slow rolling phase facilitates leukocyte interaction with endothelial chemokines, allowing full activation of integrins and leading to arrest of the cell; *leukocyte adhesion*. Immunoglobulins and integrins mediate the final intravascular stage in the adhesion cascade prior to leukocyte emigration into the tissue. This is known as *firm adhesion*: E-selectin, ICAM-1, platelet-endothelial cell adhesion molecule-1 (PECAM-1) (Bogen, Baldwin et al. 1992), JAMs and β_1 and β_2 integrins, among other CAMs, are expressed on leukocytes and endothelia, securing leukocytes to the vessel wall. Here monocytes (which once tissue-bound become macrophages) and neutrophils are able to pass through newly permeable endothelial cells of the BBB (see section 1.1.2.3) by one of two processes: paracellular migration (between cell junctions—around 94 percent of extravasations) or transcellular migration (through endothelial cells—around six percent of extravasations) (Mamdouh, Mikhailov et al. 2009). Emigrated leukocytes initiate chemotaxis of further blood-borne leukocytes to the site of inflammation through the dispersal of highly reactive, tissue-damaging components, discussed in the next section (1.2.1.3).

1.2.1.3 Cellular debris of the emigrated leukocyte

The cellular debris of the emigrated leukocyte may be considered the extensive chemical signature it leaves during/following either apoptotic or phagocytic cell death that is capable of perpetuating inflammation. The cocktail includes (but is not limited to): ROS (free radicals), cytokines, MMPs and pro-inflammatory eicosanoids (leukotrienes and some prostaglandins, see section 1.2.2.1) (Wang, Tang et al. 2007).

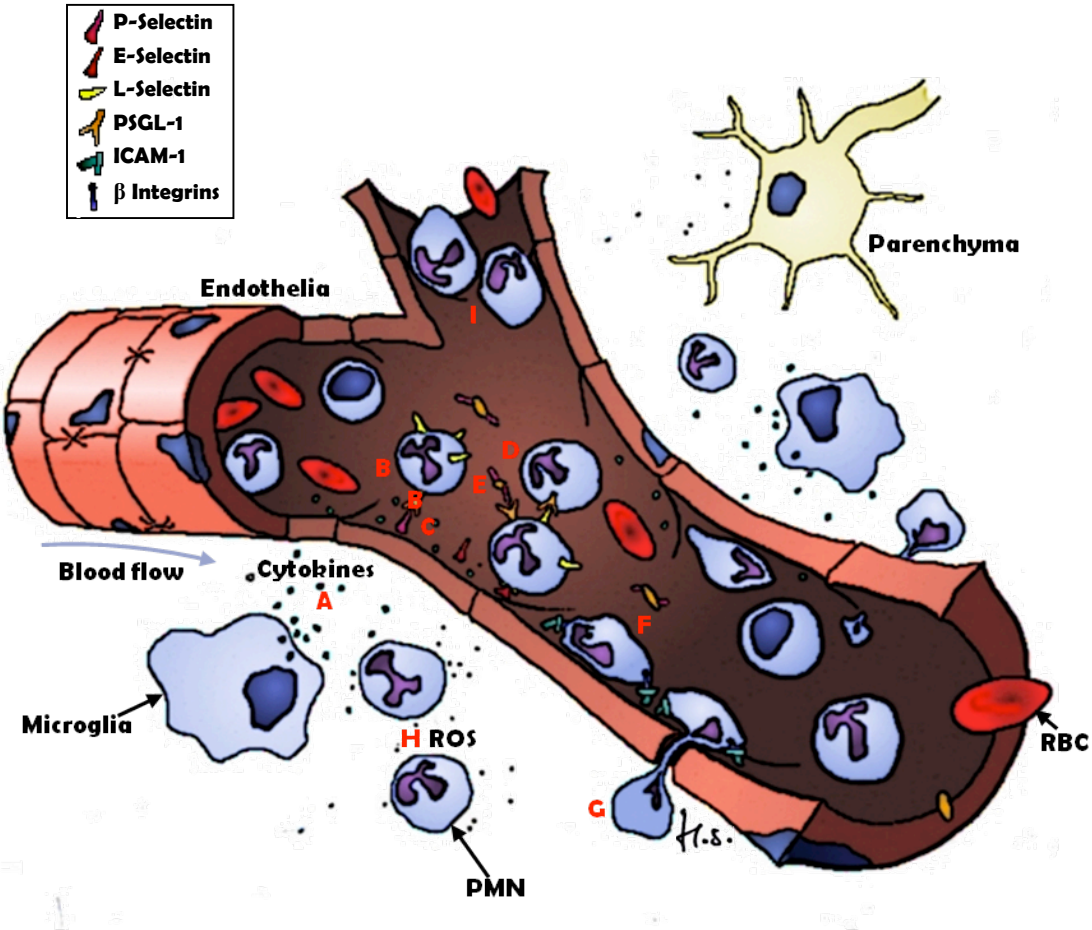

Figure 3. The leukocyte adhesion cascade (Smith Unpublished). Cytokines are release from microglia and injured tissue (A) allowing their endothelial and intravascular expression (B). These cytokines initiate chemotaxis of blood-borne neutrophils (polymorphonuclear cells, PMN) and monocytes to the site of inflammation. Leukocytes are tethered onto activated endothelial walls, mediated by cell adhesion molecules (CAMS) (C). This is followed by selectin-mediated leukocyte rolling along vessel walls. Leukocyte-leukocyte interactions enable further neutrophil recruitment (D), which is enhanced by platelet-leukocyte interactions (E). A firm adhesion phase, mediated by immunoglobulins and integrins, follows leukocyte rolling (F), following which cells exit the vessels through endothelia (G). Emigrated leukocytes release reactive oxygen species (ROS) and further inflammatory mediators (H); blood-borne leukocytes may clog smaller vessels, causing 'no-reflow' phenomenon (I). RBC, red blood cell.

A free radical is '*any species capable of independent existence that contains one or more unpaired electrons*' (Halliwell 1992). During inflammation, neutrophils use membrane-bound nicotinamide adenine dinucleotide phosphate (NADPH) oxidase through a multi-component enzyme system to reduce oxygen to superoxide (O_2^-; oxygen free radical), then to hydrogen peroxide (H_2O_2) during periods known as *respiratory bursts* (also referred to as *oxidative bursts*) (Elbim and Lizard 2009). These are capable of tissue damage through mechanisms such as DNA and protein degradation, lipid peroxidation, enzyme oxidation (Olmez and Ozyurt 2012), and stimulation of pro-inflammatory cytokines and nuclear factor-κB (NF-κB; a transcription factor central to the regulation of inflammation) (Kratsovnik, Bromberg et al. 2005). The generation of superoxide is therefore a highly effective mechanism for pathogen-removal, but its lack of specificity means that endogenous tissue is also subjected to its deleterious effects.

Neutrophils contain darkly-staining, cytosolic, azurophilic primary granules (as well as secondary, specific granules and tertiary, gelatinase granules, see section 1.2.2.1) (Borregaard and Cowland 1997). Degranulation as a result of IL-8 stimulation is key in mobilising the anti-microbial, neutrophilic defence system (Willems, Joniau et al. 1989). As well as various other bactericidal products, these contain proteases and myeloperoxidase (MPO), which neutrophils and monocytes use to produce hypochlorite (ClO^-) from Cl^- and newly generated H_2O_2 (Babior 1984). MPO itself is another component of the oxidative battery capable of destroying bacteria, with potential to cause damage to endogenous tissue. As such, an MPO activity assay is a useful tool in assessing leukocyte activation and infiltration (Williams, Paterson et al. 1982, Gavins, Dalli et al. 2007, Leoni, Patel et al. 2008).

As the potential for collateral tissue damage suggests, associations between inappropriate inflammation and non-infectious diseases are continually being drawn, in which alternative stressful stimuli provoke a response designed to tackle pathogens. The damage the 'cellular debris' causes in these cases has been linked to diseases such as rheumatoid arthritis, multiple sclerosis, asthma, atherosclerosis, reperfusion injuries—and indeed I/R injury in stroke. Recruitment of leukocytes in stroke pathogenesis has been shown to provoke proliferation of tissue damage subsequent to the initial ischaemic insult. This assertion is supported by a bulk of evidence that, as discussed in the following section (1.2.2), describes neuroprotection and improved behavioural outcome following experimental stroke with adhesion molecule-specific monoclonal antibodies (Matsuo, Onodera et al. 1994, van Lookeren Campagne, Thomas et al. 1999) or in adhesion molecule-deficient animals (Okada, Copeland et al. 1994, Zhang, Chopp et al. 1995, Zhang, Chopp et al. 1996, Prestigiacomo, Kim et al. 1999).

1.2.2 The resolution of inflammation

As extravasated and activated leukocytes release ROS and further pro-inflammatory mediators, the pro-inflammatory system is self-perpetuating to an extent. Despite this, the symptoms of any manifestation of inflammation (from a bout of influenza to a bee sting) usually subside. The mechanisms through which this occurs—through which we are protected from the deleterious effects of an aberrant bactericidal system—are part of an endogenous, parallel anti-inflammatory process. This is discussed in the following section (*The resolution of inflammation*), along with evidence which supports their potential therapeutic use.

1.2.2.1 Resolution: an active process

The termination of pro-inflammatory activity, known as the *resolution of inflammation*, is an active process (rather than a result of the gradual winding-down of pro-inflammatory activity) (Serhan, Chiang et al. 2008). It is a concerted effort between cytokines, eicosanoids and glucocorticoid-associated processes (via protein Annexin A1; AnxA1; see section 1.3.2.1) that promotes the non-phlogistic apoptosis and phagocytosis of leukocytes already in the tissue, wound-healing, and prevents further recruitment of leukocytes—particularly ROS-releasing neutrophils.

Transforming growth factor-β (TGFβ) and interleukin-10 (IL-10) are key anti-inflammatory cytokines involved in resolution, providing negative feedback on escalating inflammation. Homophilic PECAM-1 interactions allow phagocytic ingestion of apoptotic cells (Kalinowska and Losy 2006), promoting TGFβ release (Huynh, Fadok et al. 2002) which suppresses NFκB activity (Ng, Hou et al. 2005); IL-10 limits the release of cytokines and chemokines from activated dendritic cells and macrophages through STAT3-mediated gene suppression (Murray 2005). In addition to altered cytokine activity, the pro-resolution system is heavily reliant on the switch of Ω6 fatty acid-derived lipid mediators (known as *eicosanoids*) from pro-inflammatory to pro-resolving.

Fatty acids (arachidonic acid, Aα, docosahexaenoic acid, Dα, eicosapentaenoic acid, Eα) are released from leukocyte and endothelial cell membranes following an inflammatory stimulus (Figure 4). Dα and Eα are both Ω3 fatty acids which produce potent pro-resolving eicosanoids known as resolvins and protectins (Serhan, Hong et al. 2002, Schwab, Chiang et al. 2007). Aα is an Ω6 fatty acid whose derivatives produce net pro-inflammatory effects, forming prostaglandins (PGs) and leukotrienes. While the prostaglandins prostacyclin (PGI_2) and PGJ_2 are anti-inflammatory, thromboxane (TXA_2) and PGE_2 are pro-inflammatory—as are leukotrienes.

Eicosanoids are formed from Aα through either a cyclooxygenase (COX) pathway (prostaglandin synthesis, with the exception of epithelial leukotriene production) or a transcellular lipoxygenase (LOX) pathway (leukotriene synthesis). The transcellular (leukocyte-platelet-endothelia/epithelia) prerequisite for the biosynthesis of leukotrienes is fundamental in restricting their production to inflammatory states, in which leukocytes and platelets make contact with each other and endothelia. Particularly clever is that on excess inflammation, there is a switch from leukotriene production to an alternative LOX pathway which enables leukotriene conversion to lipoxins (Levy, Clish et al. 2001). Lipoxins are key endogenous effectors of resolution discussed in more detail in section 1.3.2.2.

Compounded by the failures of clinical trials for drugs targeting pro-inflammatory circuits during stroke (see section 1.1.3.2), the pharmacological potential in enhancing endogenous mechanisms of resolution is obvious. The next section assesses experimental evidence in support of this.

1.2.2.2 Evidence for therapeutic benefit in promotion of resolution

The failure of promising pre-clinical results to translate into effective therapies is assigned to a combination of poor clinical trial design and stringency within animal experiments, which, while necessary, does not inherently lend itself to the clinic. Despite this, the future of stroke research is not so bleak. As described in the previous section (1.2.2.1), for the host, implementation of the leukocyte adhesion cascade is not the end of its involvement in the progression of inflammation; the concept of active resolution of inflammation has driven a new field of research aimed at enhancing mechanisms involved. Evidence in support of the hypothesis comes from a range of *in vitro*, animal models and human studies, and has shown particular promise in the field of stroke.

Blood analyses of stroke patients have demonstrated that the presence of particular cytokines is indicative of stroke severity and often prognosis: patients with lower plasma concentrations (<6 pg/ml) of IL-10 deteriorated within 58 h of stroke onset (Vila, Castillo et al. 2003), and exogenous IL-10 administered to rats post-MCAO reduced infarct sized by around 20 percent. Following MCAO in mice, 10,17*S*-docosatriene (another DHA/Ω3 derivative) and 17R-resolvin (an EPA/Ω3 derivative produced in the presence of aspirin) alleviate the leukocyte-mediated injury (Marcheselli, Hong et al. 2003). Post-ischaemic administration of a lipoxin A4 (LXA_4: a product of the alternative, anti-inflammatory LOX pathway) analogue (LXA_4-methyl ester) improves neurological outcome; it suppresses neutrophil infiltration and lipid peroxidation levels; inhibits glial activation; reduces TNFα/IL-1β expression and up-regulates IL-10/TGFβ1 expression in a rat model of focal stroke (Ye, Wu et al. 2010). Glucocorticoid-driven protein AnxA1 offers

neuroprotection in a mouse model of focal stroke, and exogenous mimetic Annexin A1 acetylated peptide 2-26 ($AnxA1_{Ac2-26}$; see section 1.3.2.1) reduces both leukocyte recruitment to endothelia and infarct volume (Gavins, Dalli et al. 2007). Evidence to suggest the central role of eicosanoids and AnxA1 in the resolution of inflammation is abundant, as well as indications of their potential as a basis anti-inflammatory drugs (Yazid, Norling et al. 2011). Work in particular has been directed at modulating the effect of their shared receptor—this receptor is discussed in the following section (1.2.2.2).

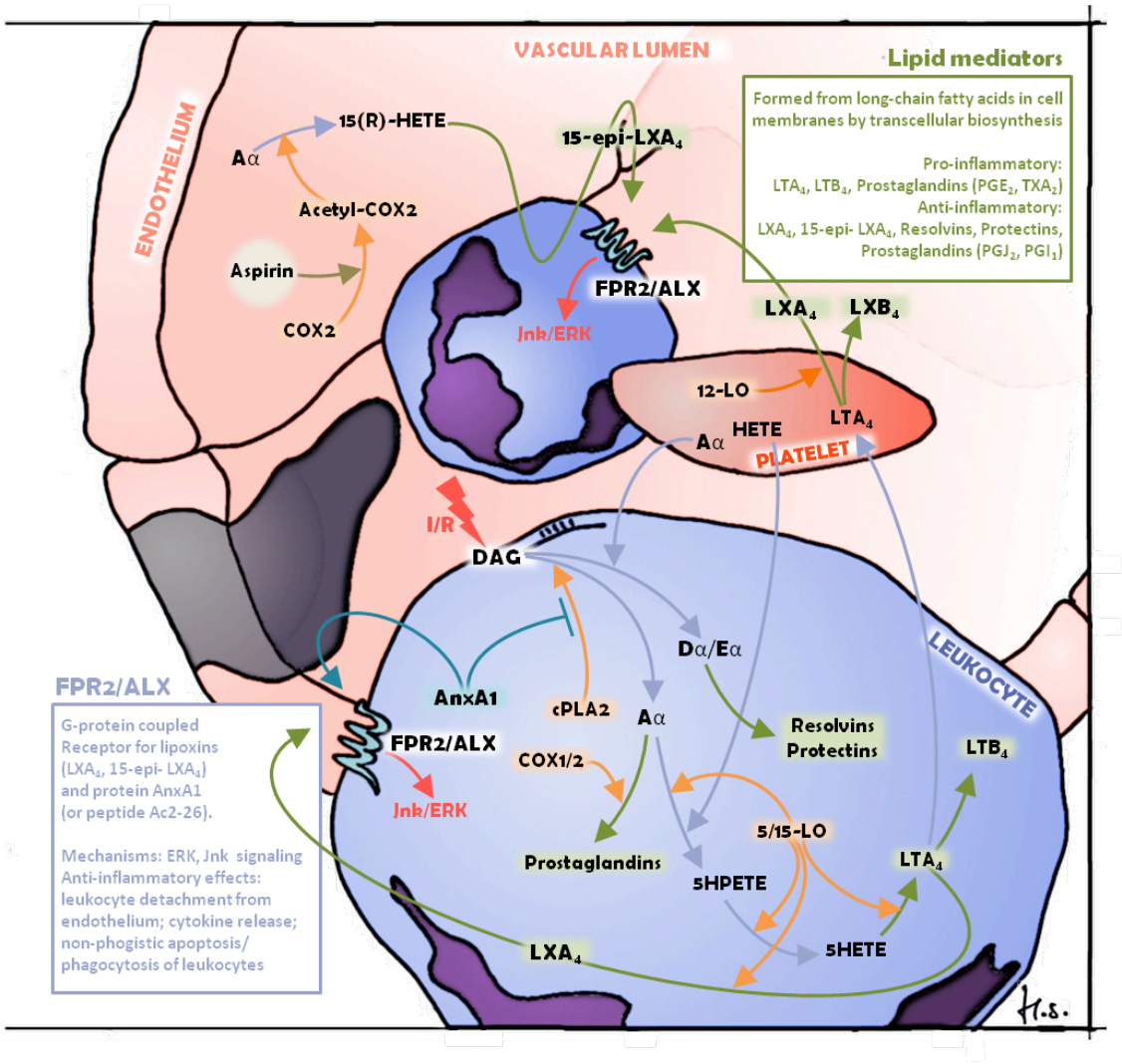

Figure 4. Eicosanoid production during inflammation (Smith Unpublished). When triggered by inflammatory stimuli (e.g. ischaemia/reperfusion, I/R), diacylglycerol (DAG) allows release of fatty acids (arachidonic acid, Aα, docosahexaenoic acid, Dα, eicosapentaenoic acid, Eα) from the cell membrane). Through transcellular biosynthetic routes these are converted to prostaglandins (PGX_X), leukotrienes (LTX_X) or lipoxins (LXX_X). Aspirin utilises a further biosynthetic route to produce 15-epi-LXA_4 in the presence of aspirin. Protein Annexin A1 (AnxA1) is an additional pro-resolving mediator which shares Formyl Peptide Receptor 2 (FPR2/ALX) with the lipoxins as a principal receptor in their anti-inflammatory activity. LO = lipoxygenase; 5HPETE = 5-hydroperoxy-eicosatetraenoic acid; 5HETE = 5-hydroxyeicosatetraenoic acid; TXA_2 = thromboxane; COX2 = cyclooxygenase 2.

1.3 The Formyl Peptide Receptors

1.3.1 Characterisation

Neutrophils are crucial in the response to acute inflammatory stimuli. They migrate to sites of tissue damage or infection, guided by gradients of endogenous chemokines and/or bacterial fragments. These mediators are recognised by toll-like receptors (TLRs) and GPCRs. Formyl peptide receptors (FPRs) on neutrophils can recognise bacterial formylated peptides and are therefore central GPCRs in host defence. Nevertheless, the roles of FPRs in the modulation of inflammation extend vastly beyond the promotion of leukocyte chemotaxis. Ligands for each of the three identified human FPRs (and the ever-expanding set of known murine orthologues) have been identified which transduce both pro- and anti-inflammatory activity. This section (*Characterisation*) will describe the fundamental aspects of FPRs, including their initial discovery, their distribution and their activity during inflammation.

1.3.1.1 Discovery and cloning of the formyl peptide receptors

FPRs belong to a seven transmembrane domain GPCR superfamily. Human formyl peptide receptor 1 (FPR1, originally FPR) was initially identified as a neutrophilic, high affinity surface binding site for *N*-formyl-Met-Leu-Phe (fMLF)—the archetypal *N*-formylated bacterial peptide (Schiffmann, Showell et al. 1975, Aswanikumar, Corcoran et al. 1977). FPR1 appeared to mediate the uptake and internalisation of formyl peptides (Niedel, Wilkinson et al. 1979, Niedel, Kahane et al. 1979) whose binding would cause the chemotaxis of neutrophils to a site of inflammation on calcium influx into the neutrophil (Boucek and Snyderman 1976). *FPR1* was cloned through functional screening of a cDNA library for differentiated human promyelocytic leukaemia (HL-60) cells—a predominantly neutrophilic promyelocyte cell line (Boulay, Tardif et al. 1990). Two related genes were subsequently cloned through low-stringency hybridisation to an *FPR1* cDNA probe: *FPR2* and *FPR3* (originally *formyl peptide-like receptors 1* and *2; FPRL1* and *2*). The three genes were found to be co-localised in a cluster on chromosome 19 (19q13.3) (Alvarez, Coto et al. 1994) and expressed by monocytes and neutrophils (FPR1/FPR2) or monocytes only (FPR3) (Durstin, Gao et al. 1994).

In parallel to these studies of the 1990s, the earlier identification of LXA_4 (the anti-inflammatory eicosanoid; see section 1.3.2.2) led to the induction of its receptor in HL-60 cells (Fiore, Romano et al. 1993), thus the identification of the LXA_4 receptor (ALX) on human neutrophils (Fiore, Maddox et al. 1994). During a screening of orphan GPCRs known to be induced within the same time

period, LXA_4 was found to bind specifically to FPR2, stimulating GTPase and pertussis toxin sensitivity—highly comparable to effects seen on its binding to the endogenous LXA_4-specific binding sites on peripheral neutrophils (Fiore, Maddox et al. 1994). ALX is also located on chromosome 19q (Bao, Gerard et al. 1992). Considerable discussion has taken place regarding the rightful nomenclature for previously-named human FPRL1 as FPR2 or ALX (Chiang, Serhan et al. 2006, Ye, Boulay et al. 2009). Those endorsing 'ALX' believe its title should relate to the functional properties of the protein (as a high affinity binding site for LXA_4) rather than its structural similarity and genomic proximity to another (FPR1)—for now the buck has stopped with FPR2/ALX.

1.3.1.2 Tissue and cellular distribution of the formyl peptide receptors

FPRs are classically receptors of the haematopoietic/myeloid cell population, having initially been discovered in rabbit and human neutrophil populations. In human, FPR1 is expressed in phagocytic leukocytes/microglia, monocytes and neutrophils; FPR2/ALX mimics this expression pattern, as does FPR3 with the exception of its presence on neutrophils (Yang, Chen et al. 2001). Monocyte differentiation into dendritic cells is coupled with a progressive decline in FPR2/ALX function but sustained FPR3 expression, whereas FPR2/ALX expression remains unchanged with monocyte differentiation into macrophages (Yang, Chen et al. 2002). A similar pattern is seen among murine myeloid cells, where Fpr1 (FPR1) and Fpr2/3 (FPR2/ALX) are expressed in neutrophils, dendritic and microglial cells (Ye, Boulay et al. 2009).

FPR expression has been described in numerous other cells/tissues, for example: astrocytes, thyroid, heart, kidney and spleen (FPR1); astrocytes, spleen, lung and testis (FPR2/ALX); spleen, adrenal glands, lung and liver (FPR3)—often endothelia of organs and tissues with secretory functions (Becker, Forouhar et al. 1998). Non-haematopoietic murine Fprs are seen in spleen, lung and liver, with Fpr3 also expressed in astrocytes and the heart (Migeotte, Communi et al. 2006, Ye, Boulay et al. 2009).

1.3.1.3 Orthology of human and mouse genes

The *FPR* gene cluster has undergone differential expansion in the mouse genome, where it encodes at least nine different receptors (Fpr1, Fpr2, Fpr3, and Fpr-related sequences (Fpr-rs) 3-8; originally Fpr and Fpr-rs 1-8) (Gao, Chen et al. 1998, Wang and Ye 2002, Tiffany, Gao et al. 2011). In fact functional FPRs can be found in other primates, rabbits, rats, guinea pig and horse as well as humans and mice, in expanded or contracted families of human receptor orthologues (Ye, Boulay et al. 2009). This diversity across mammalian species indicates strong selection pressures (Gao, Chen et al. 1998) as well as the practical difficulties of studying the receptor family in mice. Both

human and mouse FPR/Fpr families have drifted through several name changes since their discovery. Figure 5 represents structural similarities between human and mouse FPR/Fprs, and also denotes key name changes.

LXA_4 acts via FPR2/ALX in human. Mouse orthologues of human FPR2/ALX are Fpr2 and Fpr3. This has led to a lack of clarity in the literature over whether the principal physiologically relevant (rather than structurally homologous) mouse LXA_4 receptor is equivalent to Fpr2 or Fpr3. The mouse LXA_4 receptor, LXA4R, has an NCBI amino acid sequence listing distinct from both Fpr2 and Fpr3 (NCBI 2010c), although this may be due to alternative *Fpr* gene splicing. Figure 6 shows amino acid sequences of mouse Fpr2, Fpr3 and LXA4R. Differences between Fpr2/3 and LXA4R are highlighted; there is 83.48 per cent sequence homology between Fpr2 and LXA4R and 98.86 per cent between Fpr3 and LXA4R. LXA4R therefore shows higher sequence homology to Fpr3, as shown in Figure 6 and as described in detail in by Gao et al. (whose work originally demonstrated the differential expansion of the *FPR* gene cluster in human and mouse, see (Gao, Chen et al. 1998). In addition, Fpr2 and Fpr3 activity (Gao, Guillabert et al. 2007) and expression (Gao, Chen et al. 1998) may be mutually exclusive.

Despite this, the mouse LXA4R was for some time frequently referred to as Fpr2 (Dufton, Hannon et al. 2010, Dufton and Perretti 2010, Maderna, Cottell et al. 2010), as anti-inflammatory/pro-resolution action of LXA_4 were demonstrated through this receptor in genetic studies using Fpr2-null mice in particular. This colony, however, has recently been reclassified as Fpr2/3-null (despite specific targeting of Fpr2, overlap in the exon regions make a functional Fpr3 unlikely) (Dufton, Hannon et al. 2010). While not completely resolved, LXA4R is currently referred to as Fpr2/3. The emergence of subtype-specific agonists could aid in the characterisation of the mouse receptor family, as until very recently, a lack of selective antagonists or neutralising antibodies has made the identification of Fpr2 and Fpr3-specific activity difficult. An example of this is ligand for formyl peptide receptor (FPR)-like (FPRL)-2 (currently known as FPR3), F2L (Johansson 2011), which is selective for Fpr2 in the mouse (Gao, Guillabert et al. 2007).

1.3.1.4 Modulating inflammation and chemotaxis through formyl peptide receptors

The classical role for FPR1 agonists is in the promotion of chemotaxis and pathogen recognition, particularly in its role as a high affinity receptor for fMLP (Ye, Boulay et al. 2009), and the function of FPR3 remains largely unknown (Rabiet, Macari et al. 2011). Here the focus will be FPR2/ALX (mouse orthologues Fpr2/3), because of the pro-resolving pharmacological potential of some of its agonists.

The number and physical variation of FPR2/ALX ligands make the activity of the receptor difficult to define simply. It is considered a receptor whose anti-inflammatory properties are most significant with respect to pharmacological potential—indeed this theme occupies the majority of published FPR2/ALX data. In spite of this, FPR2/ALX is a low affinity receptor for fMLP (responsive in the micromolar range) (Prossnitz and Ye 1997, Kretschmer, Gleske et al. 2010) correctly indicating a role in chemotaxis; appreciation of potential receptor ligand/cell/condition-dependent pro-inflammatory activity is therefore essential for optimal use of FPR2/ALX as a drug target in the modulation of inflammation. FPR2/ALX is in general up-regulated by pro-inflammatory cytokines such as TNFα (Cui, Le et al. 2002), and may be inhibited by interleukin-4 (IL-4) on microglia following TNFα stimulation (Iribarren, Chen et al. 2005). (FPR2/ALX is also inhibited in non-cerebral tissue by IL-4 in peritonitis, see (Dai, Major et al. 2005). There have been many ligands identified for all members of the FPR family (for an up-to-date list see (Gavins 2010). Some agonists include LXA_4 (Chiang, Serhan et al. 2006), AnxA1 (Perretti, Getting et al. 2001) and related pharmacophores (see section 1.3.2.1); serum amyloid A (SAA) (Su, Gong et al. 1999); amyloid β_{1-42} ($A\beta_{42}$) (Cui, Le et al. 2002) and Trp-Lys-Tyr-Met-Val-D-Met (WKYMVM or 'W peptide') (Bae, Park et al. 2003). Antagonists include peptide Trp-Arg-Trp-Trp-Trp-Trp (WRWWWW or 'WRW4') and N-*t*-butoxycarbonyl-Phe-Leu-Phe-Leu-Phe (Boc2; for FPR2/ALX antagonism, see section 1.3.2.3) (Stenfeldt, Karlsson et al. 2007), although others are available. A possible explanation for the differential activity involves the variety of potential binding sites on FPR2/ALX (Bena, Brancaleone et al. 2012). For example, using FPR1/FPR2/ALX chimeras transfected into HEK293 cells, Bena and colleagues showed that the AnxA1-binding domain as the N-terminal and extracellular loop II whereas SAA required loops I and II.

SAA is present in serum in health, but can increase up to 1000-fold during inflammatory conditions (including Alzheimer's disease and stroke) (Kindy, Yu et al. 1999, Su, Gong et al. 1999, Brea, Sobrino et al. 2009). SAA activity through FPR2/ALX causes chemotaxis, adhesion and migration (through β_2 integrin modulation) for both monocytes *and* neutrophils, indicating a pro-inflammatory role of this mechanism (Badolato, Wang et al. 1994). Ligand-binding does, however, cause the monocytic production of cytokines such as TNFα, MCP-1 and IL-10 (Lee, Kim et al. 2006, Lee, Kim et al. 2008). While TNFα is a pro-inflammatory cytokine, IL-10 exhibits anti-inflammatory activity and MCP-1, although 'pro-inflammatory' as a chemoattractant, may be considered pro-resolving because the target cells are monocytes.

Similarly, $A\beta_{42}$ activity through human FPR2/ALX and murine Fpr2/3 has been shown to cause increased chemotaxis of microglia and monocytes in Alzheimer's disease (Cui, Le et al. 2002,

Iribarren, Chen et al. 2005). The opposing nature of monocyte-linked versus neutrophil-linked FPR activity could be considered a mechanism for reducing infiltration of neutrophils—thereby reducing potential tissue exposure to ROS—and promoting active removal of these neutrophils through increased phagocytosis by monocytes. Despite this, infiltration of activated mononuclear phagocytes into the sites of lesions is a characteristic feature of amyloidogenic diseases, and due to ROS release is associated with considerable inflammatory damage (Lee, Kim et al. 2010).

During acute inflammation and I/R, such as in ischaemic stroke, the role of FPR2/ALX is typically the promotion anti-inflammatory activity. There is involvement of LXA_4 and AnxA1 (Perretti, Chiang et al. 2002) and various related ligands, discussed in the next section (1.3.2).

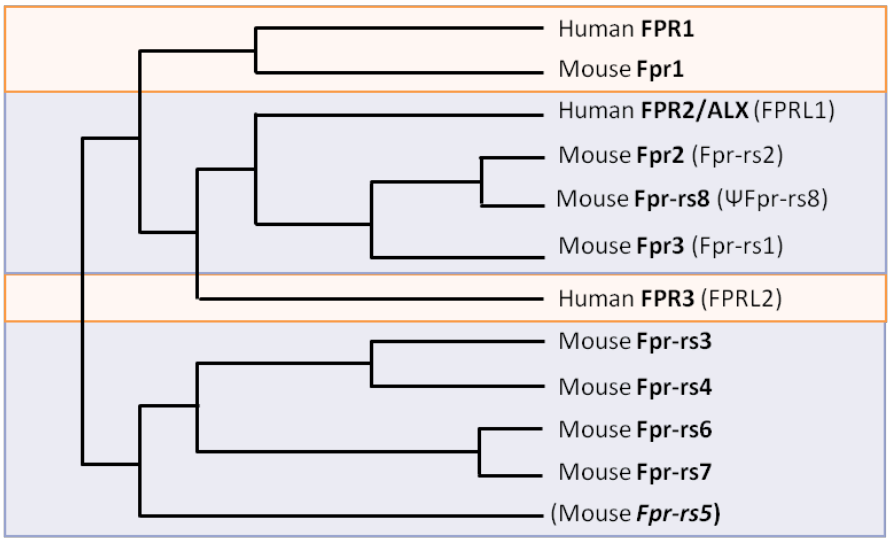

Figure 5. Structural similarities between human and mouse FPR. Early nomenclature is included where they have been commonly used in the literature; current nomenclature (as receptors will be referred to from here on) is in bold. Human and mouse orthologues shown in coloured boxes; there are no known mouse orthologues for FPR3 and no human orthologues for mouse genes Fpr-rs3-8. Brackets indicate current uncertainty regarding whether or not the mouse *Fpr-rs5* gene is actually expressed. Adapted from (Migeotte, Communi et al. 2006, Ye, Boulay et al. 2009).

Figure 6. Amino acid sequences for murine Fpr2, Fpr3 and LXA4R. Sequences aligned for comparison. Highlighted amino acids indicate those which differ from LXA4R; bold amino acids indicate extracellular loops (NCBI 2010a, NCBI 2010b, NCBI 2010c).

1.3.2 Anti-inflammatory activity of FPR2/ALX

By the early 1990s, FPR2/ALX had been discovered as the transducer for the anti-inflammatory activity of LXA_4 (Fiore, Romano et al. 1993, Fiore, Maddox et al. 1994). Other studies simultaneously demonstrated protective effects of AnxA1 in murine myocardial infarction and other inflammatory environments, but the receptor remained elusive (Romisch, Schuler et al. 1992, Vergnolle, Comera et al. 1997, Gavins, Kamal et al. 2005). In 2000, work was published demonstrating an FPR mechanism for the protein (Walther, Riehemann et al. 2000), which was later refined to support the direct interaction of AnxA1 and FPR2/ALX (Perretti, Chiang et al. 2002). The evidence for FPR2/ALX as a mutual mechanism for each of these ligands is now broad. This section (*Anti-inflammatory activity of FPR2ALX*) will describe the properties of AnxA1 and LXA_4, and how they may contribute to a pro-resolving therapy based on FPR2/ALX.

1.3.2.1 Annexin A1 and AnxA1$_{Ac2-26}$

AnxA1 is a calcium-/phospholipid-binding 37 kDa protein and an endogenous non-formyl peptide FPR agonist. It is principally active through FPR2/ALX (mouse orthologue Fpr2/3) (Walther, Riehemann et al. 2000), although may signal via FPR1 either at higher concentrations (Khau, Langenbach et al. 2011), *in vitro* (Ernst, Lange et al. 2004) or in certain models of inflammation such as zymosan-induced peritonitis (Perretti, Getting et al. 2001). AnxA1 production is stimulated by glucocorticoids (Goulding, Godolphin et al. 1990) in response to excessive inflammation, during which its key functions include: guiding leukocytes directly to the site of inflammation; the reduction leukocyte extravasation, and encouraging apoptosis and subsequent clearance of extravasated leukocytes. Annexins are characterised by a core with a unique N-terminal peptide which defines its function. $AnxA1_{Ac2-26}$, $AnxA1_{Ac2-12}$, $AnxA1_{Ac2-6}$ (particularly used in myocardial I/R) and scrambled AnxA1 peptides are AnxA1 N-terminal-derived peptides used widely experimentally as they are able to exert the biological activity of the full-length protein (La, D'Amico et al. 2001, Gavins, Kamal et al. 2005). $AnxA1_{Ac2-26}$ (Ac-AMVSEFLKQAWFIENEEQEYVQTVK) is the most commonly used of these and is used in the work in this thesis.

The purported functions of the protein are supported by a body of data. AnxA1 provides a feedback mechanism suppressing glucocorticoid-induced eicosanoid synthesis and phospholipase A2 activity (Buckingham, John et al. 2006) (Figure 4, p.36); it is a pro-engulfment ligand for phosphatidylserine during apoptosis (Arur, Uche et al. 2003) and has a role in leukocyte trafficking (Perretti, Christian et al. 2000, Gavins, Dalli et al. 2007), possibly causing leukocyte detachment

from endothelia through shedding of L-selectin (a leukocyte-bound mediator of cell rolling; see section 1.2.1.2) (Strausbaugh and Rosen 2001, de Coupade, Solito et al. 2003). Initial investigations into the clinical relevance of AnxA1 function were conducted in the rat model demonstrating reduced infarct size in a model of focal cerebral I/R after intracerebroventricular administration of an AnxA1 fragment (Relton, Strijbos et al. 1991).

Resting neutrophils store around fifty percent of cytosolic AnxA1 in their gelatinase granules (Perretti, Christian et al. 2000, Perretti and Flower 2004), which is rapidly released on neutrophil activation/adhesion to endothelia. Here it activates anti-inflammatory pathways which can result in leukocyte detachment. This activity is exemplified by intravital studies showing a significant decrease in leukocyte adhesion following AnxA1 treatment in various models, including mouse myocardial infarction (La, D'Amico et al. 2001) and focal cerebral ischaemia (Gavins, Dalli et al. 2007).

1.3.2.2 Lipoxin A4 and 15-epi-lipoxin A4

LXA_4 is an arachidonic acid-derived eicosanoid (Serhan, Hamberg et al. 1984) and also an endogenous ligand for FPR2/ALX. It is generated through a transcellular biosynthetic pathway which also produces leukotrienes (the pro-inflammatory precursor for LXA_4; Figure 4) according to LOX activity in activated leukocytes (Levy, Romano et al. 1993) (see section 1.2.2.1). The more recent discovery of an acetyl-COX2-dependent related LOX pathway induced in the presence of aspirin led to the discovery of aspirin-triggered 15-epimer-lipoxin A4 (ATL or 15-epi-LXA_4); aspirin inhibits COX2 activity through acetylation of serine residues and the acetylated COX2 is redirected to the LOX pathway (Claria and Serhan 1995). (15-epi-LXA_4 production and subsequent anti-inflammatory activity is another mechanism through which aspirin pharmacology is of cardiovascular benefit, besides its traditional inhibition of prostaglandin and thromboxane synthesis (Chiang, Bermudez et al. 2004).) 15-epi-LXA_4 is more potent and longer-lasting than its endogenous counterpart (Chiang, Fierro et al. 2000), often making it the preferred choice over LXA_4 in studies investigating the therapeutic potential of the ligand family (Fierro, Colgan et al. 2003).

There are rapidly increasing data that indicate the pro-resolving actions of lipoxins in inflammation. The broad methods through which these occur are cell specific (Migeotte, Communi et al. 2006). LXA_4 stimulates phagocytosis (1.7-fold above basal level) by bone marrow-derived macrophages in wild type mice whereas no effect is seen in Fpr2/3 knockout mice (Maderna, Cottell et al. 2010). In neutrophils, there is decreased β_2 integrin (Mac-1/CD11b/18) expression, a

reduction in ROS and pro-inflammatory cytokine production, reduced NF-κB activation and an increase in anti-inflammatory cytokine production. This reduces neutrophil activation and transmigration across epithelia. In terms of resolving inflammation, LXA_4 action on monocytes causes their non-phlogistic activation and transmigration, and an increase in phagocytosis.

In vivo evidence demonstrates the value of these effects in various disease models. LXA_4 or its analogues have been shown to be protective (by reduction of inflammation or tissue damage from I/R) in the brain (Ye, Wu et al. 2010), kidney (Munger, Montero et al. 1999) and lung (El Kebir, Jozsef et al. 2009) among other regions. Surprisingly, topical LXA_4 has been shown to increase neutrophil chemotaxis to corneal wounds in rabbits, promoting wound healing, while pro-inflammatory leukotrienes have no effect (Gronert, Maheshwari et al. 2005). This is distinct from their better-known anti-inflammatory properties but emphasizes the need to provide evidence of FPR agonists in a range of models.

1.3.2.3 FPR2/ALX inhibition

Several antagonists with a high affinity for FPR2/ALX have been widely used to study different aspects of FPR2/ALX pharmacology. WRW4 has been characterised as an antagonist for FPR2/ALX (Bae, Lee et al. 2004). The peptide was identified through library screening of WKYMVM-blocking hexapeptides and showed the most potent inhibition of WKYMVM-FPR2/ALX binding in RBL-2H3 cells. Specificity was determined by its ability to block the activity of various FPR2/ALX agonists but not fMLP (FPR1 agonist; FPR2/ALX agonist at higher concentrations). WRW4 is effective in the high nanomolar to low micromolar range (Stenfeldt, Karlsson et al. 2007), although high concentrations (above 10 μM) cause non-specific inhibition of FPR activity.

Boc2 is a non-selective antagonist (Gavins, Yona et al. 2003, Machado, Johndrow et al. 2006). Pan-antagonistic activity allows Boc2 to be used to identify general FPR activity.

1.3.3 How can we intervene to rescue the brain after stroke?

Inflammation caused by I/R in stroke provides an opportunity for damage-intervention beyond excitotoxic cell death. Coupled with the increasingly substantiated paradigm that inflammation resolution is an active process (Serhan, Chiang et al. 2008), this has directed research into the manipulation of endogenous anti-inflammatory/pro-resolving agents towards stroke therapies.

Continued study in this area seems essential given the data that have already been generated—some alluding to FPR involvement. Post-ischaemic administration of a LXA_4 analogue (LXA_4-methyl ester) improves neurological outcome, suppresses neutrophil infiltration and lipid peroxidation levels, inhibits glial activation, reduces TNFα and IL-1β expression, and up-regulates IL-10 and TGF-β1 expression in a rat model of focal stroke (Ye, Wu et al. 2010). AnxA1 offers neuroprotection in a mouse model of focal stroke, as mimetic $AnxA1_{Ac2\text{-}26}$ reduces both leukocyte recruitment to endothelia and infarct volume (Gavins, Dalli et al. 2007). There is less information available for global models, although Ischikawa and co-workers have shown leukocyte-/platelet-endothelia interactions may be reduced by angiotensin II type 1 (ANG II) receptor antagonists (including diphenyleneiodonium, 2.5 mg/kg) (Ishikawa, Sekizuka et al. 2007).

The caveat with these experiments (as with those related) is that they do not accommodate the impracticality of a regimented temporal drug-administration protocol for human stroke patients. They are, nevertheless, an excellent foundation for further work. The purpose of this project is therefore to pursue knowledge of FPR mechanisms in the resolution of inflammation in a stroke model using intravital techniques, and to investigate the potential of the receptor system in drug development.

1.4 Hypothesis

1.4.1 Hypothesis

AnxA1 and LXA_4 will mediate a protective effect in stroke (global cerebral I/R), via a mechanism of action involving member(s) of the formyl peptide receptor (FPR) family.

1.4.2 Aims

1.4.2.1 In brief

To uncover ways in which previously characterised FPR agonists mediate inflammation in global cerebral ischaemia. By providing insight into receptor mechanisms, it will supply evidence towards their potential use in stroke therapies.

1.4.2.2 In detail

1. To develop a model of global cerebral ischaemia followed by reperfusion. This should enable the visualisation through intravital microscopy of significant leukocyte-endothelial (L-E) interactions in the mouse cerebral microcirculation with respect to sham operated animals.
2. To determine changes in the cerebral microvasculature following global cerebral I/R up to 3 h post-stroke.
3. To determine the physiological/cellular responses to FPR agonists.
4. To determine the mechanism through which FPR agonists provide anti-inflammatory effects, with the use of pharmacological and genetic approaches.

Chapter Two

Materials and Methods

2.1 Materials

Table 2 and Table 3 list the sources of key products used in the experiments described within this chapter.

Table 2. List of products and reagents used in *in vivo* experiments (section 2.2).

	Product	Company	Company location
Anaesthetics	Isoflurane liquid	Attane	PA, US
	Ketamine	Fort Dodge Animal Health	Southampton, UK
	Pentobarbital sodium	VWR	PA, US
	Xylazine	Bayer Healthcare	Newbury, Berkshire, UK
Drug treatments	15-epi-lipoxin A4	Calbiochem	Darnstadt, Germany
	Ac2-26	Cambridge Research Biochemicals	Cleveland, UK
	Boc2	MP biomedicals	West Lothian, UK
	Ethanol (absolute)	Sigma-Aldrich	Poole, Dorset, UK
	Lipoxin A4	Calbiochem	Darnstadt, Germany
	Physiological saline	Baxter Healthcare	Northampton, UK
	WRWWWW (WRW4)	Tocris Bioscience	Elliswille, MO, US
Surgery	Dumont 7 forceps	Fine Science Tools	Germany
	Glass coverslips (cranial window)	BD Biosciences	Oxford, UK
	Microdrill	Fine Science Tools	Germany
	Microscissors	Fine Science Tools	Germany
	Microvessel clips	Fine Science Tools	Germany
	Needles (26, 27 and 30G)	Becton Dickenson	UK
	Polyethylene (PE)-10 tubing	Intramedic	Oxford, UK
	Silk thread (6-0)	Harvard Apparatus	Kent, UK
	Stereotactic frame (custom built)	-	-
	Surgical Scissors	Fine Science Tools	Germany
	Syringes	Becton Dickenson	UK
	Vetbond tissue adhesive	3M	UK
Misc. *in vivo* products	9.4T MRI scanner	Oxford Instruments	Oxfordshire, UK
	Artificial CSF components (CaCl, NaCl, KCl, MgCl2, Urea, Dextrose, NaHCO3)	Sigma-Aldrich	Poole, Dorset, UK
	C57BL/6 mice	Charles River UK Ltd	UK
	CoolSNAP HQ^2 black and white camera	Photometrics	Tuscon, AZ, US
	Fluroscein isothiocyanate (FITC)-labelled albumin	Sigma-Aldrich	Poole, Dorset, UK
	Heparin (sodium salt from porcine intestinal mucosa)	Sigma-Aldrich	Poole, Dorset, UK
	Intravital microscope	Olympus	Japan
	Lipopolysaccharide (LPS) from *E. coli* 0111:B4	Fisher Scientific	Loughborough, UK
	Rhodamine 6G	Sigma-Aldrich	Poole, Dorset, UK
	Slidebook 4.2 software	Intelligent Imaging Innovations, Inc.	Denver, CO, US

Table 3. List of products and reagents used in *in vitro* experiments (section 2.3).

	Product	Company	Company location
Bead array	Cytometric bead array, mouse inflammation kit	BD Biosciences	Oxford, UK
	Falcon sample acquisition tubes (75 mm)	BD Biosciences	Oxford, UK
	MultiscreenHTS vacuum manifold	Millipore	Billerica, MA, USA
	MultiscreenHTS-BV 1.2 µm filter plates	Millipore	Billerica, MA, USA
	FCAP Array 3.0 software	BD Biosciences	Oxford, UK
Blood collection/ chemotaxis assay	Chemotaxis plates	Neuroprobe Receptor Technologies	Warwickshire, UK
	fMLP	Sigma-Aldrich	Poole, Dorset, UK
	Histopaque1077 and 1119	Sigma-Aldrich	Poole, Dorset, UK
	MCP-1	PeproTech EC Ltd	London, UK
	MIP-1α	PeproTech EC Ltd	London, UK
	Vacutainer system	BD Biosciences	Oxford, UK
MPO assay	Hexadacyl trimethylammonium bromide	Sigma-Aldrich	Poole, Dorset, UK
	Hydrogen peroxide	Sigma-Aldrich	Poole, Dorset, UK
	Tetramethylbenzidine (TMB)	Sigma-Aldrich	Poole, Dorset, UK
Western-blotting	β-actin primary Ab (mouse)	Abcam	Cambridge, UK
	Anti-rabbit secondary Ab	Abcam	Cambridge, UK
	Annexin A1 primary Ab (rabbit)	Invitrogen	Carlsbad, CA, US
	Chemiluminescence kit	Thermo Scientific	MA, US
	ERK1/2 primary Ab (rabbit)	Cell Signalling Technologies	Hertfordshire, UK
	Peroxidase horse anti-mouse IgG	Vector Laboratories	Peterborough, UK
	Phospho-ERK1/2 primary Ab (rabbit)	Cell Signalling Technologies	Hertfordshire, UK
	Western blotting apparatus	Invitrogen	Carlsbad, CA, US
Misc. *in vitro* products	Falcon tubes 15 and 50 ml	BD Biosciences	Oxford, UK
	Paraformaldehyde (PFA)	Sigma-Aldrich	Poole, Dorset, UK
	Phosphate buffered saline (PBS) tablets	Sigma-Aldrich	Poole, Dorset, UK

2.2 Methods 1: *In vivo* observation of leukocyte-endothelial cell interactions in cerebral ischaemia/reperfusion

2.2.1 Mouse global stroke model

2.2.1.1 Animal preparation

Experiments were performed using male C57BL/6 mice or Fpr2/3$^{-/-}$ mice on a C57BL/6 background (backcrossed for 6 generations) (Dufton, Hannon et al. 2010)[2], weighing 23-28 g. All animal procedures were carried out under licence and complied with Home Office regulations (Guidance on the Operation of Animals, Scientific Procedures Act, 1986). Mice were maintained on a 12 h light/dark cycle during which temperature was maintained at 21-23 °C, and had access to a standard chow pellet diet and tap water *ad libitum*.

Mice were anaesthetised with an intraperitoneal (i.p.) injection (using a 30G x ½" needle) of pentobarbital sodium (100 mg/kg) diluted in dH_2O and reflexes continually checked; a top up of pentobarbital sodium (approximately 15 mg/kg) was administered if animals maintained a pedal reflex 30+ min after initial injection. Eyes were kept lubricated with physiological saline. The right jugular vein was cannulated with a 20 cm polyethylene (PE)-10 catheter for intravenous (i.v.) administration of saline, treatments and dye (see section 2.2.2.2). Body temperature was monitored throughout using a rectal thermometer and maintained at 37±1.0 °C using a heating mat on which surgery was performed (Figure 7A/B).

2.2.1.2 Bilateral Common Carotid Artery Occlusion

The common carotid arteries (CCAs) were exposed via the existing ventral midline incision at the level of the neck (created previously for cannulation of the jugular vein). In the ischaemic group, CCAs were clamped for 5 min using microvessel clips (Figure 7C)[3]. In order to prevent excess disruption to breathing, care was taken to avoid physical pressure on the trachea and disruption/clamping of the vagus nerve. The clips were then removed and resumption of blood

[2] At the time of carrying out this work, Fpr2/3 wild type mice were unavailable, therefore Fpr2/3$^{-/-}$ groups are compared to C57BL/6 data sets as published in Gavins, F. N., E. L. Hughes, N. A. Buss, P. M. Holloway, S. J. Getting and J. C. Buckingham (2012). "Leukocyte recruitment in the brain in sepsis: involvement of the annexin 1-FPR2/ALX anti-inflammatory system." FASEB J..

[3] Variations to this protocol during the development of this model, including alterations to the duration of ischaemia are included in an *Additional methods* section (3.2) in chapter 4.

flow confirmed visually. 100 µl vehicle (vehicle 2 = LXA_4, 15-epi-LXA_4; vehicle 1 = all other treatments) or treatment was administered at the start of the reperfusion period. Animals were divided into 2 reperfusion period groups: 40 min or 2 h. Treatments included FPR2/ALX agonists: LXA_4, 15-epi-LXA_4 and $AnxA1_{Ac2-26}$; FPR antagonists: Boc2 and WRW4; and $AnxA1_{Ac2-26}$ in combination with antagonists: $AnxA1_{Ac2-26}$/Boc2 and $AnxA1_{Ac2-26}$/WRW4 (n=4-9 mice/group; see Table 4 for doses). A sham group was included (n=4 mice/group); these animals underwent the procedures described above (2.2.1.1), following which the CCAs were exposed only (not clamped). After 5 min, mice underwent a mock reperfusion period (of 40 min or 2 h).

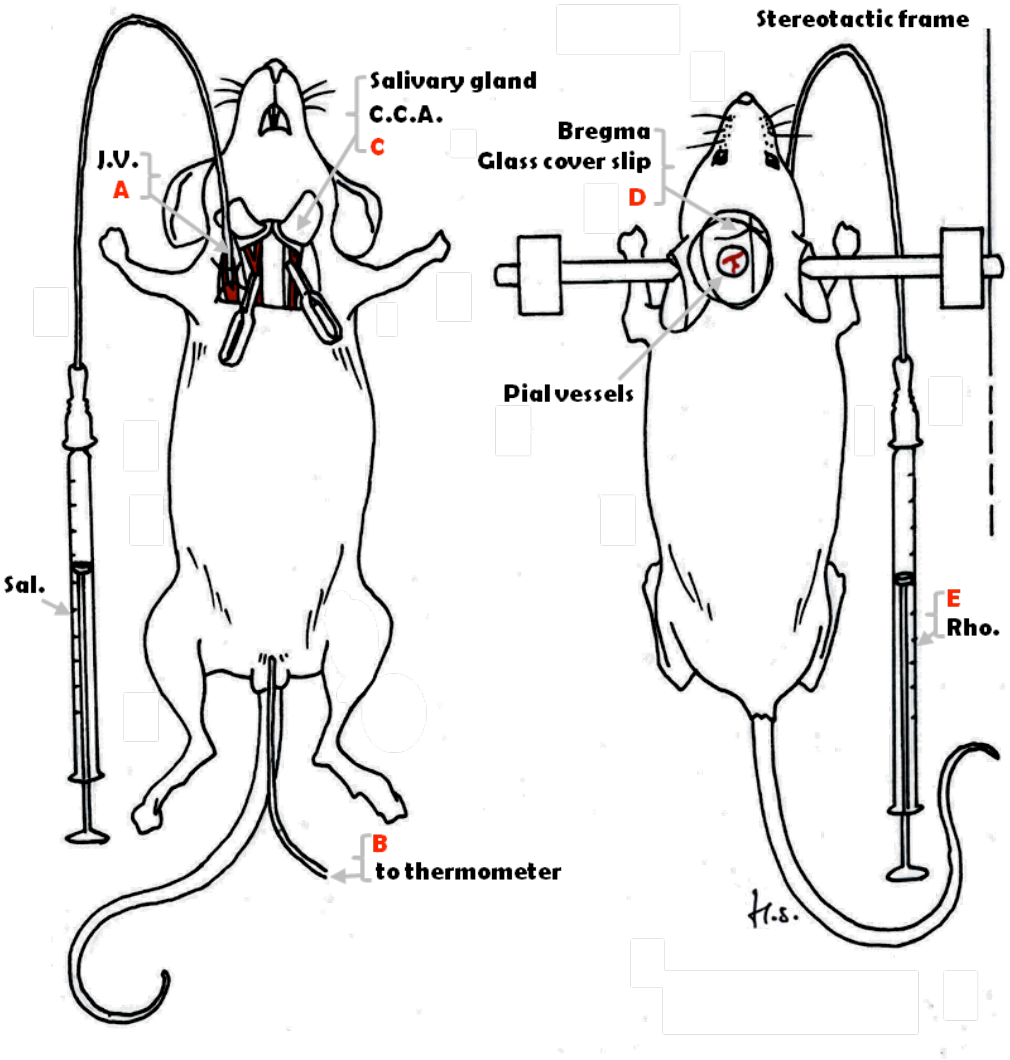

Figure 7. Animal preparation for observation of cerebral ischaemia/reperfusion; bilateral common carotid artery occlusion (Smith, unpublished). Under deep anaesthesia, the jugular vein was cannulated with a syringe initially containing saline (A), for future administration of treatments and dye. A rectal probe connected to a thermometer was inserted (B) in order that body temperature be maintained at 37 ± 0.5 °C using a heating mat (not shown). After exposure of the common carotid arteries, they were clipped using microvessel clips for 5 min (C). During the following reperfusion period, a small window was drilled through the skull of the animal (D), suffused with artificial cerebrospinal fluid and enclosed using a glass coverslip. The syringe was exchanged for one containing rhodamine 6G, 100 µl of which was administered 5 min prior to viewing under the intravital microscope (E). J.V., jugular vein; C.C.A., common carotid artery; B.P., blood pressure; Rho., Rhodamine 6G; Sal., saline.

Table 4. Doses of treatments given at the start of reperfusion following BCCAO.

	Treatment	µg or µl/100 µl saline	Concentration (µM)
Vehicles	Vehicle 1[a] (saline)	(9 g NaCl in 1 l dH_2O)	154k (0.9%w/v)
	Vehicle 2[b] (ethanol/saline)	17 µl ethanol in 83 µl saline	3.7
FPR2/ALX agonists	Ac2-26	100.0 µg	323.7
	15-epi-lipoxin A4	0.4 or 4.0 µg	11.3 or 113.5
	Lipoxin A4	0.1 or 1.0 µg	2.8 or 28.4
FPR2/ALX antagonists	Boc2	10.0 µg	127.2
	WRWWWW (WRW4)	55.0 µg	498.1
Ac2-26+ antagonists	Ac2-26/Boc2	100.0/10.0 µg	323.7/127.2
	Ac2-26/WRW4	100.0/55.0 µg	323.7/498.1

[a] Vehicle 1 corresponds to $AnxA1_{Ac2-26}$, Boc2 and WRW4.
[b] Vehicle 2 corresponds to 15-epi-lipoxin A4 and LipoxinA4.

2.2.2 Viewing leukocyte-endothelial interactions (using intravital microscopy)

2.2.2.1 Cranial window

Each mouse was set on a custom built stereotactic frame in a sphinx position, with the head gently secured in place. The left parietal bone was exposed through removal of local skin and underlying periosteum. A circular craniectomy was performed (diameter: 2-3 mm; centred approximately 3 mm from the coronal and sagittal sutures) using a high-speed micro drill; the scored circle of bone was removed using forceps, taking care not to disrupt the vasculature beneath (Figure 7D). The dura mater was left intact as fluorescently-labelled leukocytes in the pial microvasculature are visible through it. Artificial cerebrospinal fluid (aCSF; Na^+ 147.8 mEq/l, K^+ 3.0 mEq/l, Mg^{2+} 2.3 mEq/l, Ca^{2+} 2.3 mEq/l, Cl^- 135.2 mEq/l, HCO_3^- 19.6 mEq/l, $lactate^-$ 1.67 mEq/, phosphate 1.1 mM, and glucose 3.9 mM) at 37 °C was used to suffuse the tissue during this process. A 12 mm glass coverslip was placed over the exposed tissue and the area between the coverslip and tissue filled with aCSF. Mice were left to recover for 20 min before surgery.

2.2.2.2 Intravital fluorescence video microscopy

Mice were administered 100 µl rhodamine 6G (0.02 % in saline) intravenously 5 min prior to intravital microscopy (IVM); rhodamine 6G is a fluorescent dye selectively absorbed by leukocytes and allows them to be viewed using fluorescence. After 40 min or 2 h reperfusion, mice were transferred onto the viewing stage of an IVM microscope (Olympus 'BW61WI' microscope; water-immersion objective lens; magnification x 40; LUMPlan FI/IR). A 12 V, 100 W halogen light source through CY3 filter was used to observe the cerebral microcirculation through the cranial window. Time-lapse images were captured with a CoolSNAP HQ^2 black-and-white camera and recorded as a video by Slidebook 4.2 software.

2.2.2.3 Video analysis

3-5 randomly selected venular segments, 30-70 µm in diameter and with at least 100 µm of observable length, and one arteriole (in which L-E interactions were not seen) were filmed over 2 min for each mouse. Leukocyte rolling, rolling velocity and adhesion were assessed (Figure 8). Rolling leukocytes were defined as cells crossing a designated boundary within the 100 µm vessel length at a velocity discernibly slower than the central flow; these counts were represented as the number of rolling cells/mm^2 of the venular surface, over the analysed 2 min (i.e. cell

count/[diameter/1000]). Rolling velocity was calculated as the distance travelled by a rolling leukocyte/time in sec (expressed as µm/sec). Adherent leukocytes were defined as those remaining stationary within the vessel for 30≤ sec. As with the rolling cell counts these data were expressed as number of adherent cells/mm^2 as interpreted from vessel diameter, assuming a cylindrical shape (i.e. cell count/[(diameter x π x 100)/10^6]).

2.2.2.4 Plasma extravasation

Plasma extravasation in the post-capillary venules was measured. Fluroscein isothiocyanate (FITC)-labelled albumin (0.25 mg in 5 µl saline/g body weight; i.v.) was administered intravenously 5 min prior to recording. The fluorescence was switched on and 3-5 snapshots of vessels taken for each mouse. Visualization is obtained using block filter (excitation, 450–490 nm; emission, 525–620 nm). Albumin leakage was quantified by measuring mean fluorescence intensity with image analysis software (Image J). Three groups of three windows (approximately 5×5 µm) were created and positioned randomly in three regions relating to each vessel: one group was placed within the venule (Fl_{in}), another approximately 10 µm away from the vessel wall (Fl_{out}) and the remaining group on background. (This baseline measurement was made from a black background section of the image to represent an area where there is no leakage.) Mean intensity was calculated for each region and albumin leakage determined by [(Fl_{out}−baseline)/(Fl_{in}−baseline)]×100%.

2.2.2.5 Blood and tissue collection

Following methods in section 2.2.1, blood was taken by cardiac puncture through the diaphragm into the apex of the heart (26G x $^3/_8$" needle entering the left ventricle) into a heparinised 1 ml syringe (approximately 500-900 µl blood/mouse could be collected). After culling, brains were dissected out and snap frozen in liquid nitrogen. Blood was centrifuged at 4 °C, 7 700 g for 6 min to yield the plasma. Both samples were stored at -80 °C until required.

2.2.2.6 Statistical analysis

All values are expressed as mean ±SEM for all animals in each treatment group (n). Statistical analysis for IVM was conducted using either a student's *t* test (2 groups) or by ANOVA followed by Bonferroni (>2 groups). In all cases, $p<0.05$ was considered significant.

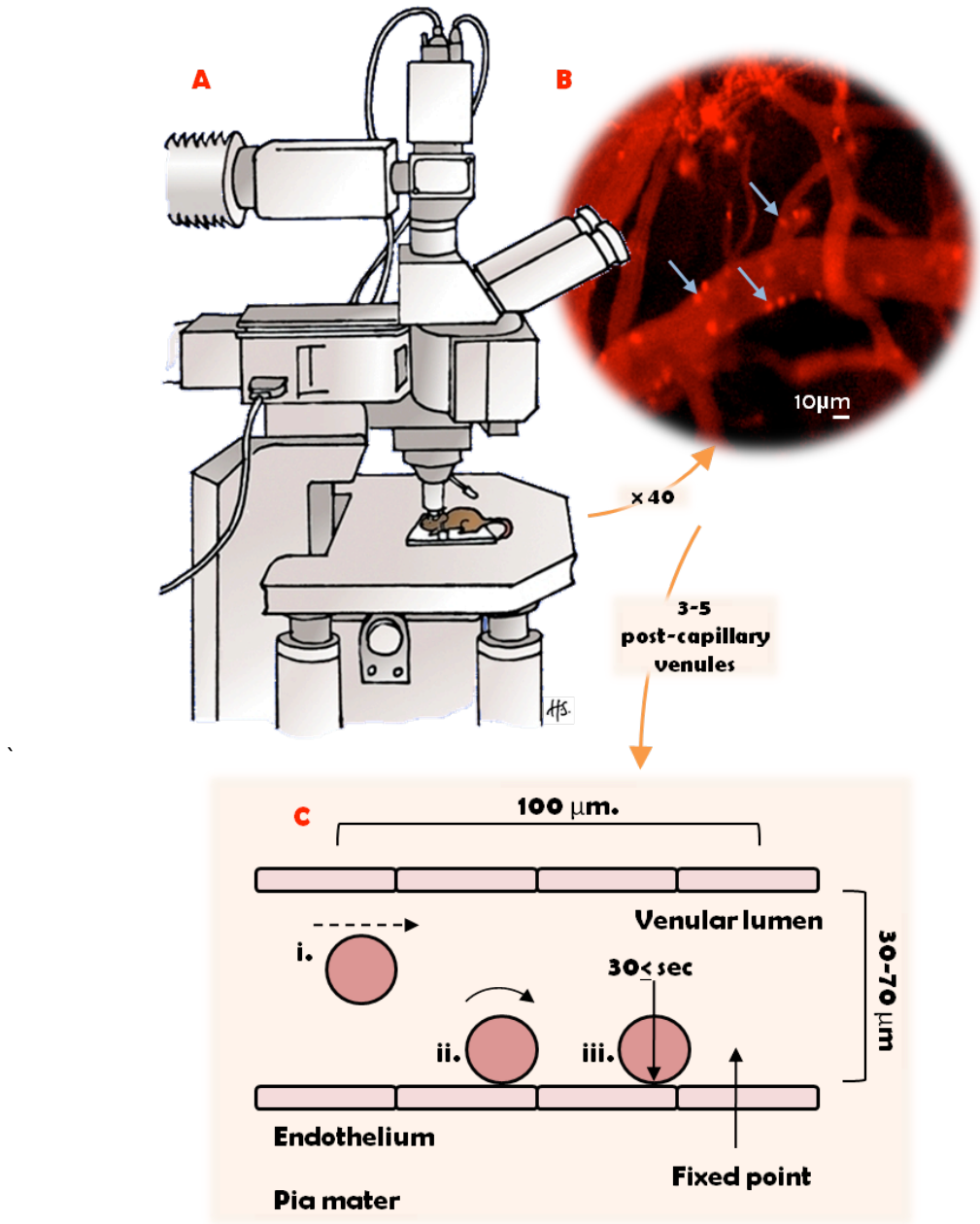

Figure 8. Intravital microscopy video analysis (Smith, unpublished). Using an intravital microscope (A), leukocytes were viewed following rhodamine 6G injection (B). Venular (3-5) segments were identified (length: 100µm; diameter: 30-70 µm) and leukocyte rolling, rolling velocity and adhesion were analysed over 2 min (C). Rolling cells (Cii.) were identified as those travelling at a velocity discernibly lower than those in the free-flowing circulation (Ci.), and were included on passing a fixed point. Rolling velocity = distance travelled / time taken (sec). Adherent cells were identified as those remaining stationary for 30< sec within the 100 µm section (Ciii.). Leukocytes=blue arrows (B) and circles (C).

2.2.3 Visualising neutrophil localisation (using magnetic resonance imaging)

2.2.3.1 Animal preparation

Experiments were performed using male C57BL/6 mice weighing 23-25 g. All animal procedures were carried out under licence and complied with Home Office regulations (Guidance on the Operation of Animals, Scientific Procedures Act, 1986). Mice were housed under conditions stated in section 2.2.1.1 and administered 10 mg/kg lipopolysaccharide (LPS; an inflammation-inducing bacterial fragment) or vehicle (saline) i.p., prior to imaging using a gadolinium (Gd)(III)-based contrast agent bonded to a peptide ligand for Fpr1 (cFLFLFK; Figure 9).

The following day, animals were anaesthetised using isoflurane (induced with 4.5% isoflurane; 2.5% O_2 and maintained under anaesthesia at 1-1.5% isoflurane; 1.5% O_2). The left jugular vein was cannulated for administration of contrast agent, using a 1.5 m length of PE-10 tubing in order that the agent could be administered from outside the MRI machine. The cannula itself (inside diameter 0.28 mm; length 1.5 m; total volume 370 µl) contained 50 µl saline at the end proximal to the mouse and, distally, 320 µl contrast agent (or Gd-DOTA control (Bousquet, Saini et al. 1988); a widely-used stable, untargeted contrast agent). Vetbond tissue adhesive was used to close the opening to reduce heat and fluid loss while mice were transferred to the MRI scanner.

Mice were placed in a stereotactic frame within a 72 mm, volume quadrature coil, with a rectal thermometer recording body temperature (maintained at 37 ± 1.0 °C) and a balloon pressure sensor below the chest to monitor respiration rate. Each of these parameters was recorded from a control room and anaesthesia adjusted according to fluctuations in the stability of each mouse.

2.2.3.2 Diffusion-weighted MRI using a gadolinium-linked contrast agent

Once animals were securely positioned, the coil was placed in the centre of the MRI machine. Wires recording vital signs and the cannula were threaded outside for access. A 9.4 tesla (9.4T) MRI machine was used, which produces a magnetic field strength able to provide appropriate resolution for imaging very small rodents. Baseline acquisitions of the whole body (7 slices, 6 averages over 1 min 30 sec), brain/head (12 slices, 6 averages over 4 min 23 sec) and abdomen (12 slices, 6 averages over 4 min 23 sec) were taken, 24 h after initial LPS injection. 1 mmol/kg contrast

agent was injected over 5 min, and subsequent acquisitions taken continuously post-injection, from the whole body, brain and abdomen in sequential rotation.

2.2.3.3 Tissue collection (for 2.2.3.2)

A 10 ml syringe containing saline was inserted into the left ventricle of the heart. A small cut was made in the right atrium and the mouse perfused with 10 ml saline, followed by 10 ml 4% PFA. The brain, lung (upper right lobe), spleen, liver (median lobe) and mesentery were removed. Samples were stored in 4% PFA at 4 °C overnight in bijou tubes then transferred into fresh tubes containing 30% sucrose. Once saturated, samples were embedded in mounting medium for cryotomy (optimum cutting temperature; OCT) and stored at -20 °C until required.

2.2.3.4 Analysis

Mice received either Gd-DOTA or Gd(III)-cFLFLFK contrast agent. Signal intensities for MRI were recorded using Image J software and relative contrast calculated where pre-injection intensity equals '0' and peak intensity equals '1'. In Figure 31 and Figure 32 means are calculated of intensities across all slices of the brain/head; error bars ±SEM in both groups.

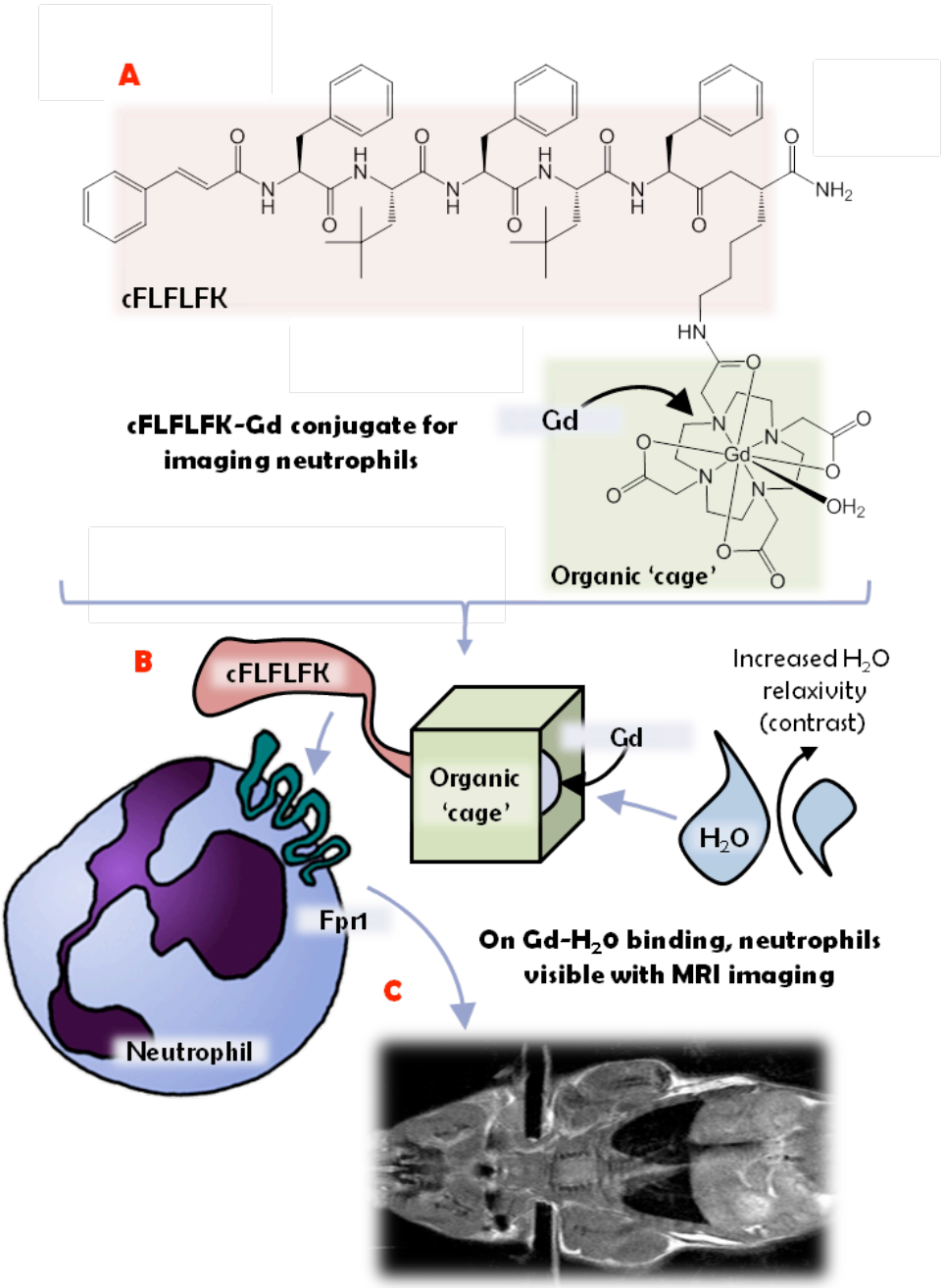

Figure 9. Using a Gd(III)-cFLFLFK conjugate contrast agent in visualising neutrophils with MRI. A Gd(III)-cFLFLFK conjugate (A) was used as a contrast agent in viewing neutrophil localisation following 10 mg/kg LPS in mice. Gd(III)-bound cFLFLFK binds to Fpr1 on neutrophils (B); Gd(III) increases H_2O relaxivity which as a result increases MRI contrast in regions of high neutrophil concentration (C). Figure 9A adapted from (Stasiuk, Smith et al. 2013); Figure 9B/C (Smith Unpublished).

2.3 Methods 2: *In vitro* tissue analyses following cerebral ischaemia/reperfusion

2.3.1 Mouse global stroke model

2.3.1.1 Plasma cytokine concentration (using bead array)

Blood was taken by cardiac puncture and stored (as described in 2.2.2.5). Samples from 4 treatment groups (n=3 mice/group; groups: sham, vehicle, $AnxA1_{Ac2\text{-}26}$ and 15-epi-LXA4; see Table 4 for doses) were defrosted on ice and levels of IL-6, IL-10, MCP-1, IFN-γ, TNF and IL-12p70 detected using a cytometric bead array kit. Cytokine concentrations were measured using a flow cytometer which calculated levels from a best-fit curve based on serial dilutions of standard solutions (n=10), then analysed using FCAP Array 3.0 software.

2.3.1.2 Leukocyte activation (using myeloperoxidase assay)

Whole brain samples from each condition were homogenised in 3 ml 0.5% hexadacyl trimethylammonium bromide (HTAB; in dH_2O). Homogenates were freeze-thawed twice to disrupt cells membranes, allowing detection of intracellular MPO. Samples were then centrifuged at 2500 g for 10 min and the protein concentration of the supernatants was measured using a NanoDrop (average of 2 measurements/sample; a 'blank' HTAB reading was recorded for a baseline measurement). Supernatants were transferred into a 96-well plate and 160 µl 0.004% tetramethylbenzidine (TMB; in dimethyl sulfoxide; DMSO) and 20 µl H_2O_2 to 20 µl was added to each. Plates were incubated for 60 min at room temperature after which an optical density reading was taken using a spectrophotometer at 450 nm.

2.3.1.3 Annexin A1 and phospho-ERK expression (using Western blots)

Whole brain samples were homogenised in 3 ml phosphate buffered saline (PBS)/proteinase inhibitor (1 tablet/10 ml PBS). Proteins were run on a NU-PAGE gel and transferred onto a nitrocellulose membrane. Primary antibodies for Anx1 (1:1000; raised in rabbit), ERK, phospho-ERK (p-ERK; both ERK and p-ERK antibodies 1:1000 and raised in rabbit) and β-actin (1:20 000; raised in mouse) were used with secondary antibodies anti-rabbit (1:30 000) and peroxidise horse anti-mouse (1:200; β-actin only). Antibodies were diluted in 5% bovine serum albumin (BSA) rather than 5% milk to prevent non-specific binding of milk phospho-proteins to the pERK antibody.

Antibodies were visualised using a chemiluminescence kit and signal intensity/volume recorded using Image J.

2.3.1.4 Statistical analysis

All values are expressed as mean ±SEM for all animals in each treatment group (n). Signal intensities were recorded using Image J software where applicable and statistical analysis was conducted using either a student's *t* test (2 groups) or by ANOVA followed by Bonferroni (>2 groups). Differences between groups in were determined by the Mann-Whitney test. In all cases, $p<0.05$ was considered significant.

2.3.2 Human blood samples

2.3.2.1 Obtaining human blood samples (control and post-stroke)

All work in this section (2.3.2) was carried out in line with the Declaration of Helsinki and received ethical approval from NHS Research Ethical Committee (Reference number: 2009, 04/Q0401/40). Verbal consent was obtained from healthy (no known chronic or acute illnesses) human volunteers for the collection of 20 ml whole blood. Blood was extracted into a syringe (containing 2 ml 1.5% ethylenediaminotetraacetic acid (EDTA) disodium salt dehydrate) via standard median cubital vein needle insertion. Samples were collected on a designated site at Hammersmith Hospital (Imperial College London) in accordance with standard operating procedures and used immediately. Verbal and written consent was obtained in order to obtain blood samples from human stroke patients, we collaborated with the 'BRAINs' trial at Charing Cross Hospital (Imperial College London). Patients were 18+ y old; had undergone radiological confirmation of stroke, and would have blood samples collected within 96 h stroke onset. 4ml of blood was collected using the Vacutainer system, sealed in a K2-EDTA tube and transported to Hammersmith Hospital in accordance with standard operating procedures for immediate use.

2.3.2.2 Blood separation

Human blood samples were added to equal quantities of Roswell Park Memorial Institute (RPMI) medium. 6 ml of the each mixture was centrifuged on a histopaque 1077 (top layer, 3 ml)/1119 (lower layer, 3 ml) gradient for 30 min (settings: 400 g; acceleration 6; brake 0; room temperature). Neutrophils and monocytes were removed from their respective layers and transferred to 15 ml falcon tubes (up to 6 ml total volume in RPMI/15ml tube). Tubes contents were increased to 12 ml with RPMI and centrifuged for 15min (400 g; acceleration 6; brake 0; room temperature). Supernatants were removed and pellets re-suspended in remaining solution. 7.5 ml cold ddH_2O was added to each tube to lyse cells, the resulting contents made isotonic by the addition of 2.5 ml/tube NaCl solution at 3.6% then centrifuged for 10 min (400 g; acceleration 6; brake 0; room temperature). Supernatants were removed and pellets resuspended in the remaining solution. 14 ml RPMI was added to each tube and samples were centrifuged again for 10 min (400 g; acceleration 6; brake 0; 400 g; room temperature). The supernatants were removed and cells counted on a haemocytometer using Turk's solution (10 µl cells/solution:90 µl Turk's),

then re-suspended at the desired concentrations[4] (5 x 10^6 monocytes/ml) in RPMI + 0.1% BSA +L-glutamine.

2.3.2.3 Assessing migratory properties of leukocytes (using chemotaxis assay)

Monocytes were treated with an FPR ligand ($AnxA1_{Ac2-26}$ or LXA_4; both 1 µM) or saline for 10 min 37^{o}C and 5% CO_2. A baseline (no treatment) control group was also included. Migratory properties of the cells following treatment were assessed using 96-well polycarbonate chemotaxis plates.

To prepare the assay, 28 µl of RPMI + 0.1% BSA + 1% L-glutamine + chemoattractant (MCP-1, 0.9 µM; fMLP, $1x10^{-5}$ µM) or vehicle (RPMI + 0.1% BSA) was added through reverse pipetting into each well. A porous membrane (pore diameter 5 µm; plate type 101-5) was placed over the plate and 25 µl of the pre-treated monocytes loaded onto the upper surface of the membrane, directly above each well. Assembled membranes/plates were incubated for 1.5 h at 37 ^{o}C and 5% CO_2 before being washed with 25 µl iced 1.5% EDTA disodium salt dehydrate/well and centrifuged for 5 min (400 g; acceleration 4; brake 4; 20 ^{o}C). The cellular contents of each well were counted using Turk's solution as described above (2.3.2.2).

2.3.2.4 Statistical analysis

All values are expressed as mean ±SEM for monocyte populations in each group (n), where groups are defined with respect to cell treatment, cell source (patients versus healthy volunteers) and chemoattractant used. Statistical analysis of emigrated cell counts was conducted using either a student's *t* test (2 groups) or by ANOVA followed by Bonferroni (>2 groups). In all cases, $p<0.05$ was considered significant.

[4] Cell concentration = no. cells x dilution factor x 10^4 = cells/ml
(Dilution factor: 10ul cells →90 µl Turk's = 1:10 = 10)

Chapter Three

Development and validation of global cerebral ischaemia/reperfusion model

3.1 Introduction

3.1.1 BCCAO model

The initial aim of this project was to develop a stroke model that would produce a post-ischaemic inflammatory response observable through intravital fluorescence video microscopy (IVM) of the exposed mouse cerebrum. BCCAO is not an exact replica of human stroke (see section 1.1.2.5); it is, however, relatively simple to execute. It provides a model of cerebral I/R which is able to be viewed using IVM—an excellent way of monitoring L-E interactions during inflammation—and may be used to demonstrate efficacy of anti-inflammatory agents. During the development of the model, changes to the protocol and mouse specifications were made to improve animal survival and consistency of outcomes. These are discussed below (*BCCAO model*) and in the following section (*Mouse specifications*; 0)[5], and results which defined the ultimate model used are described in the *Results* section (3.3) of this chapter.

3.1.1.1 Timeframe and practical hurdles

After gaining the appropriate personal and project licences for prospective experiments (3-4 months), the initial step in developing the model was learning relevant animal handling and surgery. This involved 'scruffing' mice, so that they could be given consistent, relatively painless i.p. injections; surgical procedures including cannulation of the jugular veins, BCCAO, drilling cranial windows and systemic perfusion through the heart as well as subsequent tissue collection; administration of anaesthetics, and use of the intravital microscope with a live animal. Learning these practical procedures took up to 3 months. During the subsequent 3-4 months, experiments were conducted (as described in this chapter) in order to determine the suitable anaesthetic, ischaemic and reperfusion periods, and mouse specifications—those below 20 g were far less resilient to surgery.

3.1.1.2 Duration of ischaemia and additional variations to protocol

Table 5 details technical aspects of several recent studies which involved BCCAO followed by reperfusion in various mouse strains. Database searches revealed Ishikawa and colleagues to be the only group to have used a protocol involving BCCAO-induced cerebral I/R, observed through a cranial window using IVM (Ishikawa, Cooper et al. 2003, Ishikawa, Sekizuka et al. 2007). Their

[5] *In vitro* data characterising further aspects of the model are described in subsequent results chapters 4 and 5.

method (1 h ischaemia followed by 40 min≤4 h reperfusion; see section 3.2.1.1 for further detail), including the use of silk threads as ligatures around the CCAs to produce ischaemia, was therefore used as a starting point. Following difficulties in producing a stable and consistent model using 1 h global ischaemia, various compensatory adaptations were made to the primary model, as well as alterations to ischaemic duration. For example, it was observed (and has been referred to elsewhere, see (Kittaka, Wang et al. 1996, Lavine, Hofman et al. 1998) that there is a build-up of mucus during long periods of I/R, which led to the temporary use of artificial ventilation via tracheotomies (see section 3.2.1.3). Finally, different anaesthetics were trialled in order to reduce mortality (see section 3.2.1.2) and to avoid potential neuroprotection from certain anaesthetics, such as previously observed isoflurane-induced neuroprotection in C57BL/6 mice (Zhou, Lekic et al. 2010, Gigante, Appelboom et al. 2011).

Table 5. Experimental mouse models of global cerebral ischaemia/reperfusion through BCCAO.

Model	Mice			Anaesthetic	Physiological Parameters			Duration of ischaemia	Reperfusion /IVM	Additional information
	Strain	Sex	Weight /age		Ventilation	MABP /Arterial blood gas	Body temp.			
1997 [1]	C57BL/6; see add. info.	M	21-27 g; 8-16 wks	Halothane (1.0%; 0.5%) open face mask	Spontaneous: open face mask (70% N_2O and 30% O_2)	Femoral A., PE 10 connected to pressure transducer /polygraph; Acid-base laboratory system (abl550; Radiometer); MAPB: 80.5 ± 5.3	Heating lamp 37.0-37.5˚C	5; 10; 15; 20 min	<40 d /No	Comparison with ICR, BALB/c, C3H, CBA, ddY and DBA/2 mice - C57BL/6 found most susceptible to BCCAO due to narrow PCoA /reduced collateral blood flow; greatest ischaemic damage after 20 min; 1 hr BCCAO in C57BL/6 caused 75% mortality.
1998 [2]	C57BL/6; CBA; DBA/2	M	22.5 ± 0.4; 21.8 ± 0.6; 22.8 ± 0.4 g; 8-16 wks	Halothane (2.0%; 0.5%) open face mask	Not stated	Femoral A., PE 10 connected to pressure transducer/polygraph	Heating lamp 36.0-37.5˚C	1; 5; 10; 15; 30 min	<2 d (5-30 min ischaemia); 7 d (1 - 15 min ischaemia) /No	Recommends assessment of intracranial vasculature using LDF over 1 min occlusion prior to surgery; 1 hr BCCAO in C57BL/6 caused 80% mortality.
1998 [3]	CD-1	M	35-40 g	C.H. (350 mg/kg) Xylazine, (4 mg/kg) i.p.	Controlled: Animal ventilator (Harvard), vol. 0.5 ml; rate 120 /min. 5 mins before BCCAO.	Femoral A.	Rectal probe: Blanket, heating pad, 37 ± 0.5˚C	3; 5; 10 min	24; 72h /No	Shows MABP increase of 10 mmHg during ischaemia; blood gas concentraions and mortality rate significantly improved with controlled ventilation.
2000 [4]	C57BL/6; SV129	M	8-10 wks	Halothane (3%; 1.0-1.5%; 0.5% in O_2), ventilation	Controlled: 20 gauge i.v. catheter, vol. 0.7 ml; rate 120 /min.	Femoral A., PE 10	Temporal subcutaneous needle thermistor: target 37˚C	10; 15; 20 min	3 d /No	Jugular V. cannulated for blood withdrawal; hypotension (30 ± 2 mmHg) increased CA1 neuronal death; time dependent increase in neuronal damage observed only in BCCAO + hypotension in C57/BL6.
2003 [5]	C57BL/6	M	21-25 g	α-chloralose (60 mg/kg) urethane (600 mg/kg), i.p. (lidocaine, L.A.)	Controlled (BCCAO period): Rodent ventilator (model 683, Harvard); Spontaneous: (reperfusion period): tracheotemised, PE 90.	Femoral A., PE 10	Not stated	60 min	40 min; 4 h /Yes	Femoral V. cannulated for administration of labelled platelets and rhodamine 6G; pancuronium (0.4 mg/kg) administered i.v. to assist breathing in some cases.
2005 [6]	C57BL/6	M	10-15 wks	Isoflurane (2%; 0.5-1%; 0% - during ischaemia in 70% N_2O and 30% O_2) face mask.	Spontaneous: face mask (see anaesthetic)	Femoral A., PE 10 connected to pressure transducer/polygraph	Rectal probe: heating lamp 37.6 ± 0.2˚C	20 min	<7 d /No	Increased O_2 concentration via open face mask. Neuronal loss demonstated following 20 min ischaemia.
2007 [7]	C57BL/6	M	21-25 g	α-chloralose (60 mg/kg) urethane (600 mg/kg), i.p. (lidocaine, L.A.)	Controlled (BCCAO period): Rodent ventilator (model 683, Harvard); Spontaneous: (reperfusion period): tracheotemised, PE 90	Femoral A., PE 10	Rectal probe: Overhead heat lamp, 37 ± 0.5˚C	30; 60 min	40 min; 4 h /Yes	Femoral V. cannulated for administration of labelled platelets and rhodamine 6G; >90% reduction in blood flow to observed brain tissue, as assessed by Laser Doppler Flowmetry; cranial window over frontal bone rather than parietal in BCCAO mice.

Models: [1] (Yang, Kitagawa et al. 1997); [2] (Kitagawa, Matsumoto et al. 1998); [3] (Murakami, Kondo et al. 1998); [4] (Wellons, Sheng et al. 2000) [5] (Ishikawa, Cooper et al. 2003); [6] (Murakami, Saito et al. 2005); [7] (Ishikawa, Sekizuka et al. 2007).

3.1.2 Mouse specifications

3.1.2.1 Strain

C57BL/6 mice were chosen for this project. Fpr2/3$^{-/-}$ and AnxA1$^{-/-}$ mice on a C57BL/6 background are already in existence (although non-commercially available), making this strain preferable should the work be extended.

Based on published data, C57BL/6 mice are also ideal for a complete and consistent model of global cerebral ischaemia. They have substantially smaller cross-sectional diameters of the posterior communicating artery and less collateral circulation than other strains, which would supply the brain with blood during occlusion of the CCAs (Connolly, Winfree et al. 1996, Yang, Kitagawa et al. 1997, Kitagawa, Matsumoto et al. 1998). In addition, these mice show greatest neuronal damage after an ischaemic insult when compared with ICR, BALB/c, C3H, CBA, ddY, DBA/2 (Yang, Kitagawa et al. 1997) and SV129 (Wellons, Sheng et al. 2000) strains.

3.1.2.2 Weight

In preliminary experiments, mice weighing under 19 g did not survive an ischaemic period longer than 20 min. As mice larger than 30 g will have more patent collateral afferent brain circulation (Connolly, Winfree et al. 1996), we used mice weighing between 23-28 g.

3.1.2.3 Sex

Male mice only were used so that hormonal changes during the oestrous cycle did not influence results.

3.2 Additional methods

3.2.1 Variations in BCCAO protocol

While developing the model described in *Methods* section 2.2.1, various earlier methods were trialled before arriving at the protocol which produced low mortality and consistent inflammatory responses. These methods are described in this section (*Additional methods*).

3.2.1.1 Variations in method of vessel occlusion and duration of ischaemia

Mice were anaesthetised and prepared for surgery as described previously (see section 2.2.1.1). To perform BCCAO, CCAs were exposed fully so that forceps could be slipped underneath. A silk thread was passed underneath a CCA and tied in a loose knot and the same carried out on the other side, before tightening threads around the vessels. After ischaemic periods of 5, 8, 10, 15, 30, 45 min or 1 h, knots were released and the resumption of blood flow assessed visually for 40 min reperfusion initially. A longer reperfusion period of 4 h was also used; following a 0% survival rate for 4 h (n=4), the maximum reperfusion period was reduced to 2 h. The use of ligatures was ultimately replaced with use of microvessel clips.

3.2.1.2 Anaesthetic

Animals were initially anaesthetised with an i.p. injection of ketamine (150 mg/kg) and xylazine (7.5 mg/kg) as this combination had provided deep and adequate anaesthesia in previous work by our group. Pentobarbital sodium (100 mg/kg) was used in later experiments as this seemed to avoid respiratory suppression observed during BCCAO under ketamine/xylazine anaesthesia.

3.2.1.3 Tracheotomy

Mice were tracheotomised with a PE-90 catheter attached to a rodent ventilator set to tidal volume 0.7 ml and breathing rate 120/min (Wellons, Sheng et al. 2000). Sternohyoideus and sternothyroidius muscles were separated with care not to put pressure on the trachea or cause tissue damage. The trachea was exposed and a doubled silk thread passed underneath. Two loose knots were created and a small incision was made between them. The rostral knot was tightened and the catheter passed into the incision, then secured with the caudal knot.

3.3 Results

3.3.1 Five minutes ischaemia generates a significant inflammatory response

Mice were subjected to 5, 8, 10, 15, 30, 45 min or 1 h cerebral ischaemia through BCCAO. After 40 min or 2 h reperfusion, mice were placed under an IVM microscope for viewing of the L-E interactions in the cerebral microvasculature.

Pentobarbital sodium was the chosen anaesthetic as administration achieved a long-lasting, deep anaesthesia (rare need for administrations subsequent to initial dose) with a low mortality rate which ascribed to the 'Three Rs' (reduce, refine and replace in animal experimentation). The use of a tracheotomy was abandoned after the ischaemic duration was reduced below 30 min, as the intervention no-longer had an effect on mortality (mucus production was not as extensive). For the production of BCCAO, knotted silk threads around CCAs were replaced with microvessel clips, as these provided a more consistent occlusion pressure on the vessels, and could be removed swiftly and relatively simultaneously.

Having initially used 1 h of ischaemia based on previous literature (Ishikawa, Cooper et al. 2003, Ishikawa, Sekizuka et al. 2007), the period was gradually reduced due to mortality or lack of blood flow visible through the microscope. This progression is represented in Table 6.

Ample blood flow could be seen with both 5 and 8 min of ischaemia at 40 min reperfusion. Despite this, highly variable susceptibility to ischaemia after 8 min (number of rolling leukocytes/mm^2 ranged from 13-987), or a lack of leukocyte activity, meant that the 8 min ischaemic group did not have significantly more L-E interactions than sham operated animals (Figure 10). Having established 5 min as optimal in providing consistent inflammation after 40 min (Figure 10A/C; $p<0.05$; n=7 mice/group; 5-fold increase in adhesion versus sham group), the reperfusion period was extended to 2 h to enable the production of temporally varied data from future treatment groups (n=4 mice/group). No significant change in leukocyte rolling velocity was seen after either ischaemic period (Figure 10B) at 40 min, but velocity was significantly reduced at 2 h ($p<0.05$). In addition, at 2 h leukocyte adhesion was significantly increased versus 40 min as well as 15-fold versus sham groups (Figure 10C; $p<0.05$).

Table 6. Development of global cerebral ischaemia/reperfusion model.

Mouse n =	Survival (%)	Conditions			Blood flow
		Anaesthetic (mg/kg)	Ischaemia (min)	Tracheotomy	
2	0	K 150/X 7.5	60	✗	-
5	0	K 150/X 7.5	60	✓	-
6	67	P 50	60	✓	✗
2	50	P 50	30	✓	✗
2	50	P 100	30	✓	✗
2	50	P 100	20	✗	✗
2	100	P 100	10	✗	✓/✗
7	86	P 100	5	✗	✓
9	89	P 100	8	✗	✓

Arrow denotes time/order of experiments. Both survival and good blood flow were required. K = ketamine; X = xylazine; P = pentobarbital sodium.

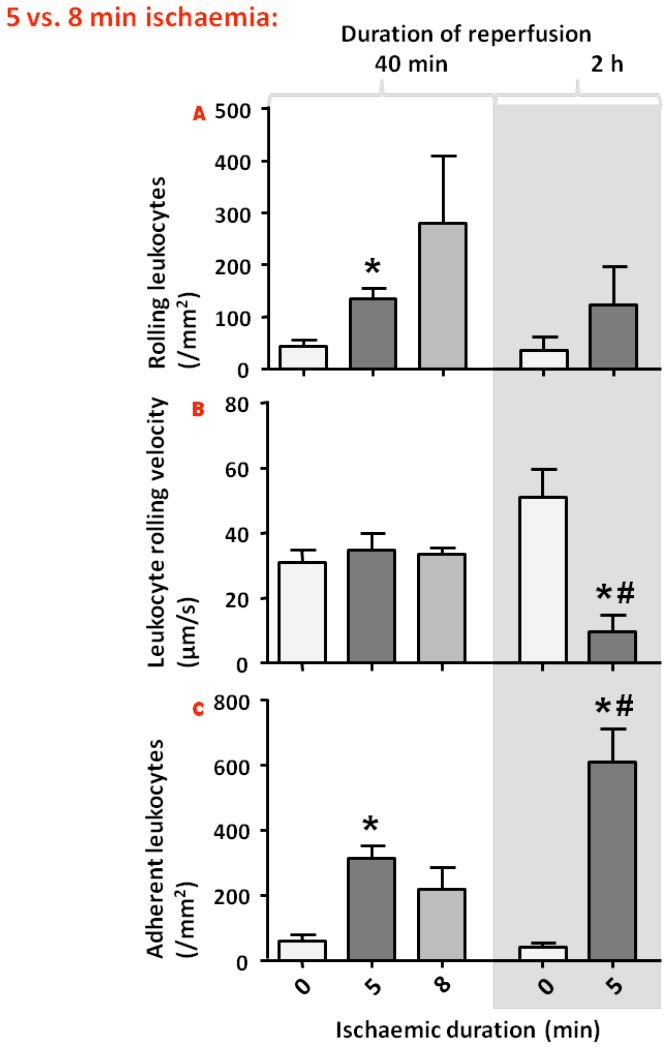

Figure 10. Different ischaemia/reperfusion durations effect leukocyte-endothelial (L-E) interactions in the cerebral microvasculature of C57BL/6 mice. Animals were subjected to BCCAO for 5 min (n=7, 40 min reperfusion; n=4, 2 h reperfusion mice/group) or 8 min (n=9 mice/group). In sham-operated animals (0 min ischaemia; n=4 mice/group), CCAs were exposed but not occluded. After 40 min/2 h reperfusion, L-E interactions were analysed over 2 min: the number of rolling leukocytes (A), the rolling cell velocity (B) and the number of adherent leukocytes (C) were counted over 100 µm vessel, and rolling and adherent cells expressed as number/mm^2. Data are mean ±SEM; p<0.05 vs. *sham or $^{\#}$0, 5 and 8 min ischaemia (all 40 min reperfusion) by unpaired *t* test.

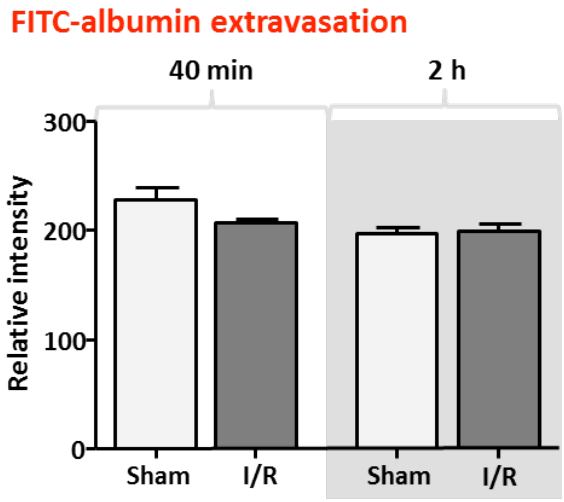

Figure 11. No albumin leakage observed following ischaemia/reperfusion (I/R) at 40 min or 2 h. Albumin leakage was measured using images of FITC-labelled albumin where fluorescence intensity was calculated as intensity inside vs. outside each vessel (n=3 mice/group; 3-5 vessels/mouse). In both sham-operated and I/R groups, fluorescently-labelled albumin remained largely intravascular indicating BBB integrity at these time points.

3.3.2 Alterations in the cerebral microvasculature following five minutes ischaemia and 40 minutes/two hours reperfusion

Cerebral I/R in this model generated an inflammatory response in which leukocytes roll and adhere to luminal (venular) blood vessel walls. This could be viewed using IVM following i.v. injection of rhodamine 6G to label the leukocytes. Leukocyte rolling, rolling velocity and adhesion were visualised then quantified as illustrated by Figure 12. With respect to sham-operated groups, cerebral I/R in mice produced discernibly more L-E interactions (as shown in representative images in Figure 13A/B). When quantified, there was significantly more cell rolling and adhesion in mice treated with vehicle (saline or saline plus ethanol), 40 min and 2 h into reperfusion compared with sham groups (see previous section 3.3.1).

Post-capillary venule leakage was assessed using intravenous FITC-labelled albumin to assess BBB integrity (fluorescently-labelled albumin would remain intraluminal under healthy conditions, but 'leak' into the parenchyma if the BBB junctions are sufficiently compromised). In sham and I/R groups, labelled albumin remained largely intraluminal (Figure 13C/D). This indicates preservation of BBB integrity at the time points observed.

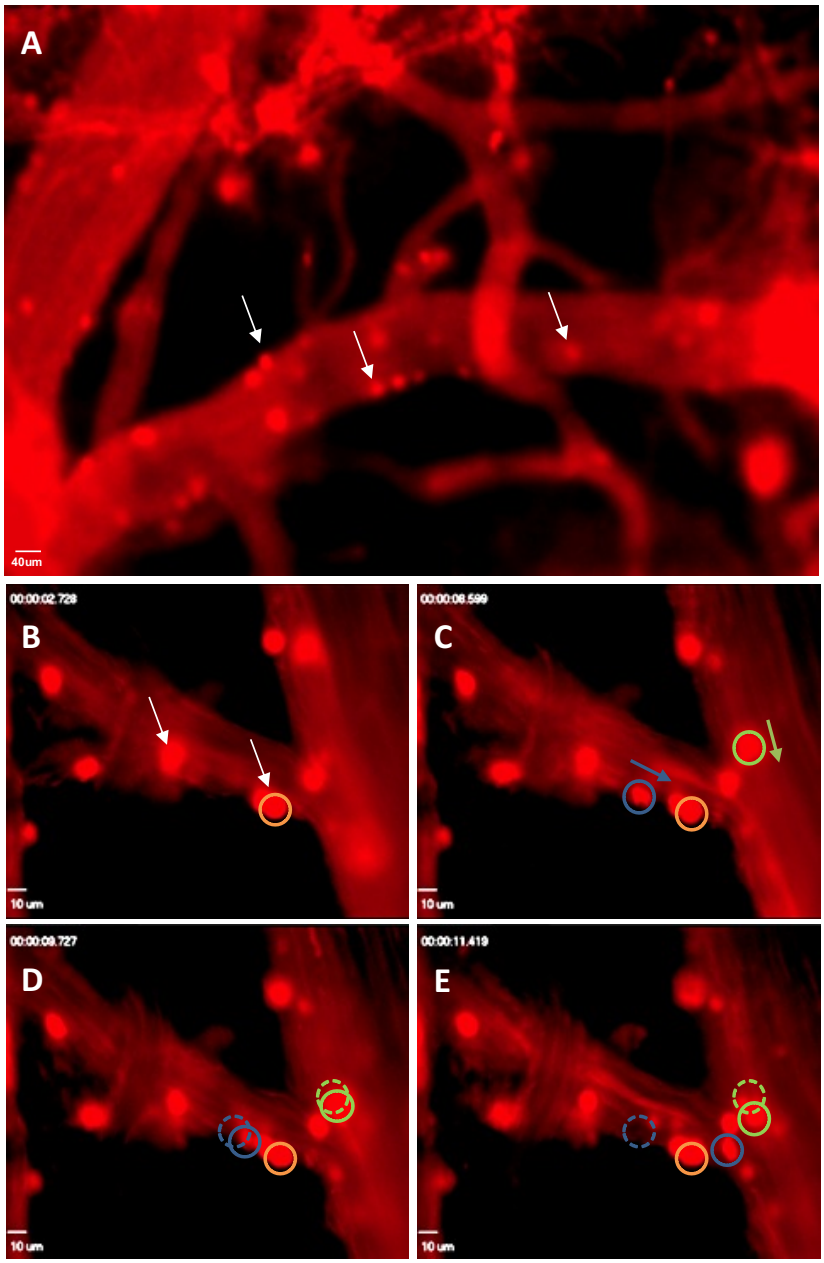

Figure 12. Leukocyte rolling and adhesion in the cerebral microcirculation following ischaemia/reperfusion (I/R). Leukocyte-endothelial interactions in the cerebral microvasculature could be seen following cerebral I/R (A). Leukocyte rolling and adhesion could be observed; B-E show video snapshots of the same vasculature over approximately 9 sec. Blue and green circles outline two different rolling cells as they are captured on the endothelial wall at 8.6 seconds (adjacent to arrows) (C) then continue to roll (dashed circles indicate location of initial capture) (D/E) in direction of blood flow (blue/green arrows). Orange circles outline an adherent cell (remains stationary throughout); white arrows = leukocytes; scale bars = 40 µm (A), 10 µm (B-E).

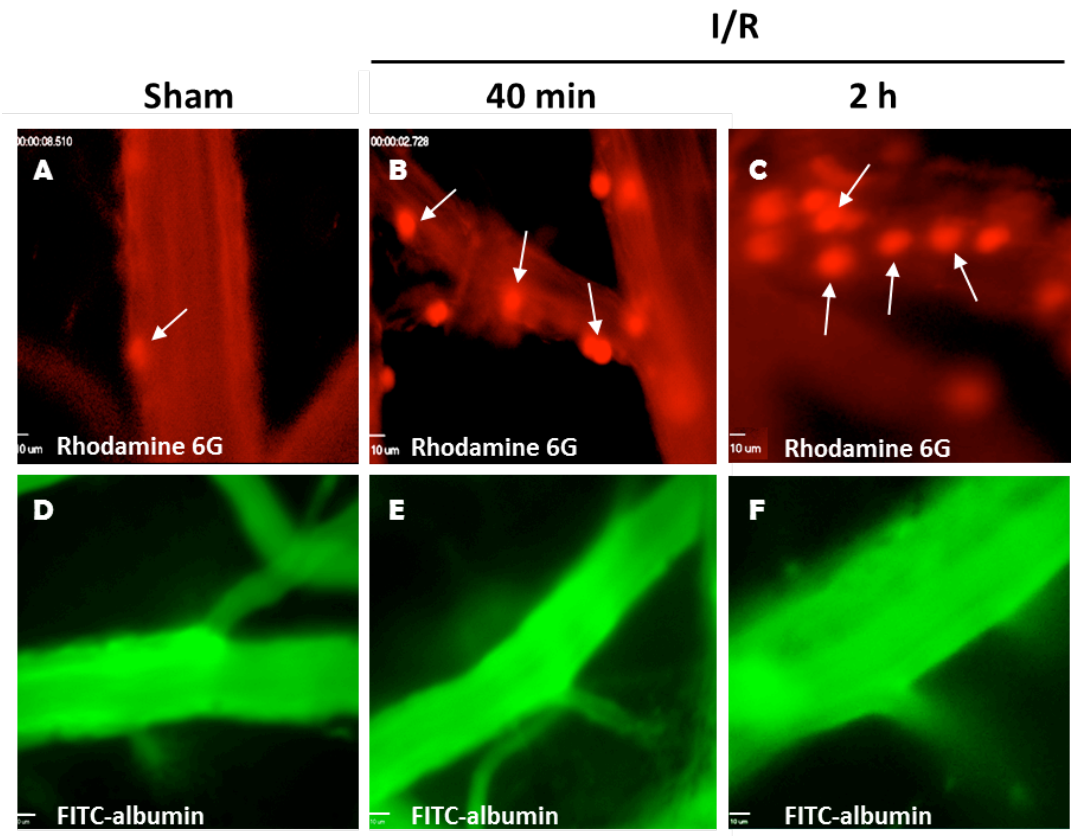

Figure 13. Cellular changes in the cerebral microcirculation following ischaemia/reperfusion (I/R). Representative images from a sham group (A, D) and I/R groups (5 min ischaemia/40 min or 2 h reperfusion) (B, C, E, F). In sham-operated mice, few or no rolling or adherent leukocytes (white arrows) could be seen interacting with the walls of the post-capillary venules using intravital microscopy (A). After I/R, leukocyte rolling and adhesion could be observed (B, C). Albumin leakage was also measured using images of FITC-albumin. In both sham-operated (D) and I/R (E, F) groups, fluorescently-labelled albumin remained largely intravascular (calculated by fluorescence intensity inside vs. outside vessel). All scale bars = 10 µm.

3.4 Conclusions

IVM was used to observe real-time L-E interactions in the pial microvasculature in a mouse model of stroke. The aim was to develop a model of global cerebral I/R which would produce an inflammatory response of consistent magnitude (with respect to numbers of rolling and adherent leukocytes) within each treatment group, and low mortality.

The model, once established, involved male C57BL/6 mice (23-28 g), anaesthetised with 100 mg/kg pentobarbital sodium and subjected to 5 min BCCAO-induced ischaemia using microvessel clips. This was followed by a 40 min or 2 h reperfusion period, which produced an IVM-visible inflammatory response up to 15-fold the magnitude of sham groups. Once developed and validated, this procedure was used to assess the effects of FPR ligands, administered at the start of reperfusion, as described in the next chapter.

Chapter Four

Effects of Formyl Peptide Receptor agonists in global cerebral ischaemia/reperfusion

4.1 Introduction

The model developed in the previous chapter provided parameters with which to assess inflammation-associated cellular and physiological responses to FPR agonists in the cerebral microvasculature following I/R. The following data describe variations in L-E interactions following cerebral I/R, primarily in response to administration of pan-FPR agonist $AnxA1_{Ac2\text{-}26}$ or FPR2/ALX agonist 15-epi-LXA_4 at the start of reperfusion.

Agonists were administered at the start of reperfusion: The receptor for LXA_4 and its epimer, 15-epi-LXA_4 (see section 1.3.2.2) has been well characterised as FPR2/ALX (mouse orthologue Fpr2/3). $AnxA1_{Ac2\text{-}26}$ is an *N*-terminal peptide of AnxA1 and has been shown to mimic the activity of the full-length protein through all members of the FPR family (see section 1.3.2.1). LXA_4, 15-epi-LXA_4 and $AnxA1_{Ac2\text{-}26}$ were therefore used to indicate pharmacological potential of Fpr2/3 mechanisms in this model of global cerebral I/R. Doses were chosen based on previously published data in which the ligands showed anti-inflammatory effects (Gavins, Dalli et al. 2007, Dufton and Perretti 2010).

Leukocyte rolling, rolling velocity and adherence were assessed in response to treatment with these agonists, as quantification of inflammation *in vivo*. Cytokines previously identified as involved in the pathogenesis of stroke were assayed using a bead array kit for mouse inflammatory cytokines ((Legos, Whitmore et al. 2000, Liesz, Hagmann et al. 2009). In addition, an MPO assay and Western blot expression analysis for proteins involved in the FPR mechanism were all carried out to characterise further the model and effects of treatments in the model. Results from these experiments are described in this chapter.

4.2 Results

4.2.1 AnxA1$_{Ac2-26}$ reduces leukocyte adhesion in cerebral microvasculature

4.2.1.1 Temporal variation (increased anti-inflammation at 2 h reperfusion)

BCCAO and reperfusion (I/R) plus treatment with vehicle (100 µl saline) cause increased L-E interactions versus sham-operated animals (Figure 14A/C). Treatment of mice with AnxA1$_{Ac2-26}$ (100 µg, 100 µl saline/mouse) reduced I/R-associated inflammation: there were significantly fewer cells adhered to the endothelia at 40 min reperfusion versus vehicle (100 µl saline/mouse) treatment groups (p<0.05; Figure 14C), although neither cell rolling nor rolling velocity was significantly altered. At 2 h of reperfusion, treatment with AnxA1$_{Ac2-26}$ reduced inflammation to sham levels; both rolling and adhesion were significantly lower (p<0.05; Figure 14A/C) and rolling velocity increased with respect to vehicle-treated mice (not significant; Figure 14B).

4.2.1.2 AnxA1 expression increased following AnxA1$_{Ac2-26}$ treatment

Western blots in Figure 15 show that I/R plus AnxA1$_{Ac2-26}$ (and to a lesser extent 15-epi-LXA$_4$; see section 4.2.2.3) treatment caused increased expression of endogenous cleaved AnxA1 (33 kDa) versus I/R plus vehicle groups (n=3 mice/all groups). This trend was not significant, but demonstrable at both 40 min and 2 h into reperfusion.

As evidence has indicated phosphorylation of ERK as a possible mechanism of action for FPR2/ALX activity (Hayhoe, Kamal et al. 2006), percentage p-ERK of total ERK was assessed in cerebral I/R brain samples. In contrast to earlier data, both AnxA1$_{Ac2-26}$ and 15-epi-LXA$_4$ treatment groups showed 5-10% decreases in the percentage p-ERK at 2 h reperfusion (not significant), but AnxA1$_{Ac2-26}$ produced no differences at 40 min.

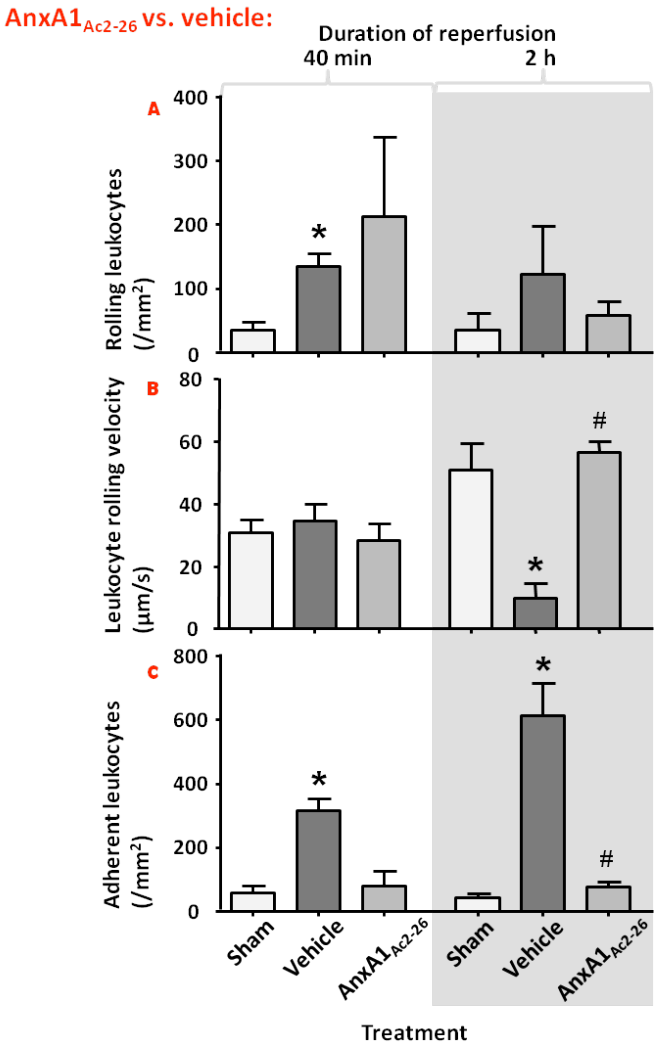

Figure 14. AnxA1$_{Ac2-26}$ inhibits leukocyte-endothelial (L-E) interactions in cerebral ischaemia/reperfusion (I/R)-induced inflammation. After 5 min BCCAO, mice were administered i.v. vehicle (100 µl saline/mouse) or AnxA1$_{Ac2-26}$ (100 µg/mouse) at the start of reperfusion. A sham-operated group (no I/R) was included. After 40 min or 2 h reperfusion, L-E interactions were analysed over 2 min: the number of rolling leukocytes (A), the rolling cell velocity (B) and the number of adherent leukocytes (C) were counted over 100 µm vessel, and rolling and adherent cells expressed as number/mm^2. Data are mean ±SEM; *p<0.05 vs. sham, $^{\#}p$<0.05 vs. vehicle by unpaired t test; n=4-7 mice/group.

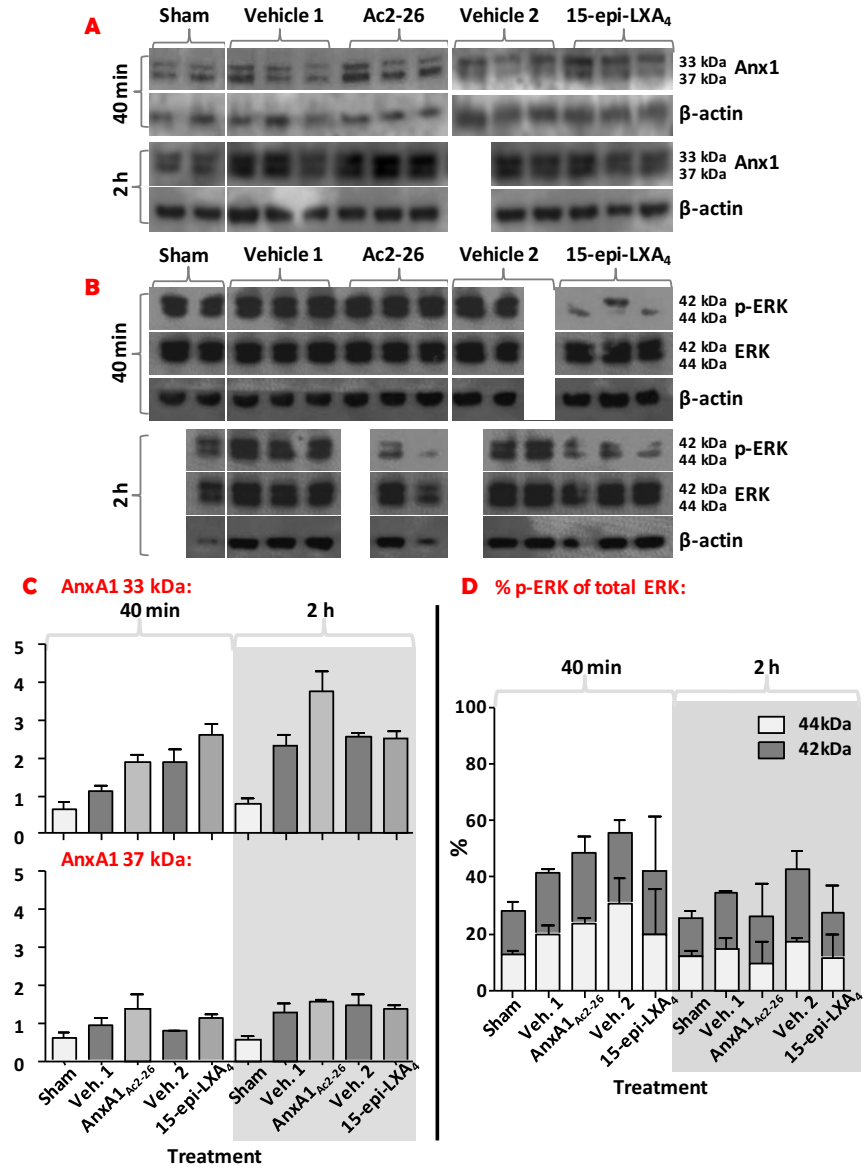

Figure 15. AnxA1 expression is increased after 5 min ischaemia/40 min or 2h reperfusion (I/R). Western blots of whole brain homogenates show a trend towards increased mobilisation of AnxA1 (A) through an increase in expression of AnxA1 (most notably the cleaved form; 33 kDa) following I/R and more so after I/R plus $AnxA1_{Ac2\text{-}26}$ treatment (100 µg/mouse) (C). There is a small increase in AnxA1 expression following 15-epi-LXA_4 treatment (0.5 µg/mouse) at 2 h, although this is not significant. Blots for p-ERK/ERK (B) show a trend towards decreased percentage p-ERK of total ERK in the 15-epi-LXA_4 group at 2 h vs. veh. 2 treatment (D), although no changes were significant. n=3 mice/group; value for each mouse = mean of triplicate experiments; veh. 1 = $AnxA1_{Ac2\text{-}26}$ vehicle, 100 µl saline/mouse; veh. 2 = 15-epi-LXA_4 vehicle, 100 µl saline+ethanol/mouse.

4.2.2 15-epi-lipoxin A4 reduces leukocyte-endothelial interactions in cerebral microvasculature

4.2.2.1 15-epi-lipoxin A4 but not lipoxin A4 reduces leukocyte-endothelial interactions

Initial experiments were conducted using the 40 min reperfusion end point. Treatment of mice with 15-epi-LXA_4 (both 0.5 and 4.0 µg; 100 µl saline plus ethanol) reduced the inflammatory response associated with I/R: both number of rolling cells and adherent cells/mm^2 endothelium were significantly reduced to levels comparable with those seen in sham-operated animals (p<0.05; Figure 16A/C). In addition, leukocyte rolling velocity significantly increased compared with vehicle (100 µl saline plus ethanol)-treated mice (p<0.05; Figure 16B). LXA_4 treatment (0.1 and 1.0 µg; 100 µl saline plus ethanol) had no effect on L-E interactions at either concentration.

4.2.2.2 Temporal and dose-dependent variation (increased anti-inflammation at 40 min reperfusion versus 2 h with low dose 15-epi-lipoxin A4)

Subsequent experiments used 15-epi-LXA_4 treatment only over the extended, 2 h reperfusion. At 2 h, only the higher dose 15-epi-LXA_4 (4.0 µg) was able to sustain anti-inflammatory effects seen at 40 min reperfusion. In higher dose animals, numbers of both rolling and adherent cells were significantly reduced at 2 h (p<0.05; Figure 17A/C) (and rolling velocity significantly increased compared with vehicle-treated mice at 40 min; p<0.05; Figure 17B). This reduction was not sustained to the same extent at 2 h reperfusion in the lower dose 15-epi-LXA_4 (0.5 µg) group: adhesion was reduced, but not with significance. An additional data set shows that a reduction in the number of rolling cells is redeemed if 15-epi-LXA_4 is administered closer to the 2 h endpoint rather than at the beginning (at 40 min reperfusion; Figure 17A/C white dashed box), although vehicle treatment itself administered at this time point also reduced L-E interactions to some extent.

4.2.2.3 Increase in AnxA1 expression following high dose 15-epi-lipoxin A4 treatment at 40 min reperfusion

Western blots in Figure 15 show that I/R plus 15-epi-LXA_4 treatment (4.0 µg; no data for 0.5 µg) caused an increase in expression of endogenous cleaved AnxA1 (33 kDa) versus I/R plus vehicle groups (n=3 mice/all groups). This trend was not significant, and occurred only at 40 min reperfusion. 15-epi-LXA_4 treatment groups showed a very slight decreasing trend in the percentage p-ERK of total ERK at 40 min and (as with $AnxA1_{Ac2\text{-}26}$) at 2 h (Figure 15).

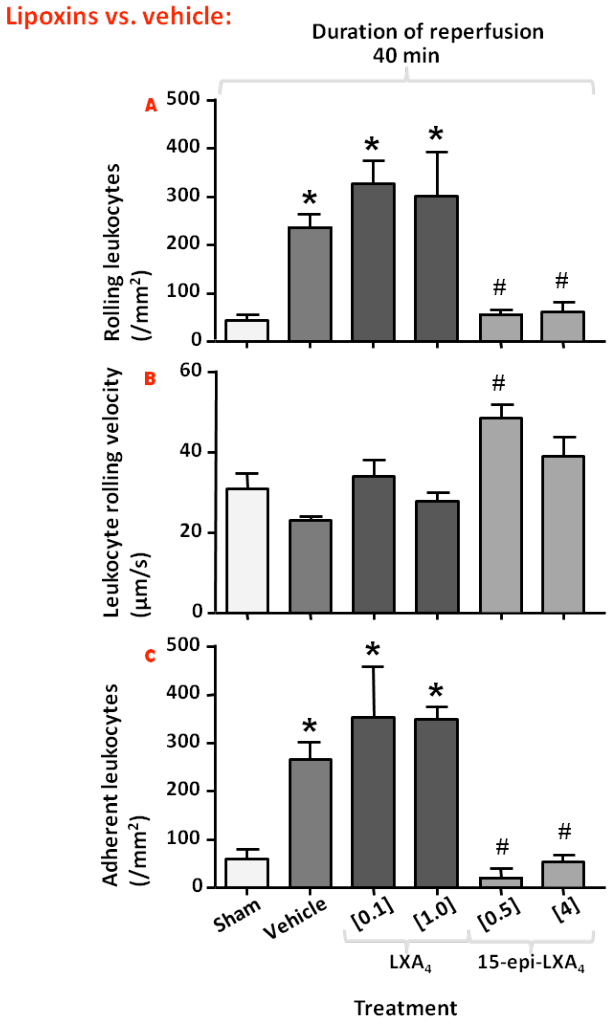

Figure 16. 15-epi-LXA_4 but not LXA_4 inhibits leukocyte-endothelial (L-E) interactions in cerebral ischaemia/reperfusion (I/R)-induced inflammation at 40 min reperfusion. After 5 min BCCAO, mice were administered i.v. LXA_4 (0.1 or 1.0 µg/mouse), 15-epi-LXA_4 (0.5 or 4.0 µg/mouse) or vehicle (100 µl saline+ ethanol/mouse) at the start of reperfusion. A sham-operated (no I/R) group was included. After 40 min or 2 h, L-E interactions were analysed over 2 min: the number of rolling leukocytes (A), the rolling cell velocity (B) and the number of adherent leukocytes (C) were counted over 100 µm vessel, and rolling and adherent cells expressed as number/mm^2. Data are mean ±SEM; *p<0.05 vs. sham, $^{\#}p$<0.05 vs. vehicle by unpaired t test; n=4-6 mice/group.

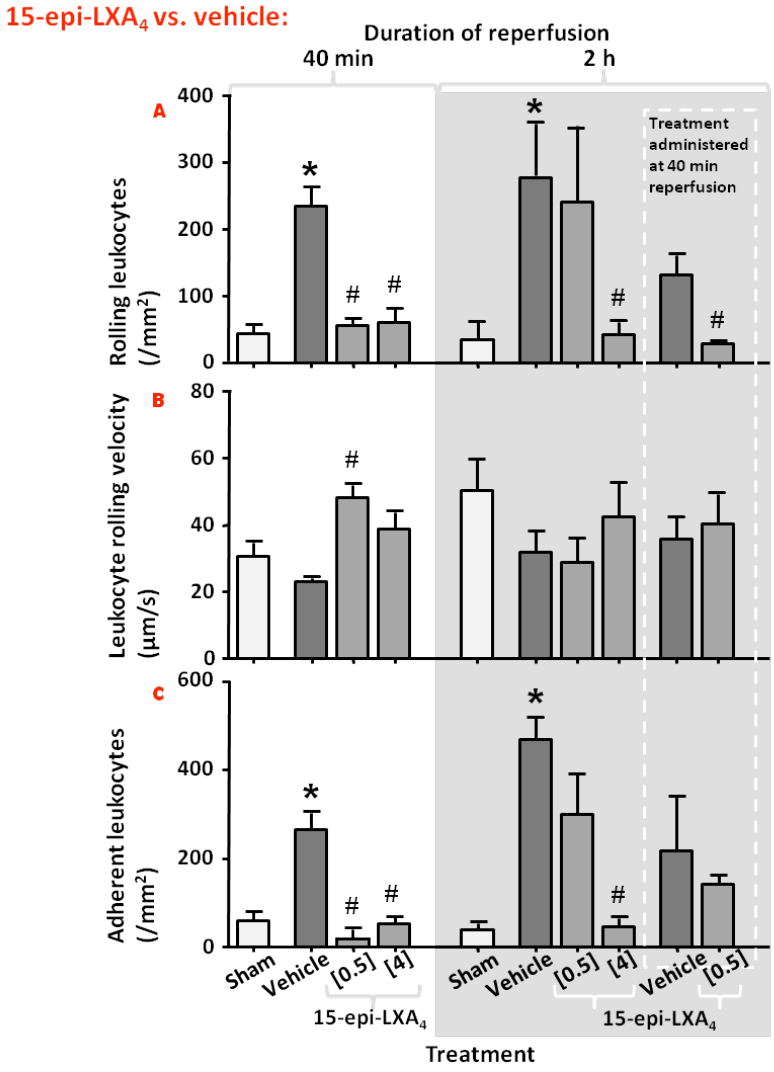

Figure 17. 15-epi-LXA_4 inhibits leukocyte-endothelial (L-E) interactions in cerebral ischaemia/reperfusion-induced inflammation. After 5 min BCCAO, mice were administered i.v. vehicle (100 µl saline+ethanol/mouse) or 15-epi- LXA_4 (0.5 or 4.0 µg/mouse) at the start of reperfusion. A sham-operated group (no I/R) was included. After 40 min or 2 h, L-E interactions were analysed over 2 min: the number of rolling leukocytes (A), the rolling cell velocity (B) and the number of adherent leukocytes (C) were counted over 100 µm vessel, and rolling and adherent cells expressed as number/mm^2. Data are mean ±SEM; *p<0.05 vs. sham, $^{\#}p$<0.05 vs. vehicle by unpaired t test; n=4-6 mice/group.

4.2.3 Changes in cytokine expression and tissue oxidation following global cerebral ischaemia/reperfusion

4.2.3.1 Increase in MCP-1 expression following AnxA1$_{Ac2-26}$ treatment

To characterise anti-inflammatory effects following treatments with FPR2/ALX ligands, serum levels of pro- and anti-inflammatory cytokines were measured using a mouse inflammation cytometric bead array kit. Levels of IFNγ and IL-12p70 were below those accurately detectable by the kit (including for LPS positive control); Figure 18 therefore shows expression of TNF, MCP-1, IL-6 and IL-10 only. MCP-1 is increased in vehicle treatment groups, at 40 min and even more so with vehicle 1 (saline) at 2 h. AnxA1$_{Ac2-26}$ but not 15-epi-LXA$_4$ increased MCP-1 levels 3 times above vehicle treatment at 2 h.

Vehicle 1 increases IL-6 expression at 40 min and 2 h, whereas AnxA1$_{Ac2-26}$ has lower levels at 40 min and extremely high levels at 2 h. This corresponded with increased IL-10 at 2 h following AnxA1$_{Ac2-26}$ treatment. Cytokines were not expressed in any of the sham groups.

4.2.3.2 Myeloperoxidase activity

An MPO assay was used on whole brain homogenates to assess oxidative activity of leukocytes at 40 min and 2 h reperfusion. Slight increases were recorded following AnxA1$_{Ac2-26}$ and vehicle 2 (15-epi-LXA$_4$ vehicle; 100µl saline plus ethanol) at 2 h reperfusion versus 40 min reperfusion and sham groups (not significant; Figure 19). No changes were recorded in lower dose 15-epi-LXA$_4$ groups (0.5 µg), and data do not include a higher dose 15-epi-LXA$_4$ (4.0 µg) group. The positive control (10 mg/kg LPS, 4 h prior to tissue collection) was lower than expected from the literature (Jeong, Jou et al. 2010), indicating that the levels through whole brain are too dispersed to measure, and with hindsight, that measuring the MPO levels in specific brain regions would have been preferable.

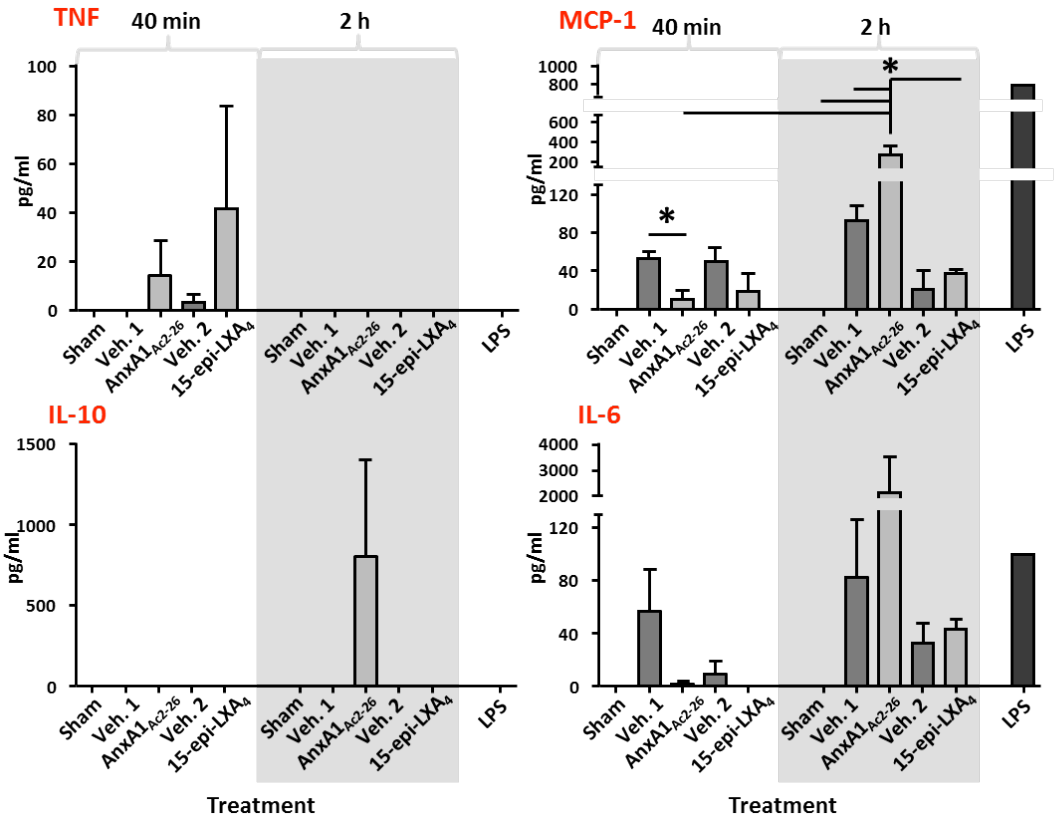

Figure 18. AnxA1$_{Ac2-26}$ increases levels of MCP-1 at 2 h. Blood samples were collected from mice in sham (no I/R), vehicle (AnxA1$_{Ac2-26}$ vehicle; 100 µl saline/mouse), AnxA1$_{Ac2-26}$, (100 µg/mouse) and 15-epi-LXA$_4$ (4.0 µg/mouse)-treated mice after 5 min BCCAO and 40 min reperfusion and blood serum was assayed for cytokine content using a bead array kit. Data are mean ±SEM; *p<0.05 by ANOVA followed by Bonferroni; n=3 mice/group; value for each mouse = mean of triplicate experiments.

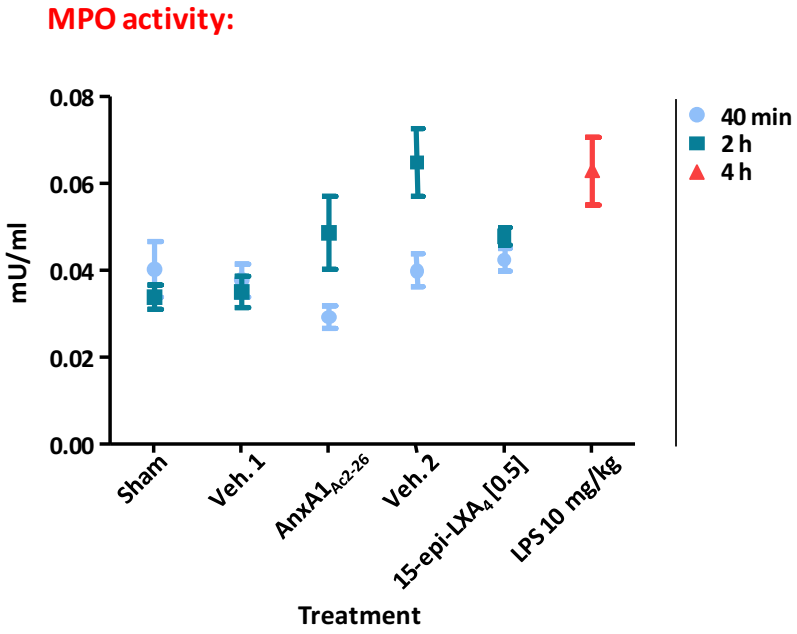

Figure 19. Myeloperoxidase (MPO) activity in whole brain samples leukocyte-endothelial interactions in cerebral I/R-induced inflammation in mice. Brains were collected from mice in sham (no I/R)**,** veh. 1 ($AnxA1_{Ac2-26}$ vehicle; 100 µl saline/mouse), veh. 2 (15-epi-LXA_4 vehicle; 100 µl saline plus ethanol), $AnxA1_{Ac2-26}$, (100 µg/mouse) and 15-epi-LXA_4 (0.5 µg/mouse)-treated mice after 5 min BCCAO and 40 min/2 h reperfusion. MPO activity was assayed and no significant differences were found between groups. Positive control = lipopolysaccharide (LPS); n=3 mice/group; value for each mouse = mean of triplicate experiments**.**

4.3 Conclusions

Both AnxA1$_{Ac2-26}$ and higher dose 15-epi-LXA$_4$ had anti-inflammatory effects in this model of global cerebral I/R at 40 min and 2 h. Both doses of 15-epi-LXA$_4$ reduced the number of rolling cells by 75% with respect to the vehicle-treated mice at 40 min, only marginally above sham-operated groups. Both 15-epi-LXA$_4$ and AnxA1$_{Ac2-26}$ reduced the number of adherent cells by 75% also, (consistent with the effect of 15-epi-LXA$_4$ on rolling cells,) again to levels almost identical to the sham-operated group. In this model, LXA$_4$ does not appear to produce the anti-inflammatory effects it has demonstrated in other models (Dufton, Hannon et al. 2010), possibly due to its lack of potency and stability (see *Discussion* chapter for further details).

The cytokines assayed were not detected at 40 min in reperfusion, suggesting that they are not involved in mediating inflammatory responses at this stage. It possible that they play a role at later time points as indicated by other groups (Legos, Whitmore et al. 2000), or are present in the cerebral tissue rather than blood serum.

These data provided the basis for further work aiming to identify an Fpr2/3 mechanism through which the effects of AnxA1$_{Ac2-26}$ were occurring. This work is described in the following chapter.

Chapter Five

Immunomodulation through Formyl Peptide Receptor 2/3 mechanisms in global cerebral ischaemia/reperfusion

5.1 Introduction

The previous chapter describes anti-inflammatory effects through both 15-epi-LXA_4 and $AnxA1_{Ac2-26}$ treatment in cerebral I/R. The ligands were selected on the basis of previous evidence which suggests the involvement of FPRs in their activity. The following data were therefore produced in order to indicate a role for FPRs (specifically FPR2/ALX) in the activity of these ligands in this model.

The LXA_4 (and 15-epi-LXA_4) receptor is well documented as FPR2/ALX (mouse orthologue Fpr2/3) (Chiang, Serhan et al. 2006). While full-length AnxA1 also seems to be FPR2/ALX-specific (Hayhoe, Kamal et al. 2006), $AnxA1_{Ac2-26}$ can be an agonist for all members of the FPR family (Ernst, Lange et al. 2004). To establish whether or not changes seen in the microvasculature in *Chapter 4* were occurring through FPR2/ALX activity, two established FPR antagonists (see section 1.3.2.3) were used in conjunction with $AnxA1_{Ac2-26}$: Boc2, a pan-antagonist of the FPR family, and WRW4, an FPR2/ALX-specific antagonist with which very little work has so far been done *in vivo*. Control groups in which animals were administered with an antagonist alone were included. Doses were again based on previously published data (Gavins, Kamal et al. 2005, Kretschmer, Gleske et al. 2010).

Interesting results from the $AnxA1_{Ac2-26}$/antagonist-treatment groups led to the acquisition of incremental cell counts from a WRW4-treatment group between 40 min and 2 h. Data are also shown from $Fpr2/3^{-/-}$ mouse groups, but should be considered preliminary due to the lack of available corresponding wild type mice (groups are instead compared with C57BL/6 mice). In all experiments, leukocyte rolling and adherence were assessed following cerebral I/R in response to the combined agonist/antagonists treatment. Results from these experiments are described in this chapter.

5.2 Results

5.2.1 Boc2 abrogates anti-adhesive effects of $AnxA1_{Ac2-26}$

Boc2 blocked the anti-adhesive properties seen with $AnxA1_{Ac2-26}$ at 40 min reperfusion (p<0.05; Figure 20C), suggesting that $AnxA1_{Ac2-26}$ reduces inflammation through an Fpr mechanism at this time point. The Boc2 control group produced inverse agonistic effects in the microvasculature: there was a marked increase in the number of rolling cells at 40 min in mice treated with $AnxA1_{Ac2-26}$/Boc2 as well as with Boc2 alone versus vehicle and sham groups (p<0.05; Figure 20A). The antagonist treatment, unlike with WRW4 (see section 5.2.2.2), produced greater levels of L-E interactions in the $AnxA1_{Ac2-26}$/Boc2 combined group than the Boc2 group.

While combined treatment with Boc2 abrogated some anti-inflammatory effects of $AnxA1_{Ac2-26}$ at 2 h, the effects were minimal compared with the earlier time point. While the number of rolling cells was increased in the $AnxA1_{Ac2-26}$/Boc2 group versus $AnxA1_{Ac2-26}$ at 2 h (i.e. effects were abrogated), this was not significant. In addition, animals receiving $AnxA1_{Ac2-26}$/Boc2 or Boc2 treatment alone produced cell activity levels significantly lower than the vehicle-treated group (p<0.05; Figure 20). This artifact is pursued further with respect to WRW4 (which produced similar but more pronounced effects) in section 5.2.2.2.

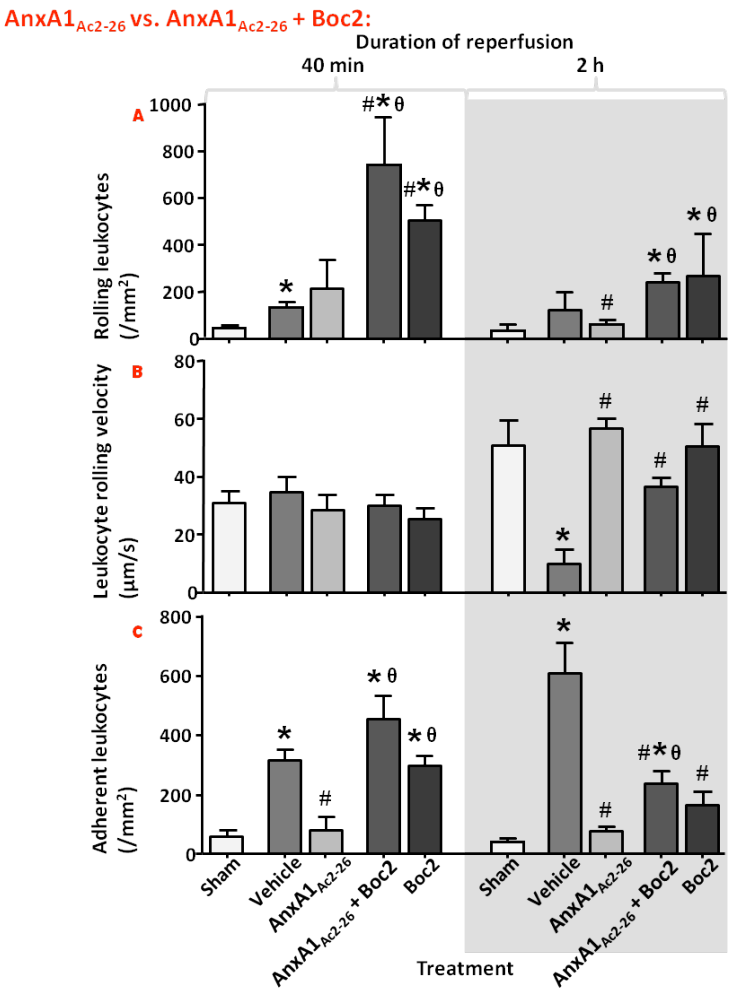

Figure 20. Pan-FPR antagonist Boc2 eliminates anti-adhesive properties of AnxA1$_{Ac2-26}$ at 40 min reperfusion. After 5 min BCCAO, mice were administered i.v. vehicle (100 µl saline/mouse), AnxA1$_{Ac2-26}$ (100 µg/mouse), Boc2 (10 µg/mouse), or AnxA1$_{Ac2-26}$ plus Boc2 at the start of reperfusion. A sham-operated group (no ischaemia/reperfusion) was included. After 40 min or 2 h reperfusion, L-E interactions were analysed over 2 min: the number of rolling leukocytes (A), the rolling cell velocity (B) and the number of adherent leukocytes (C) were counted over 100 µm vessel, and rolling and adherent cells expressed as number/mm^2. Data are mean ±SEM; *p<0.05 vs. sham, $^{\#}p$<0.05 vs. vehicle, $^{\theta}p$<0.05 vs. AnxA1$_{Ac2-26}$ by unpaired *t* test or ANOVA followed by Bonferroni; n=4-7 mice/group.

5.2.2 WRW4 abrogates anti-adhesive effects of $AnxA1_{Ac2-26}$

5.2.2.1 Temporal variation (increased efficacy at 40 min reperfusion)

WRW4 blocked the anti-adhesive properties seen with $AnxA1_{Ac2-26}$ at 40 min reperfusion ($p<0.05$; Figure 21C). As WRW4 is FPR2/ALX-selective, this indicates the significance of Fpr2/3 in mediating the effects of $AnxA1_{Ac2-26}$ in this model. As with Boc2, the WRW4 control group produced inverse agonistic effects in the microvasculature: there was a significant increase in the number of rolling cells at 40 min in mice treated with $AnxA1_{Ac2-26}$/WRW4 (4-fold versus vehicle) as well as with WRW4 alone (5-fold versus vehicle) ($p<0.05$; Figure 21A). In these groups, however, there were greater levels of L-E interactions in the WRW4 group than the $AnxA1_{Ac2-26}$/WRW4-combined group. In addition, (unlike Boc2-treatment groups) as the number of rolling cells increased, rolling velocity decreased significantly versus vehicle-treated animals at 40 min ($p<0.05$; Figure 21B).

As with the Boc2 group, combined $AnxA1_{Ac2-26}$ treatment with WRW4 also abrogated the effects of $AnxA1_{Ac2-26}$ at 2 h, but the abrogation was minimal compared with the earlier time point. While the number of rolling cells was increased in $AnxA1_{Ac2-26}$/WRW4 group versus $AnxA1_{Ac2-26}$ at 2 h, animals receiving $AnxA1_{Ac2-26}$/WRW4 or WRW4 treatment alone produced cell activity levels significantly lower than vehicle-treated groups ($p<0.05$; Figure 21). The 5-fold increase in numbers of rolling cells at 40 min and the low levels of L-E interaction at 2 h are investigated further in the next section (5.2.2.2).

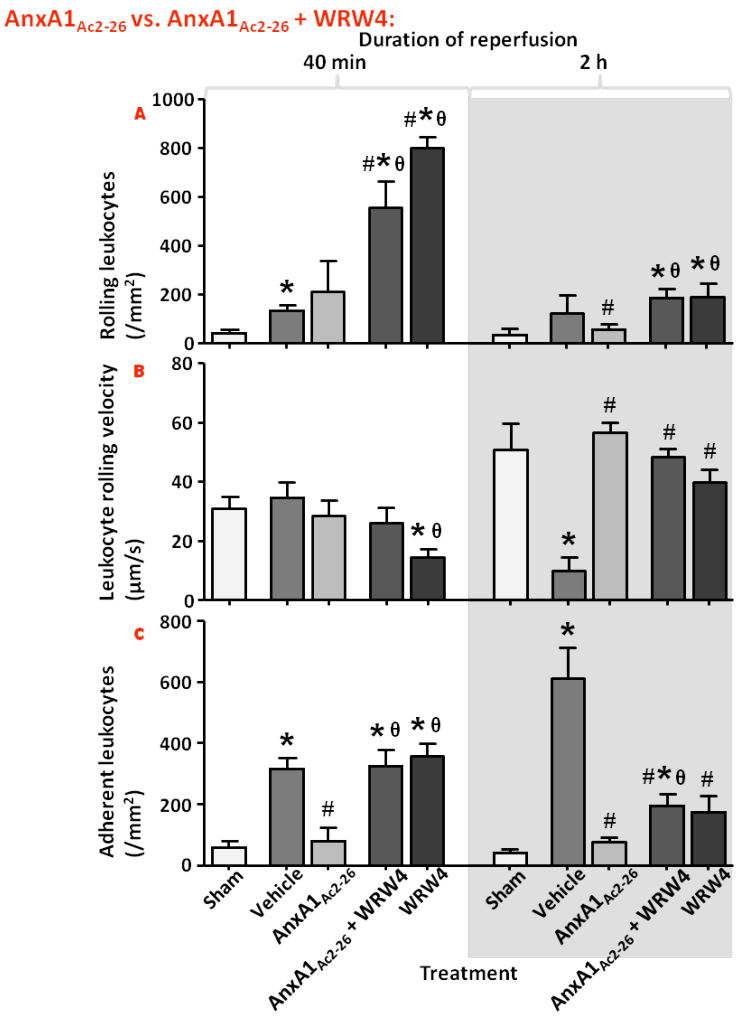

Figure 21. FPR2/ALX-selective antagonist WRW4 eliminates anti-adhesive properties of AnxA1$_{Ac2-26}$. After 5 min BCCAO, mice were administered i.v. vehicle (100 µl saline/mouse), AnxA1$_{Ac2-26}$ (100 µg/mouse), WRW4 (55 µg/mouse), or AnxA1$_{Ac2-26}$ plus Boc2 at the start of reperfusion. A sham-operated group (no ischaemia/reperfusion) was included. After 40 min or 2 h reperfusion, L-E interactions were analysed over 2 min: the number of rolling leukocytes (A), the rolling cell velocity (B) and the number of adherent leukocytes (C) were counted over 100 µm vessel, and rolling and adherent cells expressed as number/mm^2. Data are mean ±SEM; *p<0.05 vs. sham, $^{\#}p$<0.05 vs. vehicle, $^{\theta}p$<0.05 vs. AnxA1$_{Ac2-26}$ by unpaired *t* test or ANOVA followed by Bonferroni; n=4-7 mice/group.

5.2.2.2 Inflammatory activity diminishes between 40 min and 2 h reperfusion

Large numbers of rolling cells in the WRW4 (and Boc2) treatment groups at 40 min, combined with reduced rolling and adhesion at 2 h versus vehicle groups, led to recording of cell activity between the two time points. Monitoring leukocyte activity 40 min-2 h would help to clarify why treatment with antagonists produced profoundly different effects from vehicle treatment, in particular why surprisingly low levels of inflammation were seen at 2 h with antagonist versus vehicle treatment groups.

Videos were grouped into 5 x 15-20 min brackets (40≤59 min; 60≤74 min; 75≤89 min; 90≤104 min and 105≤120 min/2 h) within the 40 min-2 h period. The number of rolling leukocytes over the duration displayed a clear decreasing trend, with significant differences between the 40≤59/60≤74 and 105≤120 groups ($^{\S}p<0.05$; Figure 22A). Rolling velocity dipped at around 75≤89 min by half (not significant; Figure 22B), then resumed velocities seen in sham and (WRW4 at) 40≤59 min groups up to the 2 h end point. The number of adherent cells peaked at 75≤89 min (corresponding to the time period with the slowest recorded cell rolling velocities). The adherence during this middle segment is significantly increased versus the number of adherent cells at 40≤59 min ($^{\#}p<0.05$; Figure 22C), and the final recorded adherence levels (105≤120 min) significantly reduced versus the peak ($^{\#}p<0.05$; Figure 22C).

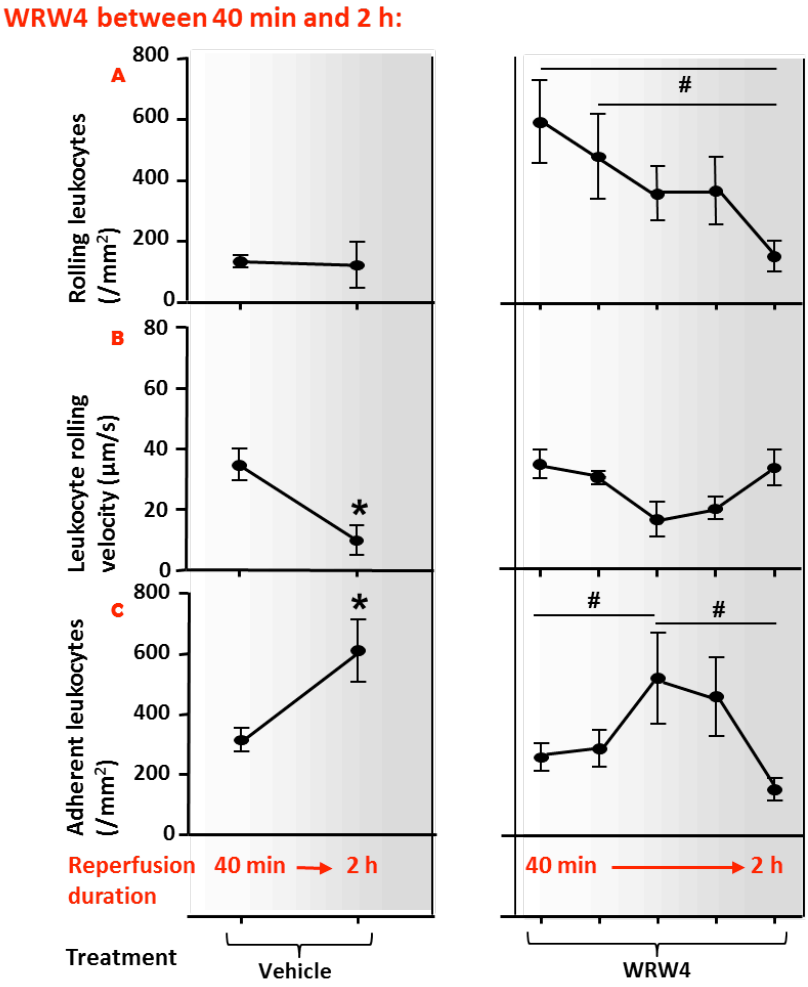

Figure 22. WRW4-treatment induces early peak in rolling followed by delayed peak in adhesion. After 5 min BCCAO, mice were administered i.v. vehicle (100 µl saline/mouse), or WRW4 (55 µg/mouse) at the start of reperfusion. A sham-operated group (no I/R) was included; WRW4 groups are shown on the right; sham and vehicle groups are shown on the left for reference. L-E interactions were analysed over 2 min between 40 min or 2 h reperfusion: the number of rolling leukocytes (A), the rolling cell velocity (B) and the number of adherent leukocytes (C) were counted over 100 µm vessel, and rolling and adherent cells expressed as number/mm^2. Time points for WRW4 groups: 40≤59 min; 60≤74 min; 75≤89 min; 90≤104 min and 105≤120 min/2 h; data are mean ±SEM; *p<0.05 vs. 40 min, p<0.05 by unpaired t test; n=4-9 mice/group.

5.2.3 Reduced leukocyte-endothelial interactions and high mortality in Fpr2/3$^{-/-}$ mice

Preliminary data were collected from Fpr2/3$^{-/-}$ mice after 40 min and 2 h reperfusion, but could not be investigated fully due to the unavailability of wild types. Fpr2/3$^{-/-}$ mice showed no significant increase in inflammation versus sham groups; in fact, the Fpr2/3$^{-/-}$ groups had adhesion levels significantly lower than C57BL/6 groups (p<0.05; Figure 23C). The differences in L-E interactions between mouse strains in the I/R groups suggest a potential pro-inflammatory role for Fpr2/3 in the endogenous response this model.

To investigate the possibility of a delayed response in these animals, preliminary data were collected from animals at 3 h reperfusion. While the C57BL/6 mice had levels of inflammation at least twice the level of 2 h groups (Figure 24), there was 100% mortality in Fpr2/3$^{-/-}$ mice after 2 h reperfusion (Figure 25).

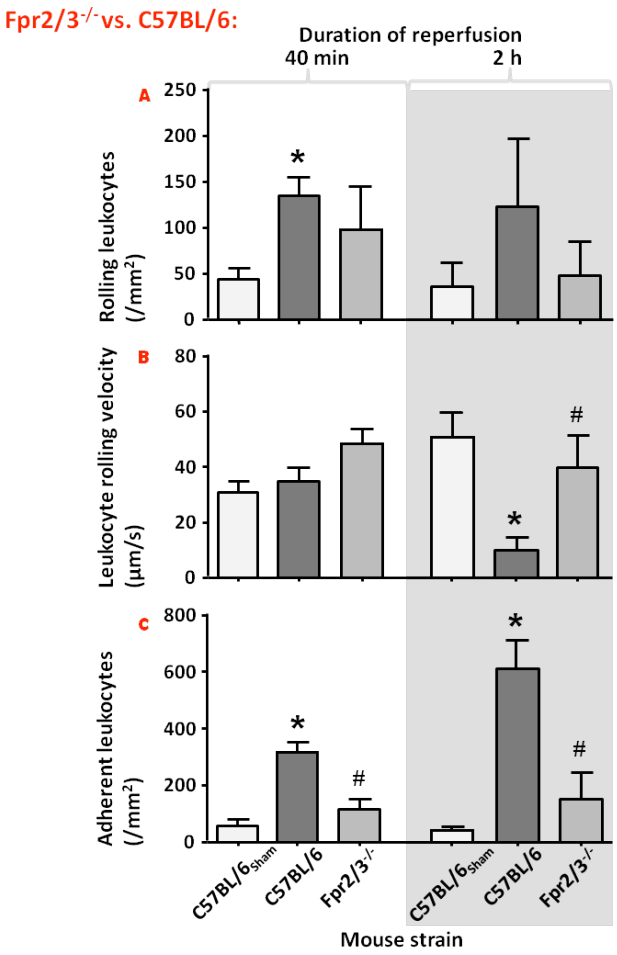

Figure 23. Cerebral ischaemia/reperfusion (I/R)-associated inflammation is reduced in Fpr2/3$^{-/-}$ mice versus C57BL/6 mice. After 5 min BCCAO, mice were administered i.v. vehicle (100 µl saline/mouse) at the start of reperfusion. A sham-operated group (no I/R) was included (C57BL/6$_{Sham}$). After 40 min or 2 h reperfusion, leukocyte-endothelial interactions were analysed over 2 min: the number of rolling leukocytes (A), the rolling cell velocity (B) and the number of adherent leukocytes (C) were counted over 100 µm vessel, and rolling and adherent cells expressed as number/mm^2. Data are mean ±SEM; *p<0.05 vs. C57BL/6$_{sham}$, $^{\#}p$<0.05 vs. C57BL/6 by unpaired t test or ANOVA followed by Bonferroni; n=3-8 mice/group.

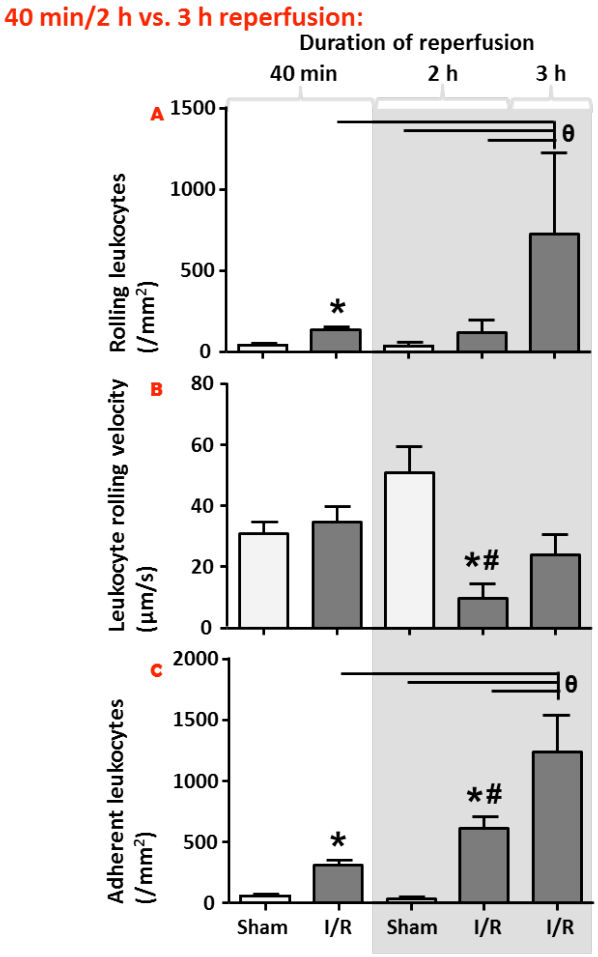

Figure 24. Cerebral ischaemia/reperfusion (I/R)-associated inflammation is increased in C57BL/6 mice at 3 h. After 5 min BCCAO, mice were administered i.v. vehicle (100 µl saline/mouse) at the start of reperfusion. A sham-operated group (no I/R) was included. After 40 min, 2 or 3 h reperfusion, leukocyte-endothelial interactions were analysed over 2 min: the number of rolling leukocytes (A), the rolling cell velocity (B) and the number of adherent leukocytes (C) were counted over 100 µm vessel, and rolling and adherent cells expressed as number/mm^2. Data are mean ±SEM; *p<0.05 vs. C57BL/6$_{sham}$, $^{\#}p$<0.05 vs. C57BL/6, $^{\theta}p$<0.05 by unpaired *t* test or ANOVA followed by Bonferroni; n=3-8 mice/group.

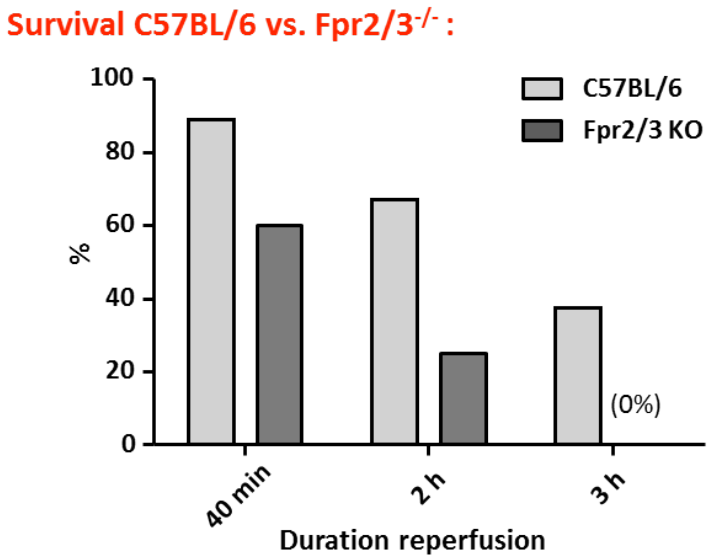

Figure 25. 100% mortality in Fpr2/3$^{-/-}$ mice after 2 h reperfusion. After 5 min BCCAO, mice were administered i.v. vehicle (100 µl saline/mouse) at the start of reperfusion. A sham-operated group (no I/R) was included. After 40 min or 2 h reperfusion, leukocyte-endothelial interactions were analysed over 2 min: the number of rolling leukocytes (A), the rolling cell velocity (B) and the number of adherent leukocytes (C) were counted over 100 µm vessel, and rolling and adherent cells expressed as number/mm^2. Data are expressed in %; n=5-12 mice/group.

5.3 Conclusions

This chapter describes data sets from mice treated with combined $AnxA1_{Ac2-26}$ and FPR antagonists, Boc2 or WRW4 alone (including longitudinal data collected between 40 min and 2 h), as well as data from $Fpr/3^{-/-}$ mice. To characterise the role of Fpr2/3 in this model, inhibition of Fpr2/3 activity was achieved through pharmacological antagonism, which produced a <5-fold increase in L-E interactions, and through the use of $Fpr2/3^{-/-}$ animals, which produced no L-E interactions significantly above sham groups. These data suggest that Fpr2/3 combination has central (albeit opposing) roles in the inflammatory response to I/R in this model.

Several points are raised in this chapter. The reduction of leukocyte rolling and adhesion at 40 min brought about by $AnxA1_{Ac2-26}$ was abrogated by combined treatment with Boc2 and WRW4, which suggests an Fpr2/3 mechanism (shared with 15-epi-LXA_4) for $AnxA1_{Ac2-26}$ at this time point. At the later time point of 2 h, anti-adhesive effects are abrogated by only 20% (compared with 100% at 40 min). Independently, the data suggest that $AnxA1_{Ac2-26}$ is acting via an alternative mechanism at 2 h. Stability and potency of compounds over the 2 h versus 4 h period must be considered, however, particularly as Boc2 and WRW4 treatment (without $AnxA1_{Ac2-}$26) gives rise to fewer adhesive leukocytes than the vehicle treatment group at 2 h. These aspects are covered further in the *Discussion* chapter, with respect to the suitability of FPR2/ALX as a target in reducing I/R injury following stroke.

.

Chapter Six

Chemotaxis of human leukocytes from stroke patients and healthy controls

6.1 Introduction

Cellular chemokinesis (movement along a chemical concentration gradient) and transmigration (across epithelia) are central processes in the leukocyte adhesion cascade. Having been granted access to blood samples from acute stroke patients at Charing Cross Hospital (London, UK), we aimed to quantify the chemotactic activity of monocytes collected from peripheral blood of stroke (MCAO) patients versus healthy volunteers.

Three chemotactic agents were selected for the assays (MCP-1, fMLP and MIP-1α) on the basis of their previously demonstrated involvement in monocyte chemotaxis (Ternowitz, Herlin et al. 1987, Jiang, Newman et al. 2008) and (in the case of fMLP) for a role as an FPR ligand (see section 1.3.1). Using an *in vitro* model of chemotaxis (quantification of cell movement across a porous membrane towards a chemoattractant), dose-response experiments using healthy monocytes defined optimal chemoattractant concentrations for use in subsequent comparative assays with monocytes from stroke patients.

To indicate a role for FPRs in the modulation of chemotaxis, monocytes from blood samples from each group were pre-treated with FPR ligands ($AnxA1_{Ac2-26}$ and LXA_4), before being assayed. The results from these experiments are described in this chapter.

6.2 Results

6.2.1 Exposure to chemoattractant increases monocyte migration

The data in this section (6.2.1) were conducted using monocytes extracted from the blood of healthy volunteers. Spontaneous monocyte migration (i.e. towards vehicle; RPMI) across a porous membrane in a chemotaxis chamber amounted to $1.0\pm0.2x10^5$ cells/ml (Figure 26). This level was increased up to 3.6 times when a chemoattractant (MCP-1, fMLP or MIP-1α) was loaded into the lower well of the chamber.

Characterised monocyte chemoattractant, MCP-1, increased migration above basal (spontaneous) level 2.4-3.6 times depending on MCP-1 concentration used (Figure 26A). Migration was significantly increased at 12.5 and 25.0 ng/ml MCP-1 ($p<0.05$) but not 50.0 and 100.0 ng/ml, with 12.5 ng/ml (the lowest concentration used) in fact providing the greatest chemoattractive effects. Despite 50.0 and 100.0 ng/ml groups not reaching significance (due to large standard errors), the higher 3 concentrations used (25.0-100.0 ng/ml) all produced over twice the basal level of migration.

Migration towards MIP-1α was increased across all doses used (25.0, 50.0 or 100.0 ng/ml) up to 3-fold above basal levels (Figure 26C), although only 50.0 ng/ml (increasing migration from $1.3x10^5$ to $3.5x10^5$ cells/ml) reached significance ($p<0.05$).

Migration towards 10^{-8}M fMLP was doubled versus basal level (Figure 26B; $2.2x10^5$ cells/ml versus $1.1x10^5$ cells/ml). This concentration produced the most consistent increases in migration among samples within the group (although not significant). A linear trend between increasing fMLP concentration and increased migration was not observed as expected, with the higher two concentrations (10^{-7}M and 10^{-6}M) not surpassing basal migratory levels. As observed across MCP-1 groups, migration instead peaked at the lower tested doses, not following a standard dose-response curve.

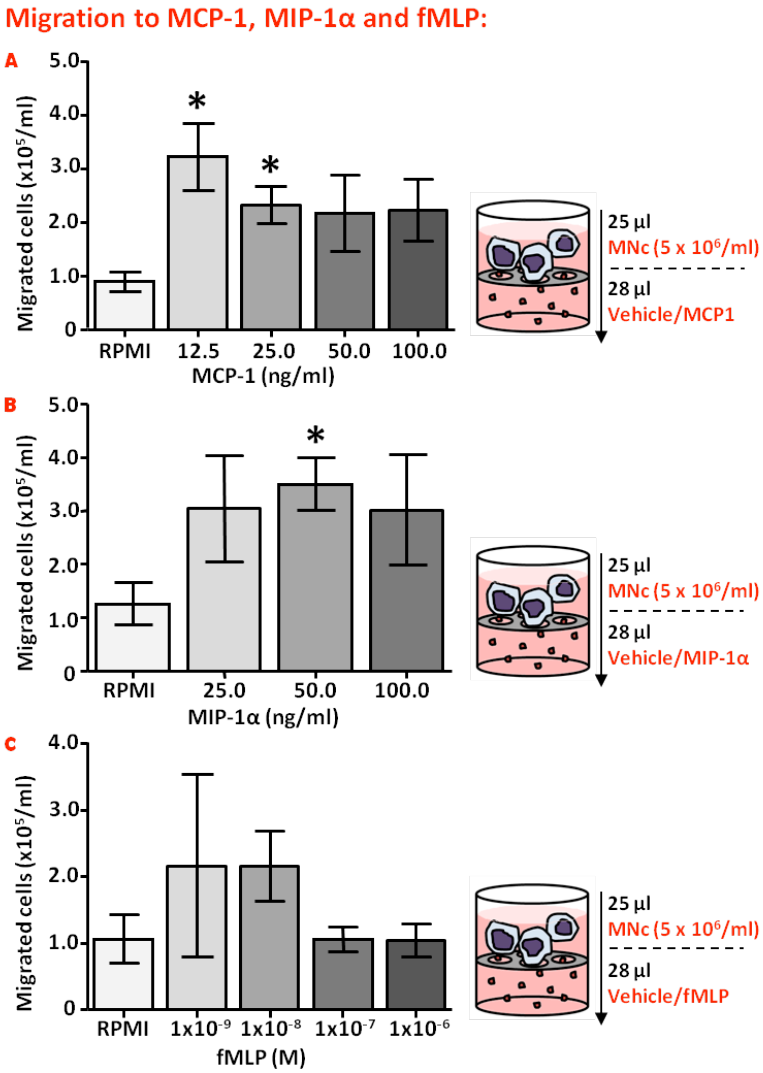

Figure 26. Monocyte (MNc) migration is significantly increased in response to MCP-1 and MIP-1α. MNc ($5x10^6$ cells/ml) from healthy volunteers were placed in a chemotaxis chamber above a characterised chemoattractant (MCP1, MIP-1α or fMLP), separated by a porous membrane (see illustrations). After 1.5 h, MNc migration towards the chemoattractant was quantified (A-C). Data are mean ±SEM; *p<0.05 vs. vehicle (RPMI) by unpaired t test; n=4 (MCP1); n=5 (MIP-1a) or n=5 (fMLP) samples/group.

6.2.2 Chemotactic responsiveness of monocytes from stroke patients versus healthy controls

6.2.2.1 Monocyte migration is increased in stroke patients

Following stroke, circulating monocytes are exposed to systemic inflammation. In order to assess priming effects this may have on migration, blood samples were obtained with permission from acute-stage stroke patients (<96 h post onset) (see section 2.3.2.1). Monocytes were extracted from samples and their migration towards a chemoattractant (MCP-1, 12.5 ng/ml or fMLP[6], 10^{-8}M) was compared with that of monocytes from healthy controls. MCP-1 was selected as a producer of the largest significant increases in monocyte migration and fMLP for its role as an FPR ligand.

Migration in monocytes from stroke patients was significantly increased versus monocytes from healthy controls (p<0.05; Figure 27). Towards MCP-1 this was particularly pronounced, producing a 4-fold increase in migrated cells ($0.3x10^5$ cells/ml to $1.2x10^5$ cells/ml Figure 27A), whereas fMLP produced a 2-fold increase (Figure 27B).

6.2.2.2 Modulation of monocyte chemotaxis through FPRs in stroke and healthy controls

In order to indicate a role for FPRs in the modulation of monocyte priming, stroke and healthy blood samples were pre-treated with FPR agonists ($AnxA1_{Ac2-26}$, LXA_4 or vehicle; saline), before being subjected to conditions described above.

Differences between FPR agonists were observed. In healthy samples, $AnxA1_{Ac2-26}$ pre-treatment caused increased migration towards both chemoattractants (Figure 27; p<0.05), particularly towards MCP-1 which resulted in 8 times the level of migration of vehicle pre-treated groups (Figure 27A; $2.4x10^5$ cells/ml versus $0.3x10^5$ cells/ml). Where healthy cells were pre-treated with LXA_4, there was again a significant increase in migration towards MCP-1 (p<0.05), but only twice the level seen in vehicle groups.

[6] During the course of this study, we received enough blood samples from stroke patients to complete experiments for 2 chemoattractants. fMLP was used rather than MIP-1□, as previous data has shown fMLP to increase chemotaxis and because of its role as an FPR ligand (hence its relevance to our wider research).

FPR agonist pre-treatments had opposing effects on healthy cells when migrating towards fMLP. Pre-treatment with $AnxA1_{Ac2-26}$ doubled migration towards the chemoattractant versus with vehicle, while LXA_4 pre-treatment halved it—both with significance (Figure 27B; $p<0.05$).

In stroke samples, $AnxA1_{Ac2-26}$ pre-treatment increased migration towards MCP-1 (Figure 27A; $p<0.05$) but only doubling levels observed in vehicle-pre-treated stroke groups (compared with the 8-fold increase in healthy $AnxA1_{Ac2-26}$ versus vehicle-pre-treated samples). Migration towards fMLP had been increased in $AnxA1_{Ac2-26}$ versus vehicle pre-treated monocytes from healthy volunteers (see above), but was significantly decreased in monocytes from stroke blood under the same conditions (Figure 27B; $AnxA1_{Ac2-26}$ versus vehicle pre-treatment; $3.4x10^5$cells/ml versus $2.7x10^5$cells/ml; $p<0.05$).

Differences were again observed in monocyte chemotaxis towards both chemoattractants following LXA_4 pre-treatment. In LXA_4-pre-treated cells, MCP-1 caused increased migration versus vehicle-pre-treated groups in stroke as well as healthy samples (Figure 27A), but—unlike in healthy controls—the increase following LXA_4 pre-treatment was not significant.

The trend towards decreased migration to fMLP in cells from stroke patients pre-treated with $AnxA1_{Ac2-26}$ was replicated with LXA_4-pre-treatment: LXA_4-pre-treatment reduced migration significantly versus vehicle pre-treatment (Figure 27B; $p<0.05$). For both stroke and healthy monocyte samples (unlike with $AnxA1_{Ac2-26}$ pre-treated groups, for which an increase was observed towards fMLP), this represented halving migration levels (Figure 27B; stroke: $3.4x10^5$ cells/ml to $1.6x10^5$ cells/ml; healthy: $1.6x10^5$ cells/ml to $0.7x10^5$ cells/ml; $p<0.05$).

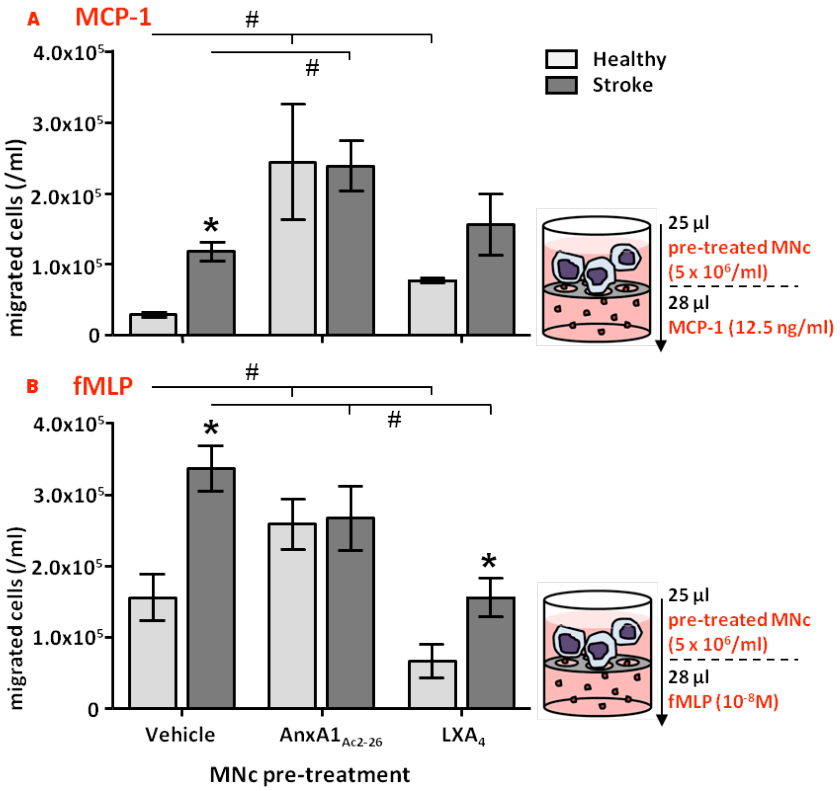

Figure 27. Monocyte (MNc) migration is increased in stroke patients versus healthy controls and modulated by FPR2/ALX agonists. MNc ($5x10^6$ cells/ml) from stroke patients and healthy controls were pre-treated with vehicle (saline) or FPR2/ALX agonists ($AnxA1_{Ac2-26}$, or lipoxins A4, LXA_4; both 1 µM; 10 min incubation), then placed in a chemotaxis chamber above a chemoattractant (MCP1, 12.5 ng/ml, A or fMLP, 10^{-8}M, B), separated by a porous membrane (see illustrations). After 1.5 h, MNc migration towards the chemoattractant was quantified (A/B). Stroke increased the chemotactic potential of MNc. Both treatments reduced migration towards fMLP but an increase in migration was recorded towards MCP-1. Data are mean ±SEM; *p<0.05 vs. healthy control by ANOVA followed by Bonferroni, $^{\#}p$<0.05 by unpaired t test; arrow = direction of MNc movement in chamber; n=4 samples/group.

6.3 Conclusions

This chapter assesses the ability of FPR agonists to modulate the chemotactic behaviour of monocytes from stroke patients and healthy volunteers. Chemoattractant concentrations were established for producing optimal migration in monocytes from healthy controls (MIP-1α, 50.0 ng/ml; MCP-1, 12.5 ng/ml and fMLP, 10^{-8}M). Subsequently, MCP-1 and fMLP were placed in the lower well of chemotaxis chambers at these optimal concentrations, and separated by a porous membrane from agonist pre-treated monocytes from stroke patients above (pretreatments: $AnxA1_{Ac2-26}$ or LXA_4; both 1 μM or vehicle, saline).

Migration towards both MCP-1 and fMLP was at least doubled in monocytes from stroke patients versus healthy controls following vehicle pre-treatment. LXA_4-pre-treated stroke versus healthy cells correlated in a similar manner to vehicle-pre-treated stroke versus healthy groups when subjected to either chemoattractant: towards MCP-1 migration was increased, whereas towards fMLP migration decreased. $AnxA1_{Ac2-26}$ increased migration in all cases (in monocytes from stroke patients and healthy controls) other than that of stroke patient monocyte migration towards fMLP. Overall, pre-treatment with FPR ligands increased migration towards MCP-1 and decreased migration towards fMLP for monocytes from stroke patients. Data suggest that FPR2/ALX activity can modulate monocyte migration and that migration is chemoattractant-dependent. Also indicated are possible divergent roles for FPR2/ALX activity in monocyte migration in healthy conditions versus stroke. This possibility is discussed further in Chapter 8 (*Discussion*).

Chapter Seven

Magnetic Resonance Imaging of inflammation using FPR-targeted agents

7.1 Introduction

The ability to trace leukocyte trafficking using non-invasive imaging techniques would be an extremely useful tool in developing targeted anti-inflammatory therapies (Dorward, Lucas et al. 2012). Cell/receptor-specific imaging agents are therefore continually being sought for use in powerful imaging modalities such as MRI (Modo, Cash et al. 2002), near-infrared fluorescence imaging (NIRF) (Xiao, Zhang et al. 2012) and positron emission tomography (PET) (Locke, Chordia et al. 2009). In stroke, not only would such imaging processes be used for diagnostic purposes, but also to provide information on disease progression over a longer period, potentially enabling treatments better tailored to an individual. This chapter contains preliminary work aiming to generate a neutrophil-specific MRI contrast agent, which would allow longitudinal tracking of neutrophil movement following an inflammatory insult within specific body structures.

MRI is able to differentiate between physical structures on the basis of water content. Gd(III) is a heavy metal widely used (in humans and experimentally) as an ionic base for contrast agents, which enhances image contrast due to its ability to increase the relaxation rate of surrounding protons within water molecules. Gd(III) is highly toxic as a solubilised free ion and is therefore chelated (retained within an organic structure or 'cage') prior to use. A ligand is covalently bound to this cage that then selectively binds the ligand receptor, enhancing image contrast in the vicinity of the target cell/receptor (see Figure 9, p.61).

FPR1 (mouse orthologue Fpr1) was selected as a suitable target for a contrast agent due to its abundance on neutrophils, its expression during inflammation and its role in neutrophil chemotaxis/trafficking. The high affinity (K_d = 17.7 nM) FPR1 ligand, peptide cFLFLFK, was selected (Locke, Chordia et al. 2009, Gavins 2010) for the Gd(III)-chelate-bound ligand. Once the agent had been generated and efficacy assessed in a series of *in vitro* Ca^{2+} flux and binding assays, it was used in an LPS model of inflammation (peritonitis through i.p. injection LPS, 10 μg/mouse) in mice to increase contrast in regions of Gd(III)-cFLFLFK binding to Fpr1 (i.e. in regions of high neutrophil concentration).

LPS is a lypoglycan endotoxin found on the cell surface of Gram-negative bacteria, which provokes an inflammatory response in the host, involving leukocyte chemotaxis to lesion sites. Prolonged periods in an MRI machine and unstable body temperature following LPS treatment/isoflurane anaesthesia produced high rates of mortality in mice. Data from three successful preliminary

experiments are described in this chapter (mice [i] and [ii], both Gd(III)-cFLFLFK, and mouse [iii], Gd-DOTA). These demonstrate the activity of a targeted contrast agent and the potential abundance of information available from an individual mouse through this technique.

7.2 Results

7.2.1 Relative retention times of Gd(III)-cFLFLFK versus Gd-DOTA

C57BL/6 mice were administered LPS (10 μg/mouse; i.p.) 24 h prior to MRI as a model of systemic inflammation. Gd(III)-cFLFLFK (Fpr1-targeted agent) or Gd-DOTA (control; both 1 mmol/kg) was injected (i.v.) and sequential acquisitions made, with slice orientation/location as illustrated in Figure 28.

A targeted contrast agent must be held within the body for several hours before being excreted. Preliminary data obtained from 3 mice [i-iii] provide information on retention times of each contrast agent and agent localisation. Figure 29 shows data from mouse [i] (Gd(III)-cFLFLFK) versus mouse [iii] (Gd-DOTA) and Figure 30, Figure 31 and Figure 32 all show data from mouse [ii] (Gd(III)-cFLFLFK) and mouse [iii] (Gd-DOTA).

Figure 29 shows coronal sections of the head pre- and post-injection of contrast agent and provides an example of how an enhanced contrast agent may be used. This slice (2 mm from the bregma in a caudal direction) was selected as it displays a region of increased contrast in both mice, with varied retention times with respect to contrast agent (Gd(III)-cFLFLFK or Gd-DOTA) across an extended period of time (240 min). In mouse [i], Gd(III)-cFLFLFK-induced increase in contrast is maintained up to 240 min, whereas Gd-DOTA (mouse [iii]) was only retained until 80 min. Detailed longitudinal data are missing from mouse [i] due to technical problems, but these images provide an initial qualitative suggestion that Gd(III)-cFLFLFK is retained longer. Figure 30 shows retention times of contrast agents (Gd(III)-cFLFLFK, mouse [ii] versus Gd-DOTA, mouse [iii][7]) across 12 corresponding slices over 80 min. (Unexpected mortality of mouse [ii] meant data were not collected beyond this time point.) In all but 2 slices, Gd-DOTA is retained longer than Gd(III)-cFLFLFK (the exceptions being around the area of the bregma, where both agents are retained equally).

[7] Mouse [i] is omitted from this comparison due to a lack detailed data available between 0-80 min (see above and Figure 29).

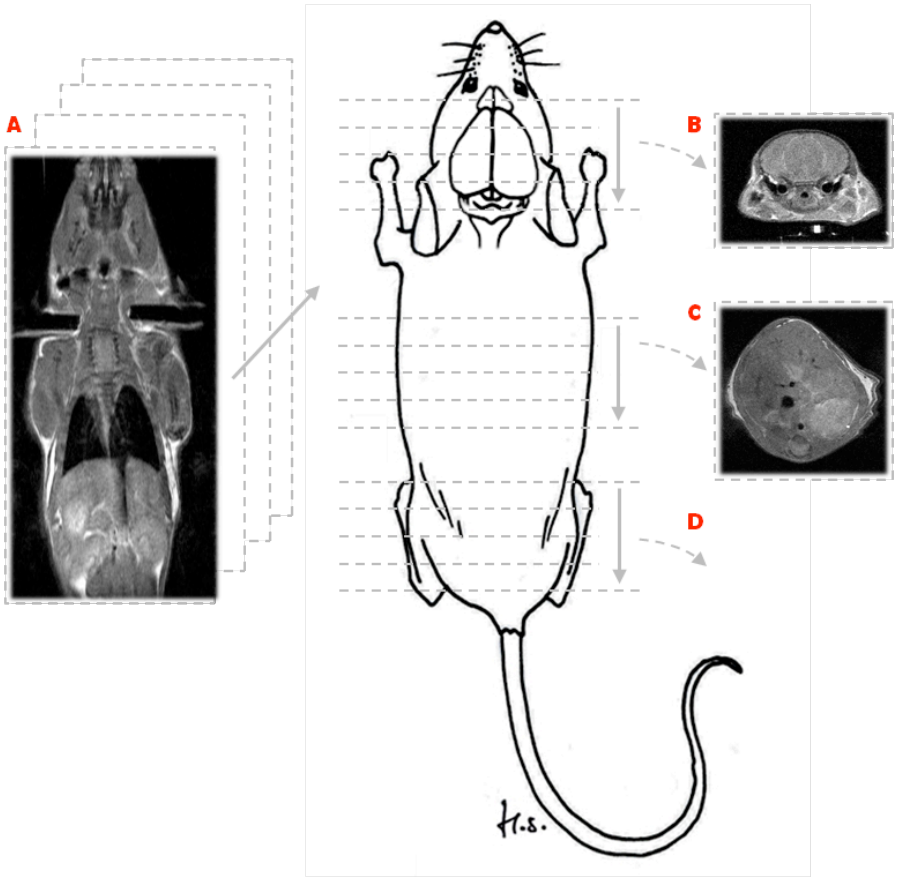

Figure 28. Acquisitions taken throughout MRI scanning (Smith Unpublished). Mice were administered LPS (10 μg/mouse; i.p.) 24 h prior to MRI as a model of systemic inflammation. Gd(III)-cFLFLFK (Fpr1-targeted agent) or Gd-DOTA (control; both 1 mmol/kg) was injected (i.v.) and sequential acquisitions made. The illustration shows 3 dimensions/regions (A-C) in which acquisitions were taken during scanning (whole body, head and abdomen). Up to 64 slices were taken during one scan, depending on how many regions were to be scanned in rotation and animal mortality. Also shown is the scanning location (D) for a potential unilateral myositis model in which LPS injection into one flank (i.e. triggering unilateral inflammation) would enable the other flank to stand as a suitable control.

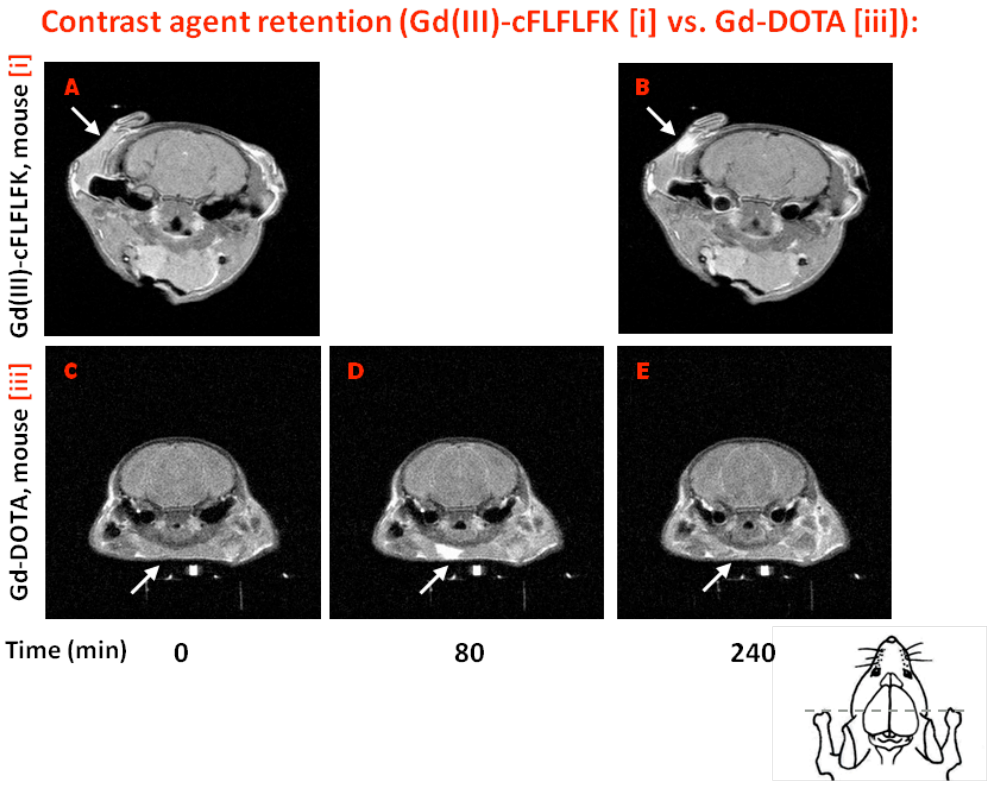

Figure 29. Increase in contrast is retained longer following Gd(III)-cFLFLFK injection versus Gd-DOTA close to the bregma. Mice were administered LPS (10 μg/mouse; i.p.) 24 h prior to MRI as a model of systemic inflammation. Gd(III)-cFLFLFK (Fpr1-targeted agent; mouse [i]) or Gd-DOTA (control; mouse [iii]; both 1 mmol/kg) was injected (i.v.) and sequential acquisitions made. Pre-injection images are shown (A/C), illustrating baseline intensity. D shows an increase in contrast in the tissue surrounding the brain at 80 min (equivalent image for mouse [i] unavailable due to technical difficulties). By 240 min, the increase in contrast seen in mouse [iii] has returned to baseline levels, whereas an increase in contrast is visible in mouse [i]. White arrow = region of interest.

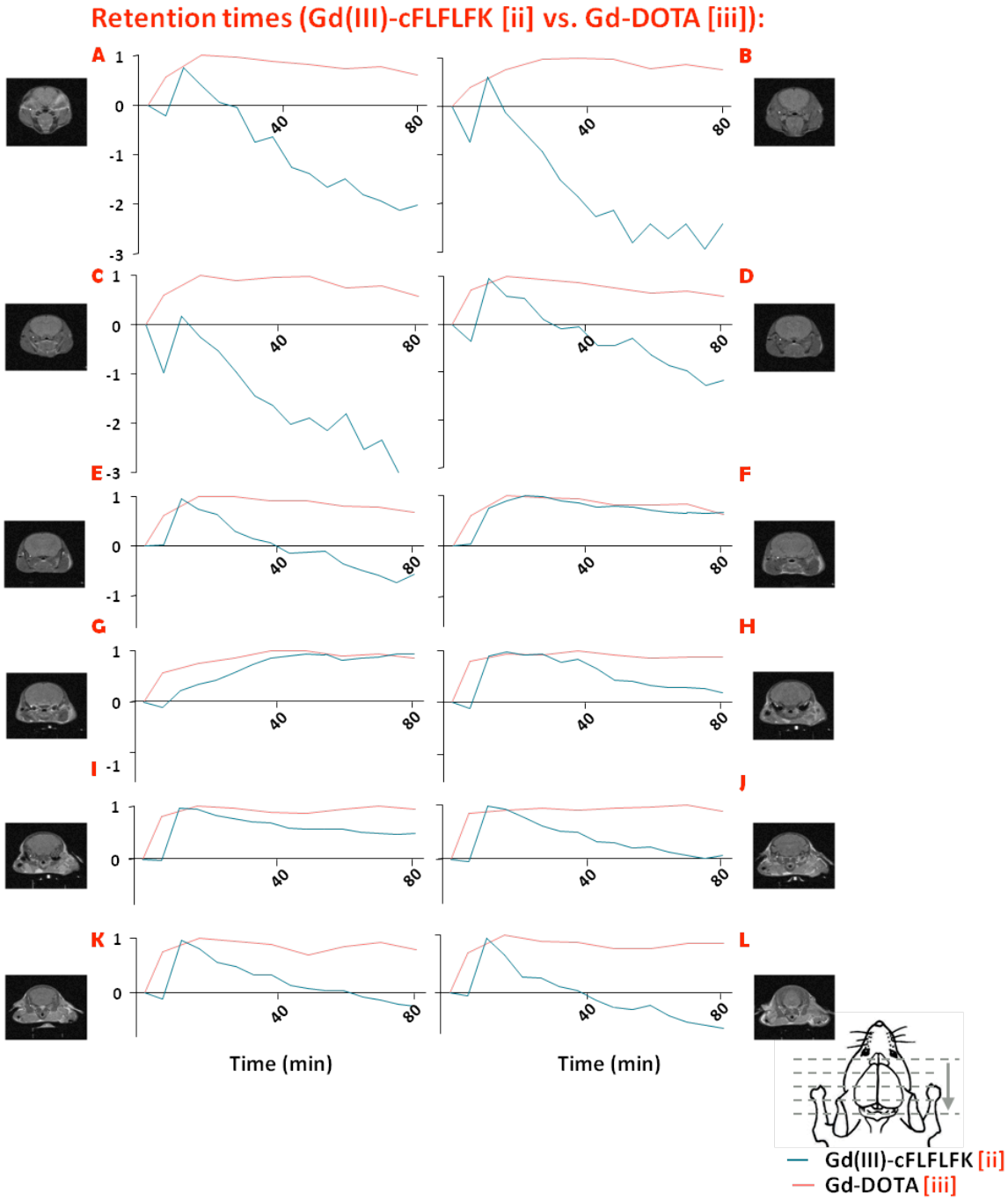

Figure 30. Retention times of Gd(III)-cFLFLFK injection versus Gd-DOTA over 12 slices (A, rostral – L, caudal). Mice were administered LPS (10 μg/mouse; i.p.) 24 h prior to MRI as a model of systemic inflammation. Gd(III)-cFLFLFK (Fpr1-targeted agent; mouse [ii]; orange lines) or Gd-DOTA (control; mouse [iii]; blue lines; both 1 mmol/kg) was injected (i.v.) and sequential acquisitions made over 80 min. In the region of the head, retention of Gd-DOTA is greater than Gd(III)-cFLFLFK.

7.2.2 Slice-dependent variations in contrast agent retention

Figure 31 and Figure 32 show grouped data from Figure 30. These demonstrate that the spread of data across slices (i.e. location-dependent variation in contrast agent retention time) is almost 7 times greater in mouse [ii], injected with Gd(III)-cFLFLFK, than the control mouse. This indicates that in mouse [iii], Gd-DOTA was retained more uniformly throughout the images regions. The variation in Gd(III)-cFLFLFK retention in mouse [ii] may therefore suggest movement of the agent to sites on inflammation (possibly the lungs or peritoneum).

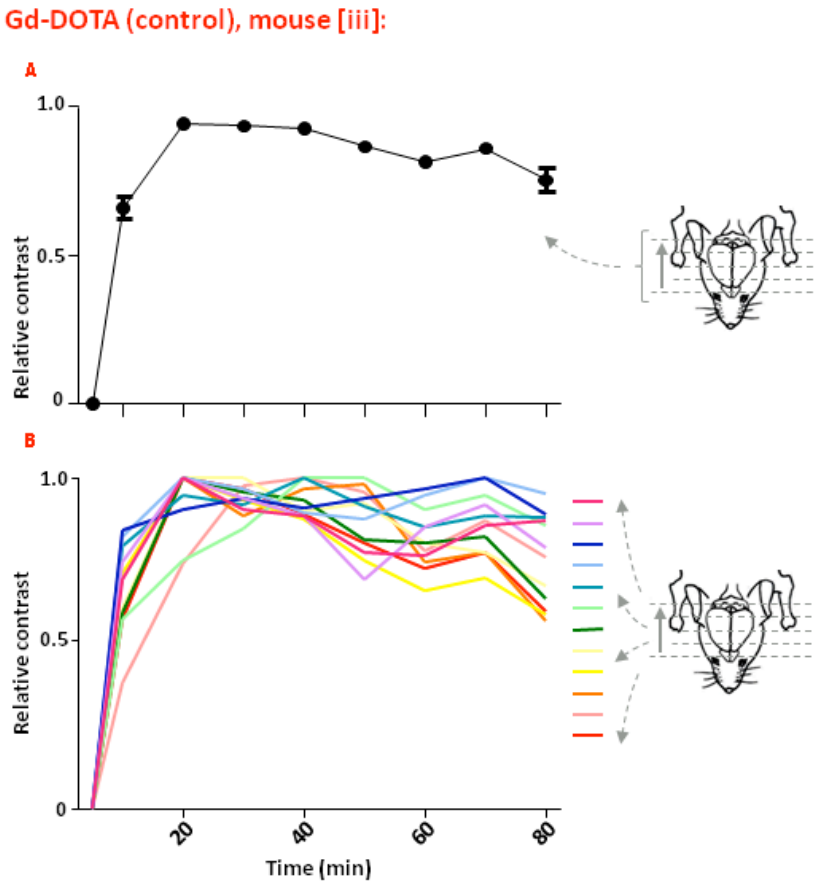

Figure 31. Retention times of Gd-DOTA across 12 head slices. Mouse [iii] was administered LPS (10 μg/mouse; i.p.) 24 h prior to MRI as a model of systemic inflammation. Gd-DOTA (control; mouse [iii]; 1 mmol/kg) was injected (i.v.) and sequential acquisitions made of 12 slices over 80 min. Figure shows mean (A) and individual (B) relative contrasts following initial injection. Data suggest that in this mouse Gd-DOTA was evenly distributed throughout the head, and retained for at least 80 min. Data in A are mean ±SEM; n=12 slices from one representative mouse.

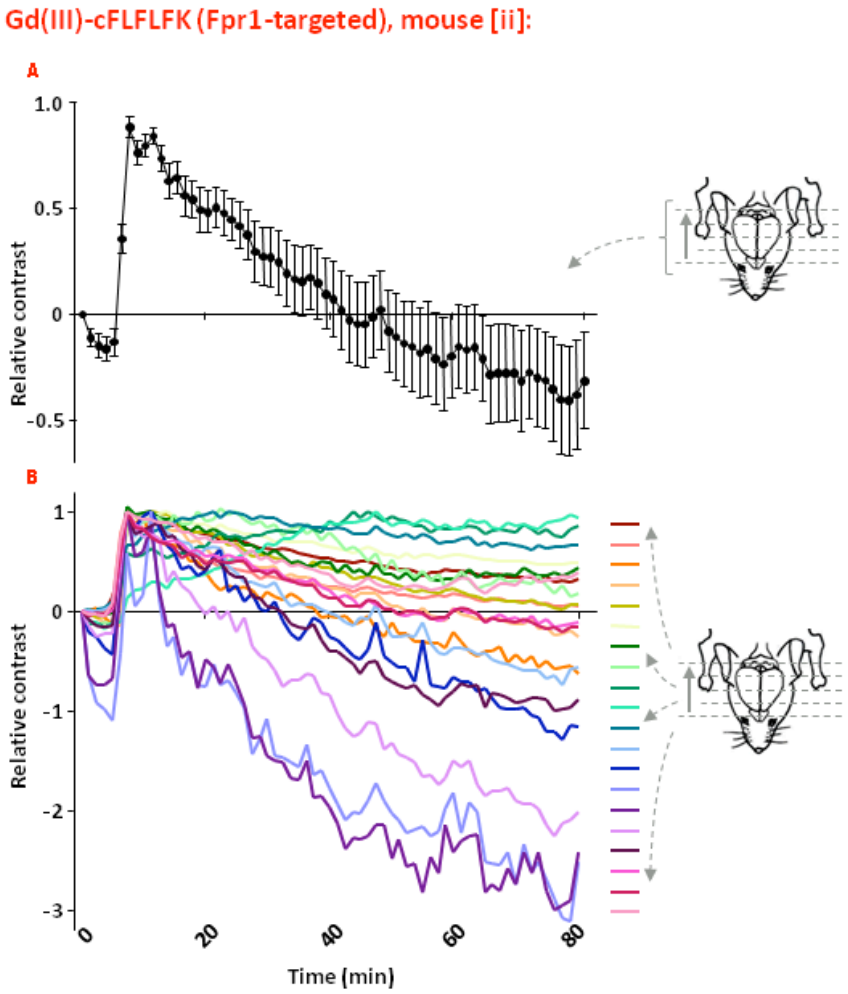

Figure 32. Retention times of Gd(III)-cFLFLFK across 12 head slices. Mice were administered LPS (10 μg/mouse; i.p.) 24 h prior to MRI as a model of systemic inflammation. Gd(III)-cFLFLFK (Fpr1-targeted agent; mouse [ii]; 1 mmol/kg) was injected (i.v.) and sequential acquisitions made of 20 slices over 80 min. Figure shows mean (A) and individual (B) relative contrasts following initial injection. Data suggest that in this mouse Gd(III)-cFLFLFK was not evenly distributed throughout the head; slices in the region of the bregma (green spectrum) were well retained for at least 80 min, but other regions (particularly the rostral slices: purple/blue spectrum) were retained Gd(III)-cFLFLFK for as little as 15 min. Data in A are mean ±SEM; n=12 slices from one representative mouse.

7.3 Conclusions

These preliminary experiments demonstrated that the short length of the coil in which mice were positioned within the MRI machine reduced the capacity for high-resolution images. Mice were therefore positioned for optimal imaging of the head. Several improvements to this model should be made to progress the work. For example, the use of a longer coil to enable visualisation of changes in contrast throughout the body would ostensibly allow the movement of Gd(III)-cFLFLFK to sites of inflammation to be monitored, establishing an accurate retention time for the agent. Another, more local model of inflammation (i.e. Figure 28D) would also fulfil this purpose.

The discrepancy between mouse [i] (Gd(III)-cFLFLFK) versus [iii] (Gd-DOTA) and mouse [ii] (Gd(III)-cFLFLFK) versus [iii] illustrate this problem. The prolonged retention is noted in mouse [i] does not occur in mouse [ii]; whether mouse [ii] displays an accurate depiction of Gd(III)-cFLFLFK retention or the agent moved elsewhere in the body as little as 15 min post injection cannot be verified without suitable whole body images or a more localised model, as mentioned above.

Further experiments are needed to draw conclusions with respect to Gd(III)-cFLFLFK retention and ultimately the effectiveness of this contrast agent in monitoring neutrophil activity. What is clear, however, is the breadth of data that may be collected from a single animal through the use of targeted contrast agents; these are explored along with potential improvements to this protocol in the following *Discussion* chapter.

Chapter Eight

Discussion

8.1 Part One: 'too much of a good thing…'

An inflammatory response is essential to the ability of a host to deal with infection. It is required for phagocytic, pathogen-removing functions of leukocytes, antigen presentation and antibody production—and without it an infectious insult is usually fatal. Yet despite its necessity, associations between the damaging effects of excessive inflammation and non-infectious diseases are continually being drawn, in which alternative stressful stimuli provoke a response intended to tackle pathogens. Inflammation in fact has a role in the pathogenesis of a variety of disorders, including autoimmune diseases such as multiple sclerosis and diabetes (Frischer *et al.,* 2009), numerous infectious diseases, and chronic diseases including rheumatoid arthritis and cancer (Lin and Karin, 2007).

In stroke, the specialist endothelia of cerebral vasculature (the BBB; usually exquisitely regulated—see section 1.1.2.3) are similarly unable to protect neural tissue from the effects of inflammation-associated I/R injury. As such, infarct size is inextricably linked to levels of inflammation during cerebral reperfusion, as demonstrated by a body of human and animal data (see sections 1.2.1.3 and 1.2.2.2).

The purpose of this thesis was therefore to investigate therapeutic modulation of inflammation in stroke. In *Part One* of this chapter, data from this thesis will be discussed, including the model of cerebral I/R developed to investigate aberrant inflammation, and subsequent evidence indicating FPRs as a potential target in stroke therapy.

8.1.1 Modelling cerebral ischaemia/reperfusion

The initial aim of this work was to develop and validate a model of global cerebral I/R that would produce consistent, non-fatal L-E interactions in the cerebral microvasculature, able to be viewed through IVM (see *Chapter 3*). This process is evaluated in this section ('*Modelling cerebral ischaemia/reperfusion*').

*

The minimum requirement for global cerebral ischaemia is occlusion of both CCAs (the collateral paired carotid system would otherwise circumvent an obstruction to blood flow). In order to produce efficacy data for targeting the FPR system in stroke, BCCAO (Smith, Bendek et al. 1984) was used in this project. Complete global ischaemia cannot be achieved by this method, as the presence of the vertebral arteries in the posterior circulation means that the stroke occurs in the frontal lobe only (Wellons, Sheng et al. 2000). Intra-species variation in susceptibility is also likely to occur (Yoshioka, Niizuma et al. 2011); in 20 percent of 8-12 week old (23-28 g) C57BL/6 mice—as used in this project—blood flow is not reduced below a threshold of 13 percent. Blood flow greater than 13 percent is considered indicative of patent posterior communicating arteries (arteries in the Circle of Willis connecting the anterior and posterior circulation, the CCAs and vertebral arteries).

The advantages of the method, however, are in its inclusion of the two most critical arteries supplying the brain, the fact that these are superficial, and that the process involves comparatively few surgical targets. The latter is a more pertinent point when considering the requirement here for a model of reperfusion, where vessels must be occluded and reopened simultaneously without destruction of their walls and result-skewing systemic inflammation. In other models of BCCAO-induced I/R, silk threads (Ishikawa, Cooper et al. 2003), microvessel clips or clamps (Yang, Kitagawa et al. 1997, Murakami, Saito et al. 2005) have previously been used to occlude vessels, since these may be removed swiftly in order to halt ischaemia and instigate subsequent reperfusion injury through resumption of cerebral blood flow. Here, microvessel clips rather than silk threads provided a consistent occluding pressure for all animals, and allowed for vessel occlusion (and reopening) to be applied simultaneously.

Where IVM has previously been used, an ischaemic period of one hour plus between 40 min and 4 h reperfusion, with controlled ventilation and α-chlorolase (60 mg/kg)/urethane (600 mg/kg) anaesthesia, had caused cerebral tissue damage commensurate with a significant inflammatory response (Ishikawa, Cooper et al. 2003, Ishikawa, Sekizuka et al. 2007). Other groups, however, have shown that damage occurs after as little as 5 min (Yang, Kitagawa et al. 1997) and 3 min (Wellons, Sheng et al. 2000) of ischaemia, and that seizures regularly occur in C57BL/6 mice after 20 min (Yoshioka, Niizuma et al. 2011). Groups also show that mortality in C57BL/6 mice reaches 75-80% (Yang, Kitagawa et al. 1997, Kitagawa, Matsumoto et al. 1998) before one hour of BCCAO-induced ischaemia is reached (which corresponds to high mortality levels seen in the preliminary work of this project). In addition to the poor cerebral blood flow (as observed through IVM) in mice after longer ischaemic durations (in *Chapter 3* only), these were the premises for our chosen, shorter duration of 5 min.

Careful selection of general anaesthesia is essential during severe surgical experiments, when hypothermia (Minamisawa, Mellergard et al. 1990), blood pressure fluctuations (Castillo, Leira et al. 2004) and respiratory depression may impact results and mortality. An anaesthetic must be safe, effective and cost-effective as well as have a defined dose and route of administration that produces consistent results. Through stroke experiments in *Chapters 3-5*, access was limited to injectable rather than inhalable anaesthetics. After preliminary experiments using ketamine (150 mg/kg)/xylazine (7.5 mg/kg) i.p., pentobarbital sodium (100 mg/kg) was used in *Chapters 4-5*. Although the recovery period from barbiturates may be several hours, the procedure required only terminal anaesthesia (i.e. there were no recovery/post-operative animal welfare aspects to consider) (Wolfensohn and Lloyd 2007).

The mortality rate when using ketamine/xylazine anaesthesia through initial surgeries reached 100 percent, necessitating an alternative despite the combination providing sufficient anaesthesia in previous work (Gavins, Hughes et al. 2012). Although ketamine/xylazine was only used during experiments in which animals received 60 min ischaemia, under the same conditions only 33 percent of mice died with pentobarbital sodium anaesthesia. Experimental stroke has been noted to increase salivary secretion (Hockstein, Samadi et al. 2004), which is also a prevalent side effect of ketamine anaesthesia. Inhalation of excess saliva may be fatal, which could explain the high mortality seen with ketamine/xylazine use. In addition, ketamine causes respiratory depression with light surgical anaesthesia alone (Wolfensohn and Lloyd 2007); while pentobarbital sodium may also cause some respiratory depression, this did not appear to affect mortality. Moderate respiratory depression would increase the level of hypoxia (particularly after one hour deep

anaesthesia), but as all animals would be affected equally, this was not considered relevant enough to disregard an otherwise effective anaesthetic.

The established model used male C57BL/6 mice (due to their relatively narrow posterior communicating artery and the availability of $Fpr2/3^{-/-}$ mice on a C57BL/6 background) anaesthetised with 100 mg/kg pentobarbital sodium and subjected to 5 min BCCAO-induced ischaemia using microvessel clips. The following 40 minute and two hour reperfusion periods fulfilled the aim of producing consistent increases in L-E interactions up to 15-fold that of sham operated groups, with low mortality in accordance with the 'Three Rs'. This model was then used to investigate the role of FPRs in cerebral I/R.

8.1.2 FPR agonists: which, when and how much?

Having established that ROS and other reactive by-products of the immune response negatively affect stroke patient outcome, it is logical to target inflammation therapeutically. This could be achieved through reducing characteristic L-E interactions or through inhibition of CAMs/pro-inflammatory cytokines, and so limiting leukocyte extravasation into the parenchyma—but these have been tried before without success (see section 1.1.3).

Figure 33 is a simplified representation of an inflammatory process. It illustrates two potential methods for targeting inflammation: inhibition of pro-inflammatory mediators, and enhancing endogenous pro-resolution mechanisms. Where anti-inflammatory treatments have failed previously, the following section (*FPR agonists: which, when and how much?*) addresses the possibility that this is due to the pre-clinical focus on inhibition of pro-inflammatory circuits rather than enhancing resolution. A level of inflammation is clearly integral to the clean-up operation following necrotic/apoptotic cell death during ischaemia, and winding this up efficiently seems to be beneficial. FPRs are a central component of endogenous resolution—are members of the FPR family suitable pharmacological targets for modulating inflammation? When is best to administer treatment? And which dose is best? These questions are discussed below in the context of this thesis (*Chapters 4*-5) and wider literature, providing evidence that an FPR2/ALX-centred anti-inflammatory treatment could be beneficial in ischaemic stroke.

*

To assess the efficacy of FPR ligands in modulating inflammation in cerebral I/R, treatments ($AnxA1_{Ac2-26}$, LXA_4 and 15-epi-LXA_4) were administered at the start of a reperfusion period, and L-E interactions monitored at the end of reperfusion (see *Chapter 4*). Peptide $AnxA1_{Ac2-26}$ is an AnxA1 pharmacomimetic, able to act through all members of the FPR family, although this is tissue specific. LXA_4 and 15-epi-LXA_4 (LXA_4 epimer) are anti-inflammatory eicosanoids, well characterised as a ligands for FPR2/ALX (mouse orthologue Fpr2/3).

Previous work has demonstrated cardioprotection following i.v. doses of 15-epi-16-(parafluoro)-phenoxy LXA_4 methyl ester (LXA_4 analogue) equivalent to 5 and 10 µg per mouse in a C57BL/6 mouse model of myocardial infarction (Gavins, Kamal et al. 2005). We observed a reduction in L-E interactions 40 min into reperfusion using just 0.5 and 4 µg, although the effects were

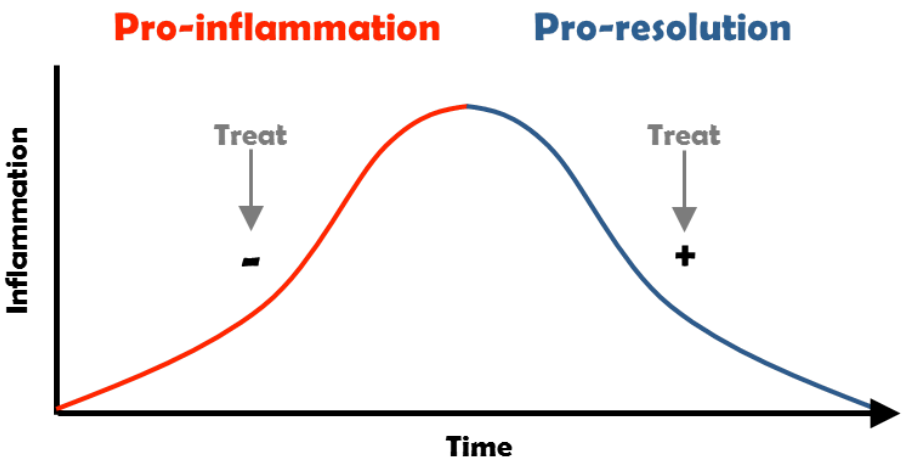

Figure 33. Therapeutic options for targeting inflammation (Smith Unpublished). During the course of an acute inflammatory episode, as associated with cerebral ischaemia/reperfusion, cellular activity promotes either a pro-inflammatory or pro-resolution environment. Each is mediated through endogenous components, which may be inhibited (pro-inflammation) or enhanced (pro-resolution) in order to reduce inflammation.

sustained until 2 h with the higher dose only (see section 4.2.2). Anti-inflammation following treatment with the lower dose could be restored to some extent if L-E interactions were observed closer to the time of drug administration; that is, a reduction in inflammation could only be seen at 2 h reperfusion when 15-epi-LXA_4 was given 40 min into reperfusion, rather than at the start.

In these subsidiary groups, however, vehicle (saline plus ethanol; 'vehicle 2' in *Chapter 4*) treatment itself also reduced interactions when given at 40 min. It is possible that the increased blood pressure caused by a bolus of liquid at this time point will be neuroprotective due to improved reperfusion, as observed elsewhere (Hillis, Ulatowski et al. 2003, Castillo, Leira et al. 2004). Alternatively, the ethanol itself may be protective: while the link between heavy alcohol consumption and stroke risk is well established, light-to-moderate consumption may be protective (Reynolds, Lewis et al. 2003, Collins, Neafsey et al. 2009). Ethanol treatment has also been shown experimentally to be protective when administered at various time points during a reperfusion period, following MCAO in rats (Wang, Wang et al. 2012). In this work by Wang and colleagues, 0.5-1.5 g/kg ethanol was used (approximately equivalent to 12.5-37.5 µl for a 25 g mouse) with dose-dependent increases in protection. The vehicle for 15-epi-LXA_4 used in this project included 17 µl ethanol per mouse, indicating potential for protection. Cytokine expression data in section 4.2.3.1 for groups treated with vehicle 2—albeit for animals treated at the beginning rather than start of reperfusion—correlate with this; IL-6 is increased in vehicle 1 (saline only) versus vehicle 2 treatment groups by 3-5 times (depending on the length of the reperfusion period).

LXA_4 at both 0.1 and 1.0 µg/mouse had no anti-inflammatory effect in this model versus vehicle-treated mice. This does not correlate with the reduction in inflammation seen by Perretti and colleagues following i.v. LXA_4 treatment in an alternative model of acute inflammation (air pouch/zymosan peritonitis) (Dufton, Hannon et al. 2010). There are two possible explanations for these results: the selected doses of LXA_4 were not sufficient to stimulate a response, or LXA_4 is not active in this model. The latter is more probable: rapid metabolic inactivation of LXA_4 occurs through oxidation/reduction at three points in the molecule, reducing its potency and affinity for FPR2/ALX (Clish, Levy et al. 2000). In light of this, the Serhan group and the majority of others preferentially use stable LXA_4 analogues in their work (Serhan, Takano et al. 1999, Levy, Lukacs et al. 2007). Endogenously, a short half-life of LXA_4 is incidental, as para-/autocrine signalling within this system does not require that its components be transported in the blood for anatomical miles without degrading. Experimentally, the extent of brain tissue which must be reached by an intravenous bolus of LXA_4 in global cerebral I/R is likely to be too distant and dispersed for there to be any significant LXA_4-FPR2/ALX binding.

We also observed a reduction in L-E interactions (in adhesion only at 40 min, but in both rolling and adhesion to a remarkable level at 2 h) after treatment with $AnxA1_{Ac2-26}$ (see section 4.2.1). It has been suggested that glucocorticoid-induced AnxA1 may cause leukocyte detachment from endothelia through shedding of L-selectin (a leukocyte-bound mediator of cell rolling) (Strausbaugh and Rosen 2001, de Coupade, Solito et al. 2003), which may be the case here.

Following observation of these anti-inflammatory effects, combined treatment of $AnxA1_{Ac2-26}$ with Boc2 (a pan-antagonist of FPRs) or WRW4 (an FPR2/ALX-selective antagonist) suggested that the anti-adhesive effects of the peptide were occurring through Fpr2/3. Not only was anti-inflammation abrogated, but a four-fold increase in rolling versus vehicle-treated groups was seen at 40 min in mice treated with either antagonist alone, suggesting a pro-inflammatory agonistic activity through Fpr2/3.

At 2 h , however, while both antagonists abrogated the anti-adhesive effects of $AnxA1_{Ac2-26}$, inflammation was significantly lower than in vehicle-treated groups. Unexpectedly, this trend was mimicked by Boc2/WRW4 treatments alone. The two-hour data sets therefore make little sense independently, considering WRW4 is a characterised FPR2/ALX antagonist and Boc2 an FPR pan-antagonist, and both would be expected to produce inflammatory levels equal to or above vehicle groups.

A possible explanation for low inflammation in antagonist groups at 2 h is that the 5 min ischaemia is enough to produce a limited level of inflammation, which can be pharmacologically manipulated into shorter, intense L-E activity. As the ischaemic insult is not tonic, the inflammatory episode has entered the resolution phase by 2 h in these groups (that is, the bell curve in Figure 33 is contracted). Exaggerated acute activity brought about by the antagonists may have a direct and/or indirect cause: on WRW4-binding, Fpr2/3 may elicit down-stream signalling cascades that directly induce leukocyte activation. This could be through p38 MAPK and JNK signalling, as is the case with serum amyloid A (a pro-inflammatory FPR2/ALX agonist) (Lee, Kim et al. 2010). Alternatively, antagonists may block endogenously produced anti-inflammatory ligands binding to Fpr2/3. The latter is implicated by an increase in total and cleaved AnxA1 expression in animals following stroke seen in Western-blotting data (see sections 4.2.1.2 and 4.2.2.3 and supported by (Brancaleone, Dalli et al. 2011), which indicates an endogenous role for the protein in this model (thus an implied requirement for AnxA1 receptor—FPR2/ALX—availability).

To understand the progression of L-E interactions between 40 min and 2 h following WRW4 treatment (the group which had produced the most pronounced 'high inflammation at 40 min/low

at 2 h ' trend), longitudinal experiments were conducted on mice between the two time points (see section 5.2.2.2). The data demonstrate that the high numbers of rolling cells in mice after 40 min reperfusion following WRW4 treatment gradually dissipate towards 2 h , and that the number of adherent cells peaks between the two time points. The vehicle treatment groups exhibit very different cellular activity: the number of rolling cells never encroaches on levels seen in the WRW4 treatment group at 40 min, but the number of adherent cells gradually accumulates to a level which is greater than the WRW4 group at 2 h .

The pronounced pro-inflammatory activity subsequent to antagonist treatment described above, as well as agonist, treatment time and dose-dependent differences in outcome illustrate the delicate nature of targeting FPR2/ALX. This is supported by wider literature, in which outwardly contradictory consequences of $AnxA1_{Ac2-26}$ activity in particular are described. While the anti-inflammation triggered by $AnxA1_{Ac2-26}$ treatment and endogenous AnxA1 expression is established, evidence also indicates a pro-inflammatory role for cleaved AnxA1 (33 kDA) in neutrophil transmigration across endothelia (Williams, Milne et al. 2010). AnxA1 in this pro-inflammatory capacity is N-terminally-truncated by proteolytic cleavage (following exocytosis/cell-surface expression), which suggests that an AnxA1 pharmacomimetic based on its N-terminal (rather than the full-length protein) may be more suitable therapeutically. This is confounded to an extent by the ability of $AnxA1_{Ac2-26}$ to act through all members of the FPR family (that is, including pro-inflammatory FPR1), while full-length AnxA1 is FPR2/ALX-selective (Ye, Boulay et al. 2009). Despite this, IVM data in *Chapters 4-5* as well as data in the literature indicate the primary role of the N-terminal peptide as anti-inflammatory. Despite possible dose-dependent responses from $AnxA1_{Ac2-26}$ treatment, this suggests that AnxA1 N-terminal peptides have pro-resolving therapeutic potential.

Pro-/anti-inflammatory $AnxA1_{Ac2-26}$ activity is further nuanced by cell-specific activity. Chemotaxis is broadly a pro-inflammatory process, control over which may reduce overall inflammatory levels. Yet data here show a very large increase in expression of chemotactic protein MCP-1 following $AnxA1_{Ac2-26}$ treatment (see section 4.2.3.1). Although encouraging the movement of neutrophils to sites of inflammation is evidently pro-inflammatory, an increase in MCP-1 expression may be an example of $AnxA1_{Ac2-26}$ as a pro-*resolution* agent; MCP-1 is specifically involved in the chemoattraction of monocytes—the phagocytosing, noxious material-disposing cells, vital for efficient resolution. This is interesting in conjunction with data in section 6.2.2 showing increased human monocyte migration following $AnxA1_{Ac2-26}$ pre-treatment, and work by McArthur and colleagues (McArthur, Reutlingsperger et al. 2012), which describes delayed monocyte migration

in AnxA1$^{-/-}$ mice and a role for AnxA1 in monocyte chemotaxis. It is, however, contradicted by earlier work that suggests AnxA1 interferes with monocyte adhesion (Solito, Romero et al. 2000) and transendothelial migration (Perretti, Ingegnoli et al. 2002), and that AnxA1$^{-/-}$ mice have increased MCP-1 expression (Gavins, Dalli et al. 2007). More work is required to investigate the effect of AnxA1 and related peptides on monocyte chemotaxis and migration—could this be model or dose-dependent?

Cytokine expression data in section 4.2.3.1 also strongly indicate an increase in IL-6 following AnxA1$_{Ac2-26}$ treatment. High plasma concentrations of IL-6 (10+ pg/ml) in acute phase stroke have been demonstrated to correlate with poor clinical outcomes (Waje-Andreassen, Krakenes et al. 2005). This is could be a matter of concern, yet there is an abundance of evidence for an anti-inflammatory role for IL-6 (Tilg, Trehu et al. 1994, Xing, Gauldie et al. 1998), partly through an increase in anti-inflammatory IL-10 and possibly MCP-1 levels (Biswas, Delfanti et al. 1998, Steensberg, Fischer et al. 2003)—interestingly IL-10 and MCP-1 are also increased in AnxA1$_{Ac2-26}$ treatment groups. Further work is required here to clarify both a possible link between AnxA1$_{Ac2-26}$ treatment, IL-6 expression and stroke outcome, and an endogenous link between AnxA1, MCP-1 and monocyte chemotaxis in the context of inflammation resolution in a variety of models. In both cases, the potential influence of such links on the pharmacological use of AnxA1-mimetics should also be investigated.

AnxA1$_{Ac2-26}$ and 15-epi-LXA$_4$ are undeniably useful in characterising a role for FPR2/ALX in I/R. Data in *Chapters 4-5* suggest they may be effective in reducing I/R injury following stroke, but also that determining optimal time points for administration is necessary before translation to the clinic. Anti-inflammatory/pro-resolution activity of these ligands has been declared widely in other models (Gavins, Dalli et al. 2007, El Kebir, Jozsef et al. 2009, Ye, Wu et al. 2010), and is demonstrated here, validating future work into FPR2/ALX mechanisms for development of a stroke therapy (see *Part Two*). The data discussed here and in the following section (8.1.3) are summarised in Figure 34A.

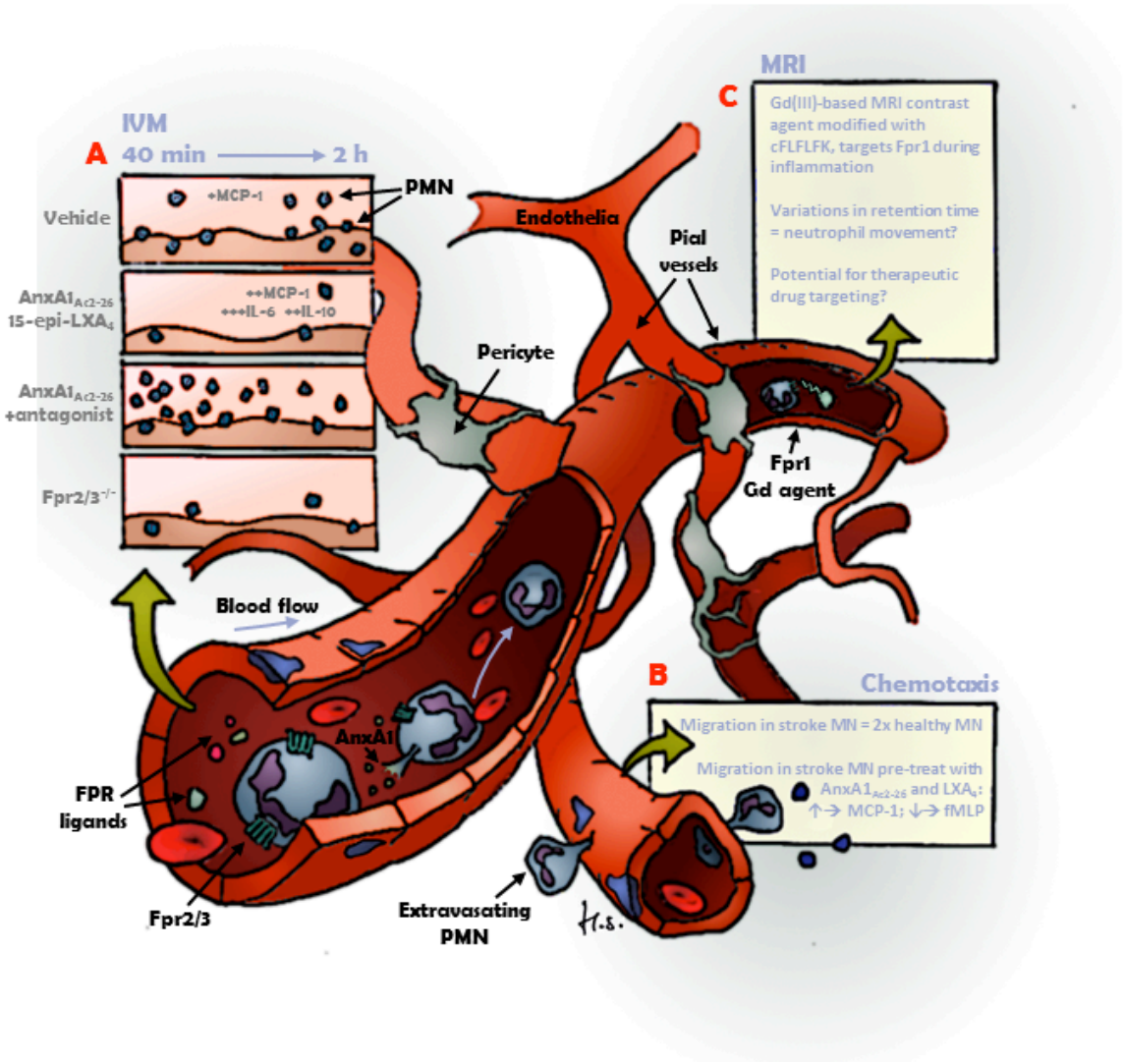

Figure 34. Mouse cerebral microvasculature; summary of thesis (Smith Unpublished). This thesis investigated the potential in FPR-targeted stroke treatments. *Chapters 3-5* describe administration of various FPR ligands and their effects on leukocyte-endothelial (L-E) interactions (A) in a model of global cerebral ischaemia reperfusion (5 min ischaemia/40 min or 2 h reperfusion). Vehicle treatment (saline/saline plus ethanol) increased L-E interactions at 40 min and adhesion more so at 2 h. Both $AnxA1_{Ac2-26}$ and 15-epi-LXA_4 (but not LXA_4) reduced these levels to those seen in sham-operated animals; $AnxA1_{Ac2-26}$ was more effective at 2 h and anti-inflammation through 15-epi-LXA_4 treatment was only sustained at 2 h in a higher dose treatment group (4 µg vs. 0.5 µg/mouse). Co-treatment of agonists with an FPR antagonist (FPR2/ALX-selective and pan-FPR)

abrogated the anti-inflammatory effects, but treatment with antagonist alone produced lower levels of L-E interactions than vehicle groups at 2 h. Longitudinal studies showed a contracted inflammatory process in these groups, with resolution being instigated by 2 h. Studies using Fpr2/3$^{-/-}$ mice (as compared with C57BL/6 mice due to lack of available wild types) showed low levels of inflammation but 100% mortality after 3 h (versus 60% in C57BL/6 mice). In agonist treatment groups, AnxA1$_{Ac2-26}$ induced an increased in expression of endogenous full-length AnxA1 and produced considerable increases in serum levels of MCP-1, IL-6 and IL-10. The second section of this thesis (*Chapter 6*) compares the intrinsic migratory properties of monocytes (MN) from stroke patients vs. healthy controls (B). Migration in stroke monocytes was twice that of healthy monocytes, and pre-treatment of cells with either AnxA1$_{Ac2-26}$ or 15-epi-LXA$_4$ caused increased migration towards MCP-1 and decreased towards fMLP. Finally, *Chapter 7* describes preliminary data using a specifically designed MRI contrast agent, targeting FPR1/Fpr1 (C). Retention times of the agent across the body would allow tracking of FPR1-expressing inflammatory cell activity over several hours. As well as the physiological information this provides, it may enable directed treatment in patients. PMN, polymorphonuclear cell.

8.1.3 FPRs, chemotaxis and visualising inflammation

In addition to the central studies in *Chapters 3-5* described above, two subsidiary projects were conducted in conjunction with FPRs, I/R and imaging (see *Chapters 6-7)*. The opportunity arose to retrieve blood samples from stroke patients, from which monocytes were extracted then assessed for migratory properties under various conditions. Secondly, collaboration with chemists led to the production of an FPR1-targeted contrast agent, which was used to track leukocyte movement in mice following an inflammatory insult. The results from these experiments are discussed in this section ('*FPRs, chemotaxis and visualising inflammation*') and illustrated in Figure 34B/C.

*

Monocytes are central to the inflammatory process, and their increased migration towards sites of injury is observed in stroke as well as in other inflammatory situations. Within an infarct, monocytes may release TNFα, nitric oxide synthase and various proteolytic enzymes, which exacerbate tissue damage. In later stages of inflammation, however, monocytes are integral to the resolution phase, during which they release anti-inflammatory mediators, perform phagocytosis and promote non-phlogistic apoptosis of dead cells. *Chapter 6* examines the chemotaxis of monocytes (from stroke patients and healthy controls) towards MCP-1, MIP-1α and fMLP, following pre-treatment with FPR ligands. Below explores the hypothesis that during stroke, peripheral monocytes possess greater intrinsic migratory potential—are there differences between monocytes collected from stroke patients versus healthy controls? And crucially, are FPR ligands able to modulate monocyte chemotaxis?

Using an *in vitro* model of chemotaxis/transendothelial migration (see section 2.3.2.3), monocyte migration towards MCP-1, MIP-1α and fMLP was confirmed in accordance with published data. In initial experiments using healthy monocytes, each chemoattractant enhanced directed monocyte migration: of the concentration ranges used (MCP-1, 12.5-100.0 ng/ml; MIP-1α, 25.0-100.0 ng/ml and fMLP, $1x10^{-9}$-$1x10^{-6}$ M), migration was optimal towards chemoattractants at 12.5 ng/ml, 50.0 ng/ml and $1x10^{-6}$ M, respectively—none produced a linear positive correlation between concentration and monocyte movement. While all other concentrations produced either significantly increased migration or a clear trend towards it, the higher two concentrations of fMLP produced migration equivalent only to the spontaneous migration observed towards the vehicle (RPMI). This is in agreement with other work (Resnati, Pallavicini et al. 2002), which describes an

inhibitory effect on migration towards higher doses of fMLP (possibly due to receptor downregulation).

Selecting the optimal doses of MCP-1 and fMLP above (MCP-1 as a producer of the largest significant increases in monocyte migration and fMLP for its role as an FPR ligand), activity in monocytes from stroke patients (<96 h post-stroke onset) was compared with that of healthy controls (see section 6.2.2).

Migration by monocytes from stroke patients was either two (towards fMLP) or four (towards MCP-1) times the level observed with monocytes from healthy controls, when neither received pre-treatment. This indicates that circulating monocytes develop enhanced chemotactic potential in response to systemic inflammation/cytokine release, secondary to the localised stroke (Ormstad, Aass et al. 2011). This has been observed in under other inflammatory conditions (Simmons, Brown et al. 1987, Offner, Subramanian et al. 2006) and may occur through varied mechanisms, including increased TNFα, IL-12, IL-6 and IL-8 expression (Kostulas, Kivisakk et al. 1998, Kouwenhoven, Carlstrom et al. 2001), or up-regulation of CCR2 (the MCP-1 receptor, therefore specific to MCP-1) (Offner, Subramanian et al. 2006).

Migration towards fMLP was increased in monocytes from stroke patients versus healthy controls. Although fMLP is a bacterial chemotactic peptide, not involved in the sterile inflammation of stroke, human formylated peptides are released from damaged mitochondria. These mitochondrial peptides are equally active through FPR1 and FPR2/ALX (Rabiet, Huet et al. 2005). fMLP was used to investigate a role for FPRs in intrinsic monocyte activation, despite the bacterial peptide preferentially binding FPR1 (Kinzer-Ursem, Sutton et al. 2006), as both receptors have similar roles in leukocyte chemotaxis and are upregulated on monocytes following stroke (Grond-Ginsbach, Hummel et al. 2008).

To investigate a role for FPR ligands in modulating migration, cells were pre-treated with $AnxA1_{Ac2-26}$ and LXA_4. Migration towards fMLP was decreased in monocytes from stroke patients pre-treated with $AnxA1_{Ac2-26}$ and further (by half) in LXA_4 pre-treated cells, possibly through receptor desensitisation of FPRs or chemoattractant receptors (Walther, Riehemann et al. 2000). This contrasts with behaviour of cells migrating towards MCP-1, for which $AnxA1_{Ac2-26}$ doubled migration and LXA_4 had no effect versus the vehicle pre-treated group. The lack of activity in LXA_4 versus $AnxA1_{Ac2-26}$ groups may represent an FPR1-specific response to $AnxA1_{Ac2-26}$, as the peptide is able to activate all members of the FPR family, whereas LXA_4 is FPR2/ALX-selective. Also notable here is that *in vivo* work (see section 4.2.3.1) showed a large increase in serum levels of MCP-1

following $AnxA1_{Ac2\text{-}26}$ treatment. These data demonstrate differential activity of FPR agonists within different environments, involving fMLP plus $AnxA1_{Ac2\text{-}26}$/FPR, and MCP-1/CCR2, $AnxA1_{Ac2\text{-}26}$/FPR—possibly reflecting pro-inflammatory/pro-resolution phases of an inflammatory episode and/or receptor crosstalk (Bennett, Fox et al. 2011).

Migration in monocytes from healthy controls followed similar trends to stroke monocytes, with the exception of $AnxA1_{Ac2\text{-}26}$ pre-treated cells towards fMLP (these showed an increase in migration versus the vehicle pre-treated group, compared with a decrease in migration by stroke cells). It is only LXA_4, therefore, that produced a consistent reduction in migration in both stroke and healthy monocytes. While anti-migratory properties of LXA_4 on neutrophils and other PMN cells are established (Chiang, Serhan et al. 2006), other *in vitro* data show that monocytes are activated by the eicosanoid (Maddox and Serhan 1996, Maddox, Hachicha et al. 1997). These represent both the anti-inflammatory and pro-resolving roles of LXA_4. The discrepancy between data in this thesis and in the cited publications is the precise use of LXA_4; work by Serhan and colleagues uses LXA_4 in the lower well of the chemotaxis chamber, creating a gradient for monocyte movement from the upper well, whereas in *Chapter 6*, cells are pre-treated with LXA_4, potentially retaining monocytes in the upper well.

Work using the chemotaxis chamber has clearly demonstrated an increase in the intrinsic migratory capacity of monocytes after stroke, and that this can be modulated using FPR agonists. Appropriately timed monocyte transmigration into the parenchyma is key in efficient resolution of inflammation following stroke. Further work is required to clarify the effects of FPR agonists, using either *in vivo* studies or a more complex cocktail of chemoattractants (that is, not fMLP or MCP-1 independently) in the lower well of the chamber, to represent an *in vivo* situation.

*

Visualising leukocyte movement during inflammation *in vivo* may be of great use in targeting or personalising therapies in the clinic. FPR1 is expressed on human neutrophils and monocytes, and Fpr1 on murine neutrophils (as well as several other tissue/cell types; see section 1.3.1.2). FPR1 is constitutively expressed (Wenzel-Seifert, Hurt et al. 1998), but the *FPR1* gene/FPR1 mRNA is upregulated under inflammatory stress (exposure to LPS, for example) (Mandal, Novotny et al. 2005), making the receptor an ideal target for an imaging agent intended to track leukocyte activity through an inflammatory process. *Chapter 7* describes the use of an FPR1-targeted MRI contrast agent in mice following an LPS challenge. MRI is used clinically in the diagnosis of several pathologies, such as heart disease (Donahue, Burstein et al. 1994), cancer (Sukerkar, MacRenaris

et al. 2011) and musculoskeletal disorders (Blemker, Asakawa et al. 2007) as well as stroke (Fiebach, Schellinger et al. 2002). It provides detailed structural images of tissue, organs and blood flow in the subject through measuring the relaxation rate of protons within water molecules, which manifests in varying black-and-white contrast across an image. This contrast may be enhanced by the use of certain ionic metals such as Gd(III) within a stable organic chelate (or case), either non-specifically or in regions of a specific target, if the chelate is engineered to contain the ligand for a target receptor (Caravan 2006, Mewis and Archibald 2010). Using this premise, a contrast agent was generated which was bound to cFLFLFK, a high affinity ligand for FPR1/Fpr1 (Stasiuk, Smith et al. 2013).

Preliminary work using LPS (10 µg per mouse) to generate ubiquitous inflammation showed that the contrast agent was retained in the body and that longitudinal image acquisitions would enable tracking of the contrast agent. Future work using this technique would be best used with an internal control for each mouse (i.e. using an asymmetrical lesion rather than a comparison of an inflamed mouse versus a healthy control). For example, Figure 28D (p.117) illustrates a model of unilateral myositis in which an LPS injection into one flank only enables the other flank to stand as a suitable control. Ultimately this could be applied to a unilateral model of stroke such as MCAO, potentially revealing neutrophil activity under varying conditions (different ischaemic durations or treatments, for example), as well as the involvement of FPR1.

8.2 Part Two: the future for FPR2/ALX

The aim of this thesis was to characterise a role for FPR2/ALX in the resolution of inflammation in a model of cerebral I/R and so to provide evidence for an FPR2/ALX-targeted stroke therapy. *Part Two* describes potential further work, which would involve a combination of the three strategies listed below and are loosely based on varying/expanding the treatment regimen, the stroke model or the disease:

1. Treatment regimen: focusing on the most promising FPR ligand for use in the model of global cerebral I/R, with experiments designed to acquire detailed dose-response data and optimal treatment times—possibly using longitudinal groups (see WRW4 groups in section 5.2.2.2).
2. Model: replicating agonist and agonist-plus-antagonist experiments described in *Chapters 4-5* in other stroke models (MCAO or BCCAO plus hypoxia, for example); in female mice; in aged mice; in comorbid mice or in other species/mouse strains, and incorporating function/behavioural studies.
3. Disease: apply the same treatment combinations in other models of inflammation, including other models of general pathogenic and sterile inflammation.

The agonist/dose-dependent variations described in *Part One* raise questions regarding how anti-inflammatory treatments might be used in the clinic—which dose to use, when to administer and perhaps how frequently—for optimal results. These aspects are also discussed in *Part Two*, along with the outlook for future FPR-related stroke research and novel promising therapies.

8.2.1 Continuation of this work

Varying points 1 and 2 (treatment regimen and stroke model) are certainly priorities in establishing the potential of an FPR-targeted stroke therapy. While point 3 is important, the variety of disease models being tested with respect to FPRs is extensive, including (among others) emphysema (Cardini, Dalli et al. 2012), Alzheimer's Disease (Cui, Le et al. 2002) and sepsis (Kim, Kim et al. 2010). The extension of this body of work would therefore be of more practical use if concentrated on stroke research.

Key findings of this thesis strongly indicate the importance of expanding treatment regimens and the stroke model. Variation of outcome based on dose and time of treatment (15-epi-LXA_4; see section 4.2.2.2), as well as agonist used ($AnxA1_{Ac2-26}$, LXA_4 and 15-epi-LXA_4; see sections 4.2.1.1, 4.2.2.1 and 4.2.2.2), implies that treatments need to be investigated further. The impact $AnxA1_{Ac2-26}$ treatment had on cytokine expression (see section 4.2.3.1) and the difference in expression patterns following administration of the peptide versus 15-epi-LXA_4 could also be investigated further with respect to agonist doses. Do the effects indicate differing mechanisms or are they simply dose-dependent? Would a larger dose of 15-epi-LXA_4 produce a similar increase in MCP-1, IL-6 and IL-10?

Differences in inflammation levels between time points (particularly antagonist groups; see section 5.2.2) imply that the treatments could be applied in a different/expanded stroke model. This may include use of an MCAO model and observation of additional time points during reperfusion. Broader information with respect to the model used is particularly vital, considering limitations with models have been such a source for failure with previous stroke treatments (see section 1.1.3). Parameters such as MABP, $PaCO_2$, PaO_2 and cerebral blood flow could also be measured for further insight into treatment mechanisms. Several studies have used models that assess early cell damage and infarct volumes. Although important, these approaches have had little capacity to measure improved functional outcome (Alessandrini, Namura et al. 1999, Yepes, Sandkvist et al. 2000). The huge survival rate of those affected by stroke has channelled research into the fields of neuroprotection and regeneration of tissue (Smith and Gavins 2012), necessitating animal models in which neural repair and functional/behavioural recovery can be demonstrated. In rodents, the MCAO model produces a delineated infarct (with the potential for modulation of infarct volume therapeutically), and allows for flexibility in ischaemic duration producing a non-fatal lesion with

significant functional/behavioural deficits. Further experiments could therefore combine MCAO data with BCCAO data.

Future work using the BCCAO or MCAO model of stroke could be conducted longitudinally, as in the WRW4 experiments of section 5.2.2.2. There is potential for the use of permanent cranial windows (Levasseur, Wei et al. 1975) (with the milder MCAO surgery), which would enable viewing of the cerebral microvasculature in the same mice—even the same vessels—over several hours, days and potentially weeks. This would allow the continual observation of the progression of L-E interactions and reduce the overall numbers of animals needed.

In such experiments with longer reperfusion times, anaesthetic should also be changed. Inhalation anaesthetics are generally preferable where recovery of the animal is anticipated. These drugs are eliminated via the lungs, whereas injected anaesthetics are metabolised by the liver, which takes considerably longer. A quick recovery is ideal, in order to hasten endogenous control over post-operative aberrations in normal physiology (in body temperature and blood pressure, for example). Reversal agents to injectable anaesthetics are also now widely available and should ideally be used (Wolfensohn and Lloyd 2006)(Wolfensohn and Lloyd 2006)(Wolfensohn and Lloyd 2006)(Wolfensohn and Lloyd 2006).

The severity of the BCCAO surgery would make MCAO preferable in assessing improved survival and functional outcome—both of which must be demonstrated in any potential treatment. A variety of tests could be used, including motor and somatosensory function tests, and those assessing asymmetry of movement (MCAO only). The cylinder test is particularly useful in studying spontaneous forelimb use, for which a rodent is placed in a glass cylinder and individual front paw placements are counted as they explore the cylinder vertically (Li, Blizzard et al. 2004). While a healthy mouse will use each paw approximately half the time, this will be biased towards the paw on the side ipsilateral to the infarct (due to neuronal crossing) in mice post-MCAO. This assessment is simple, objective and has the capacity to illustrate grey areas in the severity of brain damage, and therefore mild improvements.

Other tests include the Bederson scale and other neurological scoring tests, which are useful in their ability to assess a range of behavioural facets, yet often require subjective categorising of an animal into one of as few as four categories (Schaar, Brenneman et al. 2010). A binary outcome with respect to survival could also be measured, using a threshold time point following stroke at which 75 percent (for example) of mice receiving no treatment are still alive, as a simple

comparison of improvement in treated mice. Ultimately a combination of functional/behavioural tests will be necessary, in order to draw out sufficient efficacy evidence from a pre-clinical model.

8.2.2 The outlook for targeting FPR2/ALX in stroke

With the exceptions of tPA and hypothermia under selective conditions, promising research into stroke therapies has so far been unproductive. The good news is that the transforming pathological processes throughout stroke and during subsequent weeks, months, and years present several opportunities for intervention as the disease progresses and also suggest that the most effective treatment may be a combined therapeutic approach. There are several treatments close to or entering clinical trials, which could be used in conjunction with a pro-resolving treatment. These include (but are not limited to) ROS inhibitors (Edaravone Acute Infarction Study 2003)—targeting primary ischaemic damage—and stem cells (Smith and Gavins 2012)—aiming to promote neuroregeneration.

The variation between human ischaemic duration, lesion volumes/locations, ages and comorbidities must be appreciated—even a treatment that is extremely successful experimentally may be far too prescriptive in its potential applications to have the impact hoped for in a stroke therapy. There are three key questions that must be addressed in establishing the potential of a novel stroke therapy—beyond the fundamental one of whether or not it works: when is a treatment best administered? How much needs to be administered (and will this vary between patients)? And who is likely to benefit?

In light of these, how effective is an FPR2/ALX-targeted therapy likely to be?

The use of clot buster is severely limited by the official 4.5 hour treatment window from stroke onset. An ideal therapy would be beneficial administered at any point, preferably in the ambulance and prior to lengthy diagnostic imaging, without the risk of exacerbating a haemorrhage. Although the efficiency of an FPR2/ALX ligand is likely to vary depending on when it is administered (see section 4.2.2.2), there is not the risk of haemorrhage. This means an anti-inflammatory treatment could potentially be given as soon as a patient is in contact with clinical staff, with few side effects anticipated.

Full investigations need to include detailed dose-response experiments as well as data concerning when is best to deliver treatment. Precisely when and how much treatment should be administered may well be established in the future through use of biomarkers—ideally several biomarkers—in order to generate ‘co-ordinates’ indicating the health status of a patient.

Many attempts have been made to identify suitable biomarkers in stroke, including several soluble agents. Changes in expression of endothelial junctional proteins indicate BBB breakdown, for example, therefore soluble BBB adhesion factors are potentially useful biomarkers of disease progression. Unfortunately the search for a suitable candidate has been unsuccessful so far. JAM subtype JAM-C predominates in human and mouse brain endothelia under healthy conditions and so is unsuitable (Williams, Martin-Padura et al. 1999, Arrate, Rodriguez et al. 2001, Sonobe, Takeuchi et al. 2009). JAM-A, although expressed in mouse brain endothelia (Sonobe, Takeuchi et al. 2009), is not detected in human brain under normal conditions but expressed in low amounts in certain abnormal conditions such as multiple sclerosis (Padden, Leech et al. 2007). In practice, these levels are not sufficient for JAM-A to be considered a suitable biomarker for BBB breakdown (Haarmann, Deiss et al. 2010).

For a biomarker to be particularly useful, it should be studied in conjunction with a potential therapy. It is far more useful, arguably, to link specific interleukin/soluble CAM levels with the suitability of a patient for a certain therapy, rather than their likelihood of a poor outcome. A marker of the progress of inflammation (i.e. where the process lies on the bell curve in Figure 33) will be extremely useful in optimising the pharmacological resolution of inflammation. It is possible that cleaved AnxA1 itself may be a good indicator of this (Lim and Pervaiz 2007), or serum levels of MCP-1 (Worthmann, Dengler et al. 2012).

A concern with any novel therapy is how many people will benefit. Many pre-clinical studies do not include aged animals with comorbidities such as hypertension, hypercholesterolaemia, obesity and diabetes, and the majority do not investigate whether or not females are likely to benefit. Several studies do accommodate these factors (Vannucci, Willing et al. 2001, Zhang, Nair et al. 2004, Soleman, Yip et al. 2012), but the high cost of keeping females (!) or elderly mice is often prohibitive, particularly in the early stages of investigating a particular compound.

Despite all these provisos, the future is bright for FPRs. Resolvins are Eα/Dα-derived eicosanoids, structurally and functionally similar to LXA_4 and active through FPR2/ALX (Figure 4, p.36). A resolvin analogue has recently been patented for use in the treatment of corneal inflammation, illustrating the potential in eicosanoid-FPR2/AX therapies (Lima-Garcia, Dutra et al. 2011, Pei, Zhang et al. 2011). Through this work, analgesic effects of AnxA1 and resolvins have also been observed. This therapy is topically applied, however, which highlights a potential drawback with eicosanid-FPR2/ALX treatments for stroke. The problem for biologists is not that the lipoxins are ineffective; it is that they are tremendously unstable outside a freezer and have a short half-life once inside an organism. Foreseeable logistical problems include proximity of -80 °C freezers to

patients and unknown levels of compound degradation—therefore dose—in unpredictable clinical circumstances. Stable analogues of the lipoxins are being generated and tested, and ultimately this is a hurdle for chemists, where collaborations will be beneficial.

*

The pathophysiological development of stroke involves interactions between numerous cell types over several hours, days and weeks, as described in section 1.1.2. A combination of therapies is ultimately likely to be of greatest benefit in stroke patients: clot dispersion, followed by mediation of a subsequent inflammatory response and neuro-/vasculogenesis, backed by solid imaging.

The preferred pro-resolving agent for use is yet to be identified, and considerations should be made about their stability and best route of administration into the patient, as well as the optimal time (should one exist) to administer the therapy. It is also important to identify mechanisms that can be used to enhance the resolution of inflammation, while still permitting an extent of pro-inflammatory activity in order to remove dead cells within the brain parenchyma. The use of pro-resolving agents as a stroke treatment is new, and their efficacy has yet to be disproved. Despite the failure of previous anti-inflammatory therapies in clinical trials, data describing the enhancement of endogenous resolution in this thesis and wider literature suggest a positive future for modulating FPR2/ALX as a therapy for stroke. The possibility that this treatment may not be as temporally restrictive as tPA is certainly encouraging.

The following is a quotation from pioneering endocrinologist Professor Hans Selye (1907-82), which I first heard used by Professor Nick Goulding in his 2012 *Paton Lecture* on stress at the *British Pharmacological Society* winter meeting. I have borrowed the phrase to close this thesis, as it captures perfectly the potential in targeting the resolution of inflammation. Each mention of 'stress' is replaced by 'inflammation', in the confidence that the two afflictions are so intertwined as not to corrupt Selye's sentiment:

> *"If I may venture a prediction…research on [inflammation] will be most fruitful if it is guided by the principle that we must learn to imitate—and if necessary correct and complement—the body's own autopharmacologic efforts to combat the [inflammation] factor in disease."*
>
> *—Hans Selye,*
> *(The General adaptation syndrome and the diseases of adaptation, 1946)*

Papers

The following papers have been published in conjunction with this thesis at the time of final submission, and are inserted after this page:

- 'Targeting the Melanocortin system for Anti-Stroke Therapy', *Trends in Pharmacology* (Feb 2011) Holloway PM*, **Smith HK***, Renshaw D, Flower RJ, Getting SJ, Gavins FNE. (*Joint first authors.)

- 'PISCES: the sign of things to come in stem cell therapy for stroke', *FASEB* (Mar 2012) **Smith HK**, Gavins FNE.

- 'Gd^{3+} cFLFLFK conjugate for MRI: a targeted contrast agent for Formyl Peptide Receptor 1 in inflammation', *ChemComm* (2012) Stasiuk GJ, **Smith HK**, Wylezinska-Arridge M, Lopez Tremoleda J, Trigg W, Kaur Luthra S, Morisson Iveson V, Gavins FNE, Long NJ.

The following paper is in preparation to be submitted 2013:

- 'Fpr2/Fpr3 mechanism reduces inflammation in a global model of stroke', **Smith HK**, Gavins FNE.

References

Abdelkarim, G. E., K. Gertz, C. Harms, J. Katchanov, U. Dirnagl, C. Szabo and M. Endres (2001). "Protective effects of PJ34, a novel, potent inhibitor of poly(ADP-ribose) polymerase (PARP) in in vitro and in vivo models of stroke." Int J Mol Med **7**(3): 255-260.

Adams, H. P., Jr., B. H. Bendixen, L. J. Kappelle, J. Biller, B. B. Love, D. L. Gordon and E. E. Marsh, 3rd (1993). "Classification of subtype of acute ischemic stroke. Definitions for use in a multicenter clinical trial. TOAST. Trial of Org 10172 in Acute Stroke Treatment." Stroke **24**(1): 35-41.

Adams, H. P., Jr., G. del Zoppo, M. J. Alberts, D. L. Bhatt, L. Brass, A. Furlan, R. L. Grubb, R. T. Higashida, E. C. Jauch, C. Kidwell, P. D. Lyden, L. B. Morgenstern, A. I. Qureshi, R. H. Rosenwasser, P. A. Scott and E. F. Wijdicks (2007). "Guidelines for the early management of adults with ischemic stroke: a guideline from the American Heart Association/American Stroke Association Stroke Council, Clinical Cardiology Council, Cardiovascular Radiology and Intervention Council, and the Atherosclerotic Peripheral Vascular Disease and Quality of Care Outcomes in Research Interdisciplinary Working Groups: the American Academy of Neurology affirms the value of this guideline as an educational tool for neurologists." Stroke **38**(5): 1655-1711.

Alessandrini, A., S. Namura, M. A. Moskowitz and J. V. Bonventre (1999). "MEK1 protein kinase inhibition protects against damage resulting from focal cerebral ischemia." Proc Natl Acad Sci U S A **96**(22): 12866-12869.

Alvarez, V., E. Coto, F. Setien and C. Lopez-Larrea (1994). "A physical map of two clusters containing the genes for six proinflammatory receptors." Immunogenetics **40**(2): 100-103.

Arai, K. and E. H. Lo (2009). "Experimental models for analysis of oligodendrocyte pathophysiology in stroke." Exp Transl Stroke Med **1**: 6.

Ardehali, M. R. and G. Rondouin (2003). "Microsurgical intraluminal middle cerebral artery occlusion model in rodents." Acta Neurol Scand **107**(4): 267-275.

Arrate, M. P., J. M. Rodriguez, T. M. Tran, T. A. Brock and S. A. Cunningham (2001). "Cloning of human junctional adhesion molecule 3 (JAM3) and its identification as the JAM2 counter-receptor." Journal of Biological Chemistry **276**(49): 45826-45832.

Arur, S., U. E. Uche, K. Rezaul, M. Fong, V. Scranton, A. E. Cowan, W. Mohler and D. K. Han (2003). "Annexin I is an endogenous ligand that mediates apoptotic cell engulfment." Dev Cell **4**(4): 587-598.

Aswanikumar, S., B. Corcoran, E. Schiffmann, A. R. Day, R. J. Freer, H. J. Showell and E. L. Becker (1977). "Demonstration of a receptor on rabbit neutrophils for chemotactic peptides." Biochem Biophys Res Commun **74**(2): 810-817.

Babior, B. M. (1984). "Oxidants from phagocytes: agents of defense and destruction." Blood **64**(5): 959-966.

Bacher, A., J. Y. Kwon and M. H. Zornow (1998). "Effects of temperature on cerebral tissue oxygen tension, carbon dioxide tension, and pH during transient global ischemia in rabbits." Anesthesiology **88**(2): 403-409.

Badolato, R., J. M. Wang, W. J. Murphy, A. R. Lloyd, D. F. Michiel, L. L. Bausserman, D. J. Kelvin and J. J. Oppenheim (1994). "Serum amyloid A is a chemoattractant: induction of migration, adhesion, and tissue infiltration of monocytes and polymorphonuclear leukocytes." J Exp Med **180**(1): 203-209.

Bae, Y. S., H. Y. Lee, E. J. Jo, J. I. Kim, H. K. Kang, R. D. Ye, J. Y. Kwak and S. H. Ryu (2004). "Identification of peptides that antagonize formyl peptide receptor-like 1-mediated signaling." J Immunol **173**(1): 607-614.

Bae, Y. S., E. Y. Park, Y. Kim, R. He, R. D. Ye, J. Y. Kwak, P. G. Suh and S. H. Ryu (2003). "Novel chemoattractant peptides for human leukocytes." Biochem Pharmacol **66**(9): 1841-1851.

Bao, L., N. P. Gerard, R. L. Eddy, Jr., T. B. Shows and C. Gerard (1992). "Mapping of genes for the human C5a receptor (C5AR), human FMLP receptor (FPR), and two FMLP receptor homologue orphan receptors (FPRH1, FPRH2) to chromosome 19." Genomics **13**(2): 437-440.

Barber, P. A., T. Foniok, D. Kirk, A. M. Buchan, S. Laurent, S. Boutry, R. N. Muller, L. Hoyte, B. Tomanek and U. I. Tuor (2004). "MR molecular imaging of early endothelial activation in focal ischemia." Ann Neurol **56**(1): 116-120.

Barkalow, F. J., M. J. Goodman and T. N. Mayadas (1996). "Cultured murine cerebral microvascular endothelial cells contain von Willebrand factor-positive Weibel-Palade bodies and support rapid cytokine-induced neutrophil adhesion." Microcirculation **3**(1): 19-28.

Baskaya, M. K., A. M. Rao, A. Dogan, D. Donaldson and R. J. Dempsey (1997). "The biphasic opening of the blood-brain barrier in the cortex and hippocampus after traumatic brain injury in rats." Neurosci Lett **226**(1): 33-36.

Becker, E. L., F. A. Forouhar, M. L. Grunnet, F. Boulay, M. Tardif, B. J. Bormann, D. Sodja, R. D. Ye, J. R. Woska, Jr. and P. M. Murphy (1998). "Broad immunocytochemical localization of the formylpeptide receptor in human organs, tissues, and cells." Cell Tissue Res **292**(1): 129-135.

Belayev, L., R. Busto, W. Zhao, G. Fernandez and M. D. Ginsberg (1999). "Middle cerebral artery occlusion in the mouse by intraluminal suture coated with poly-L-lysine: neurological and histological validation." Brain Res **833**(2): 181-190.

Bena, S., V. Brancaleone, J. M. Wang, M. Perretti and R. J. Flower (2012). "Annexin A1 interaction with FPR2/ALX: identification of distinct domains and downstream associated signalling." J Biol Chem.

Bennett, L. D., J. M. Fox and N. Signoret (2011). "Mechanisms regulating chemokine receptor activity." Immunology **134**(3): 246-256.

Bernard, S. A., T. W. Gray, M. D. Buist, B. M. Jones, W. Silvester, G. Gutteridge and K. Smith (2002). "Treatment of comatose survivors of out-of-hospital cardiac arrest with induced hypothermia." N Engl J Med **346**(8): 557-563.

Biswas, P., F. Delfanti, S. Bernasconi, M. Mengozzi, M. Cota, N. Polentarutti, A. Mantovani, A. Lazzarin, S. Sozzani and G. Poli (1998). "Interleukin-6 induces monocyte chemotactic protein-1 in peripheral blood mononuclear cells and in the U937 cell line." Blood **91**(1): 258-265.

Blemker, S., D. Asakawa, G. Gold and S. Delp (2007). "Image-based musculoskeletal modeling: Applications, advances, and future opportunities." Journal of magnetic resonance imaging **25**(2): 441-451.

Boden-Albala, B. and R. L. Sacco (2000). "Lifestyle factors and stroke risk: exercise, alcohol, diet, obesity, smoking, drug use, and stress." Curr Atheroscler Rep **2**(2): 160-166.

Bogen, S. A., H. S. Baldwin, S. C. Watkins, S. M. Albelda and A. K. Abbas (1992). "Association of murine CD31 with transmigrating lymphocytes following antigenic stimulation." Am J Pathol **141**(4): 843-854.

Bogousslavsky, J., G. Van Melle and F. Regli (1988). "The Lausanne Stroke Registry: analysis of 1,000 consecutive patients with first stroke." Stroke **19**(9): 1083-1092.

Borregaard, N. and J. B. Cowland (1997). "Granules of the human neutrophilic polymorphonuclear leukocyte." Blood **89**(10): 3503-3521.

Bottiger, B. W., C. Grabner, H. Bauer, C. Bode, T. Weber, J. Motsch and E. Martin (1999). "Long term outcome after out-of-hospital cardiac arrest with physician staffed emergency medical services: the Utstein style applied to a midsized urban/suburban area." Heart **82**(6): 674-679.

Bottiger, B. W., J. J. Krumnikl, P. Gass, B. Schmitz, J. Motsch and E. Martin (1997). "The cerebral 'no-reflow' phenomenon after cardiac arrest in rats--influence of low-flow reperfusion." Resuscitation **34**(1): 79-87.

Boucek, M. M. and R. Snyderman (1976). "Calcium influx requirement for human neutrophil chemotaxis: inhibition by lanthanum chloride." Science **193**(4256): 905-907.

Boulay, F., M. Tardif, L. Brouchon and P. Vignais (1990). "Synthesis and use of a novel N-formyl peptide derivative to isolate a human N-formyl peptide receptor cDNA." Biochem Biophys Res Commun **168**(3): 1103-1109.

Bousquet, J. C., S. Saini, D. D. Stark, P. F. Hahn, M. Nigam, J. Wittenberg and J. T. Ferrucci, Jr. (1988). "Gd-DOTA: characterization of a new paramagnetic complex." Radiology **166**(3): 693-698.

Boysen, G. and H. Christensen (2001). "Stroke severity determines body temperature in acute stroke." Stroke **32**(2): 413-417.

Brancaleone, V., J. Dalli, S. Bena, R. J. Flower, G. Cirino and M. Perretti (2011). "Evidence for an anti-inflammatory loop centered on polymorphonuclear leukocyte formyl peptide receptor 2/lipoxin A4 receptor and operative in the inflamed microvasculature." J Immunol **186**(8): 4905-4914.

Brea, D., T. Sobrino, M. Blanco, M. Fraga, J. Agulla, M. Rodriguez-Yanez, R. Rodriguez-Gonzalez, N. Perez de la Ossa, R. Leira, J. Forteza, A. Davalos and J. Castillo (2009). "Usefulness of haptoglobin and serum amyloid A proteins as biomarkers for atherothrombotic ischemic stroke diagnosis confirmation." Atherosclerosis **205**(2): 561-567.

Brott, T., J. R. Marler, C. P. Olinger, H. P. Adams, Jr., T. Tomsick, W. G. Barsan, J. Biller, R. Eberle, V. Hertzberg and M. Walker (1989). "Measurements of acute cerebral infarction: lesion size by computed tomography." Stroke **20**(7): 871-875.

Buckingham, J. C., C. D. John, E. Solito, T. Tierney, R. J. Flower, H. Christian and J. Morris (2006). "Annexin 1, glucocorticoids, and the neuroendocrine-immune interface." Ann N Y Acad Sci **1088**: 396-409.

Caceres, M. J., C. L. Schleien, J. W. Kuluz, B. Gelman and W. D. Dietrich (1995). "Early endothelial damage and leukocyte accumulation in piglet brains following cardiac arrest." Acta Neuropathol **90**(6): 582-591.

Caravan, P. (2006). "Strategies for increasing the sensitivity of gadolinium based MRI contrast

agents." Chem.Soc.Rev.(35): 512-523.

Cardini, S., J. Dalli, S. Fineschi, M. Perretti, G. Lungarella and M. Lucattelli (2012). "Genetic ablation of the fpr1 gene confers protection from smoking-induced lung emphysema in mice." Am J Respir Cell Mol Biol **47**(3): 332-339.

Carmichael, S. T. (2005). "Rodent models of focal stroke: size, mechanism, and purpose." NeuroRx **2**(3): 396-409.

Castillo, J., R. Leira, M. M. Garcia, J. Serena, M. Blanco and A. Davalos (2004). "Blood pressure decrease during the acute phase of ischemic stroke is associated with brain injury and poor stroke outcome." Stroke **35**(2): 520-526.

Chiang, N., E. A. Bermudez, P. M. Ridker, S. Hurwitz and C. N. Serhan (2004). "Aspirin triggers antiinflammatory 15-epi-lipoxin A4 and inhibits thromboxane in a randomized human trial." Proc Natl Acad Sci U S A **101**(42): 15178-15183.

Chiang, N., I. M. Fierro, K. Gronert and C. N. Serhan (2000). "Activation of lipoxin A(4) receptors by aspirin-triggered lipoxins and select peptides evokes ligand-specific responses in inflammation." J Exp Med **191**(7): 1197-1208.

Chiang, N., C. N. Serhan, S. E. Dahlen, J. M. Drazen, D. W. Hay, G. E. Rovati, T. Shimizu, T. Yokomizo and C. Brink (2006). "The lipoxin receptor ALX: potent ligand-specific and stereoselective actions in vivo." Pharmacol Rev **58**(3): 463-487.

Chiu, D., D. Krieger, C. Villar-Cordova, S. E. Kasner, L. B. Morgenstern, P. L. Bratina, F. M. Yatsu and J. C. Grotta (1998). "Intravenous tissue plasminogen activator for acute ischemic stroke: feasibility, safety, and efficacy in the first year of clinical practice." Stroke **29**(1): 18-22.

Claria, J. and C. N. Serhan (1995). "Aspirin triggers previously undescribed bioactive eicosanoids by human endothelial cell-leukocyte interactions." Proc Natl Acad Sci U S A **92**(21): 9475-9479.

clinicaltrials.gov (2011). "http://clinicaltrials.gov/ct2/results?cond=%22Stroke%22."

Clish, C. B., B. D. Levy, N. Chiang, H. H. Tai and C. N. Serhan (2000). "Oxidoreductases in lipoxin A4 metabolic inactivation: a novel role for 15-onoprostaglandin 13-reductase/leukotriene B4 12-hydroxydehydrogenase in inflammation." J Biol Chem **275**(33): 25372-25380.

Collins, M. A., E. J. Neafsey, K. J. Mukamal, M. O. Gray, D. A. Parks, D. K. Das and R. J. Korthuis (2009). "Alcohol in moderation, cardioprotection, and neuroprotection: epidemiological considerations and mechanistic studies." Alcohol Clin Exp Res **33**(2): 206-219.

Connolly, E. S., Jr., C. J. Winfree, D. M. Stern, R. A. Solomon and D. J. Pinsky (1996). "Procedural and strain-related variables significantly affect outcome in a murine model of focal cerebral ischemia." Neurosurgery **38**(3): 523-531; discussion 532.

Conroy, B. E., G. DeJong and S. D. Horn (2009). "Hospital-based stroke rehabilitation in the United States." Top Stroke Rehabil **16**(1): 34-43.

Cui, Y., Y. Le, H. Yazawa, W. Gong and J. M. Wang (2002). "Potential role of the formyl peptide receptor-like 1 (FPRL1) in inflammatory aspects of Alzheimer's disease." J Leukoc Biol **72**(4): 628-635.

Cui, Y. H., Y. Le, X. Zhang, W. Gong, K. Abe, R. Sun, J. Van Damme, P. Proost and J. M. Wang (2002). "Up-regulation of FPR2, a chemotactic receptor for amyloid beta 1-42 (A beta 42), in murine microglial cells by TNF alpha." Neurobiol Dis **10**(3): 366-377.

Dai, Y., J. Major, M. Novotny and T. A. Hamilton (2005). "IL-4 inhibits expression of the formyl peptide receptor gene in mouse peritoneal macrophages." J Interferon Cytokine Res **25**(1): 11-19.

Davis, S. M. and G. A. Donnan (2009). "4.5 hours: the new time window for tissue plasminogen activator in stroke." Stroke **40**(6): 2266-2267.

de Boer, J. H., C. E. Hack, A. J. Verhoeven, G. S. Baarsma, P. T. de Jong, A. J. Rademakers, W. A. de Vries-Knoppert, A. Rothova and A. Kijlstra (1993). "Chemoattractant and neutrophil degranulation activities related to interleukin-8 in vitreous fluid in uveitis and vitreoretinal disorders." Invest Ophthalmol Vis Sci **34**(12): 3376-3385.

de Coupade, C., E. Solito and J. D. Levine (2003). "Dexamethasone enhances interaction of endogenous annexin 1 with L-selectin and triggers shedding of L-selectin in the monocytic cell line U-937." Br J Pharmacol **140**(1): 133-145.

del Zoppo, G. J., G. W. Schmid-Schonbein, E. Mori, B. R. Copeland and C. M. Chang (1991). "Polymorphonuclear leukocytes occlude capillaries following middle cerebral artery occlusion and reperfusion in baboons." Stroke **22**(10): 1276-1283.

Denes, A., E. Pinteaux, N. J. Rothwell and S. M. Allan (2011). "Interleukin-1 and stroke: biomarker, harbinger of damage, and therapeutic target." Cerebrovasc Dis **32**(6): 517-527.

Donahue, K. M., D. Burstein, W. J. Manning and M. L. Gray (1994). "STUDIES OF GD-DTPA RELAXIVITY AND PROTON-EXCHANGE RATES IN TISSUE." MAGNETIC RESONANCE IN MEDICINE **32**(1): 66-76.

Donnan, G. A., M. Fisher, M. Macleod and S. M. Davis (2008). "Stroke." Lancet **371**(9624): 1612-1623.

Dorward, D. A., C. D. Lucas, A. G. Rossi, C. Haslett and K. Dhaliwal (2012). "Imaging inflammation: molecular strategies to visualize key components of the inflammatory cascade, from initiation to resolution." Pharmacol Ther **135**(2): 182-199.

Dufton, N., R. Hannon, V. Brancaleone, J. Dalli, H. B. Patel, M. Gray, F. D'Acquisto, J. C. Buckingham, M. Perretti and R. J. Flower (2010). "Anti-inflammatory role of the murine formyl-peptide receptor 2: ligand-specific effects on leukocyte responses and experimental inflammation." J Immunol **184**(5): 2611-2619.

Dufton, N. and M. Perretti (2010). "Therapeutic anti-inflammatory potential of formyl-peptide receptor agonists." Pharmacology & Therapeutics **127**(2): 175-188.

Dunne, J. L., C. M. Ballantyne and K. Ley (2000). "Role of LFA-1 and MAC-1 in slow rolling and leukocyte adhesion during cytokine-induced inflammation." Faseb Journal **14**(4): A705-A705.

Durstin, M., J. L. Gao, H. L. Tiffany, D. McDermott and P. M. Murphy (1994). "Differential expression of members of the N-formylpeptide receptor gene cluster in human phagocytes." Biochem Biophys Res Commun **201**(1): 174-179.

EAST (2001). "Use of anti-ICAM-1 therapy in ischemic stroke: results of the Enlimomab Acute Stroke Trial." Neurology **57**(8): 1428-1434.

Edaravone Acute Infarction Study, G. (2003). "Effect of a novel free radical scavenger, edaravone (MCI-186), on acute brain infarction. Randomized, placebo-controlled, double-blind study at multicenters." Cerebrovasc Dis **15**(3): 222-229.

El Kebir, D., L. Jozsef, W. Pan, L. Wang, N. A. Petasis, C. N. Serhan and J. G. Filep (2009). "15-epi-lipoxin A4 inhibits myeloperoxidase signaling and enhances resolution of acute lung injury." Am J Respir Crit Care Med **180**(4): 311-319.

Elbim, C. and G. Lizard (2009). "Flow cytometric investigation of neutrophil oxidative burst and apoptosis in physiological and pathological situations." Cytometry A **75**(6): 475-481.

Emsley, H. C., C. J. Smith, R. F. Georgiou, A. Vail, S. J. Hopkins, N. J. Rothwell, P. J. Tyrrell and I. Acute Stroke (2005). "A randomised phase II study of interleukin-1 receptor antagonist in acute stroke patients." J Neurol Neurosurg Psychiatry **76**(10): 1366-1372.

Ernst, S., C. Lange, A. Wilbers, V. Goebeler, V. Gerke and U. Rescher (2004). "An annexin 1 N-terminal peptide activates leukocytes by triggering different members of the formyl peptide receptor family." J Immunol **172**(12): 7669-7676.

Fiebach, J. B., P. D. Schellinger, O. Jansen, M. Meyer, P. Wilde, J. Bender, P. Schramm, E. Juttler, J. Oehler, M. Hartmann, S. Hahnel, M. Knauth, W. Hacke and K. Sartor (2002). "CT and diffusion-weighted MR imaging in randomized order: diffusion-weighted imaging results in higher accuracy and lower interrater variability in the diagnosis of hyperacute ischemic stroke." Stroke **33**(9): 2206-2210.

Fierro, I. M., S. P. Colgan, G. Bernasconi, N. A. Petasis, C. B. Clish, M. Arita and C. N. Serhan (2003). "Lipoxin A4 and aspirin-triggered 15-epi-lipoxin A4 inhibit human neutrophil migration: comparisons between synthetic 15 epimers in chemotaxis and transmigration with microvessel endothelial cells and epithelial cells." J Immunol **170**(5): 2688-2694.

Fiore, S., J. F. Maddox, H. D. Perez and C. N. Serhan (1994). "Identification of a human cDNA encoding a functional high affinity lipoxin A4 receptor." J Exp Med **180**(1): 253-260.

Fiore, S., M. Romano, E. M. Reardon and C. N. Serhan (1993). "Induction of functional lipoxin A4 receptors in HL-60 cells." Blood **81**(12): 3395-3403.

Fischer, U., M. Arnold, K. Nedeltchev, R. A. Schoenenberger, L. Kappeler, P. Hollinger, G. Schroth, P. Ballinari and H. P. Mattle (2006). "Impact of comorbidity on ischemic stroke outcome." Acta Neurol Scand **113**(2): 108-113.

Fisher, M. (1997). "Characterizing the target of acute stroke therapy." Stroke **28**(4): 866-872.

Flavin, M. P., G. Zhao and L. T. Ho (2000). "Microglial tissue plasminogen activator (tPA) triggers neuronal apoptosis in vitro." Glia **29**(4): 347-354.

Ford, G. A. (2008). "Clinical pharmacological issues in the development of acute stroke therapies." Br J Pharmacol **153 Suppl 1**: S112-119.

Gao, J. L., H. Chen, J. D. Filie, C. A. Kozak and P. M. Murphy (1998). "Differential expansion of the N-formylpeptide receptor gene cluster in human and mouse." Genomics **51**(2): 270-276.

Gao, J. L., A. Guillabert, J. Hu, Y. Le, E. Urizar, E. Seligman, K. J. Fang, X. Yuan, V. Imbault, D. Communi, J. M. Wang, M. Parmentier, P. M. Murphy and I. Migeotte (2007). "F2L, a peptide derived from heme-binding protein, chemoattracts mouse neutrophils by specifically activating Fpr2, the low-affinity N-formylpeptide receptor." J Immunol **178**(3): 1450-1456.

Gavins, F., G. Yilmaz and D. N. Granger (2007). "The evolving paradigm for blood cell-endothelial cell interactions in the cerebral microcirculation." Microcirculation **14**(7): 667-681.

Gavins, F. N. (2010). "Are formyl peptide receptors novel targets for therapeutic intervention in ischaemia-reperfusion injury?" Trends Pharmacol Sci **31**(6): 266-276.

Gavins, F. N., J. Dalli, R. J. Flower, D. N. Granger and M. Perretti (2007). "Activation of the annexin 1 counter-regulatory circuit affords protection in the mouse brain microcirculation." FASEB J **21**(8): 1751-1758.

Gavins, F. N., E. L. Hughes, N. A. Buss, P. M. Holloway, S. J. Getting and J. C. Buckingham (2012). "Leukocyte recruitment in the brain in sepsis: involvement of the annexin 1-FPR2/ALX anti-inflammatory system." FASEB J.

Gavins, F. N., E. L. Hughes, N. A. Buss, P. M. Holloway, S. J. Getting and J. C. Buckingham (2012). "Leukocyte recruitment in the brain in sepsis: involvement of the annexin 1-FPR2/ALX anti-inflammatory system." FASEB J **26**(12): 4977-4989.

Gavins, F. N., A. M. Kamal, M. D'Amico, S. M. Oliani and M. Perretti (2005). "Formyl-peptide receptor is not involved in the protection afforded by annexin 1 in murine acute myocardial infarct." FASEB J **19**(1): 100-102.

Gavins, F. N., S. Yona, A. M. Kamal, R. J. Flower and M. Perretti (2003). "Leukocyte antiadhesive actions of annexin 1: ALXR- and FPR-related anti-inflammatory mechanisms." Blood **101**(10): 4140-4147.

Gigante, P. R., G. Appelboom, B. Y. Hwang, R. M. Haque, M. L. Yeh, A. F. Ducruet, C. P. Kellner, J. Gorski, S. E. Keesecker and E. S. Connolly, Jr. (2011). "Isoflurane preconditioning affords functional neuroprotection in a murine model of intracerebral hemorrhage." Acta Neurochir Suppl **111**: 141-144.

Goulding, N. J., J. L. Godolphin, P. R. Sharland, S. H. Peers, M. Sampson, P. J. Maddison and R. J. Flower (1990). "Anti-inflammatory lipocortin 1 production by peripheral blood leucocytes in response to hydrocortisone." Lancet **335**(8703): 1416-1418.

Granger, C. V., B. B. Hamilton and R. C. Fiedler (1992). "Discharge outcome after stroke rehabilitation." Stroke **23**(7): 978-982.

Graves, D. T. and Y. Jiang (1995). "Chemokines, a family of chemotactic cytokines." Crit Rev Oral Biol Med **6**(2): 109-118.

Grond-Ginsbach, C., M. Hummel, T. Wiest, S. Horstmann, K. Pfleger, M. Hergenhahn, M. Hollstein, U. Mansmann, A. J. Grau and S. Wagner (2008). "Gene expression in human peripheral blood mononuclear cells upon acute ischemic stroke." J Neurol **255**(5): 723-731.

Gronert, K., N. Maheshwari, N. Khan, I. R. Hassan, M. Dunn and M. Laniado Schwartzman (2005). "A role for the mouse 12/15-lipoxygenase pathway in promoting epithelial wound healing and host defense." J Biol Chem **280**(15): 15267-15278.

Haarmann, A., A. Deiss, J. Prochaska, C. Foerch, B. Weksler, I. Romero, P. O. Couraud, G. Stoll, P. Rieckmann and M. Buttmann (2010). "Evaluation of soluble junctional adhesion molecule-A as a biomarker of human brain endothelial barrier breakdown." PLoS One **5**(10): e13568.

Halliwell, B. (1992). "Oxygen Radicals as Key Mediators in Neurological Disease - Fact or Fiction." Annals of Neurology **32**: S10-S15.

Hankey, G. J. (1999). "Smoking and risk of stroke." J Cardiovasc Risk **6**(4): 207-211.

Hawkins, B. T. and T. P. Davis (2005). "The blood-brain barrier/neurovascular unit in health and disease." Pharmacol Rev **57**(2): 173-185.

Hayhoe, R. P., A. M. Kamal, E. Solito, R. J. Flower, D. Cooper and M. Perretti (2006). "Annexin 1 and its bioactive peptide inhibit neutrophil-endothelium interactions under flow: indication of distinct receptor involvement." Blood **107**(5): 2123-2130.

HCASG (2002). "Mild therapeutic hypothermia to improve the neurologic outcome after cardiac arrest." N Engl J Med **346**(8): 549-556.

Henkels, K. M., K. Frondorf, M. E. Gonzalez-Mejia, A. L. Doseff and J. Gomez-Cambronero (2011). "IL-8-induced neutrophil chemotaxis is mediated by Janus kinase 3 (JAK3)." FEBS Lett **585**(1): 159-166.

Hill, M. D. and V. Hachinski (1998). "Stroke treatment: time is brain." Lancet **352 Suppl 3**: SIII10-14.

Hillis, A. E., J. A. Ulatowski, P. B. Barker, M. Torbey, W. Ziai, N. J. Beauchamp, S. Oh and R. J. Wityk (2003). "A pilot randomized trial of induced blood pressure elevation: effects on function and focal perfusion in acute and subacute stroke." Cerebrovasc Dis **16**(3): 236-246.

Hockstein, N. G., D. S. Samadi, K. Gendron and S. D. Handler (2004). "Sialorrhea: a management challenge." Am Fam Physician **69**(11): 2628-2634.

Holloway, P. M., H. K. Smith, D. Renshaw, R. J. Flower, S. J. Getting and F. N. Gavins (2011). "Targeting the melanocortin receptor system for anti-stroke therapy." Trends Pharmacol Sci **32**(2): 90-98.

Huynh, M. L., V. A. Fadok and P. M. Henson (2002). "Phosphatidylserine-dependent ingestion of apoptotic cells promotes TGF-beta1 secretion and the resolution of inflammation." J Clin Invest **109**(1): 41-50.

Iribarren, P., K. Chen, J. Hu, X. Zhang, W. Gong and J. M. Wang (2005). "IL-4 inhibits the expression of mouse formyl peptide receptor 2, a receptor for amyloid beta1-42, in TNF-alpha-activated microglia." J Immunol **175**(9): 6100-6106.

Ishikawa, M., D. Cooper, J. Russell, J. W. Salter, J. H. Zhang, A. Nanda and D. N. Granger (2003). "Molecular determinants of the prothrombogenic and inflammatory phenotype assumed by the postischemic cerebral microcirculation." Stroke **34**(7): 1777-1782.

Ishikawa, M., E. Sekizuka, N. Yamaguchi, H. Nakadate, S. Terao, D. N. Granger and H. Minamitani (2007). "Angiotensin II type 1 receptor signaling contributes to platelet-leukocyte-endothelial cell interactions in the cerebral microvasculature." Am J Physiol Heart Circ Physiol **292**(5): H2306-2315.

Jiang, L., M. Newman, S. Saporta, N. Chen, C. Sanberg, P. R. Sanberg and A. E. Willing (2008). "MIP-1alpha and MCP-1 Induce Migration of Human Umbilical Cord Blood Cells in Models of Stroke." Curr Neurovasc Res **5**(2): 118-124.

Johansson, B. B. (2011). "Current trends in stroke rehabilitation. A review with focus on brain plasticity." Acta Neurol Scand **123**(3): 147-159.

Jones, T. H., R. B. Morawetz, R. M. Crowell, F. W. Marcoux, S. J. FitzGibbon, U. DeGirolami and R. G. Ojemann (1981). "Thresholds of focal cerebral ischemia in awake monkeys." J Neurosurg **54**(6): 773-782.

Kalinowska, A. and J. Losy (2006). "PECAM-1, a key player in neuroinflammation." Eur J Neurol **13**(12): 1284-1290.

Kaste, M. and O. Waltimo (1976). "Prognosis of patients with middle cerebral artery occlusion." Stroke **7**(5): 482-485.

Khau, T., S. Y. Langenbach, M. Schuliga, T. Harris, C. N. Johnstone, R. L. Anderson and A. G. Stewart (2011). "Annexin-1 signals mitogen-stimulated breast tumor cell proliferation by activation of the formyl peptide receptors (FPRs) 1 and 2." FASEB J **25**(2): 483-496.

Kim, S. D., Y. K. Kim, H. Y. Lee, Y. S. Kim, S. G. Jeon, S. H. Baek, D. K. Song, S. H. Ryu and Y. S. Bae (2010). "The agonists of formyl peptide receptors prevent development of severe sepsis after microbial infection." J Immunol **185**(7): 4302-4310.

Kindy, M. S., J. Yu, J. T. Guo and H. Zhu (1999). "Apolipoprotein Serum Amyloid A in Alzheimer's Disease." J Alzheimers Dis **1**(3): 155-167.

Kinzer-Ursem, T. L., K. L. Sutton, A. Waller, G. M. Omann and J. J. Linderman (2006). "Multiple receptor states are required to describe both kinetic binding and activation of neutrophils via N-formyl peptide receptor ligands." Cell Signal **18**(10): 1732-1747.

Kitagawa, K., M. Matsumoto, G. Yang, T. Mabuchi, Y. Yagita, M. Hori and T. Yanagihara (1998). "Cerebral ischemia after bilateral carotid artery occlusion and intraluminal suture occlusion in mice: evaluation of the patency of the posterior communicating artery." J Cereb Blood Flow Metab **18**(5): 570-579.

Kittaka, M., L. Wang, N. Sun, S. S. Schreiber, N. W. Seeds, M. Fisher and B. V. Zlokovic (1996). "Brain capillary tissue plasminogen activator in a diabetes stroke model." Stroke **27**(4): 712-719.

Kofler, J., T. Otsuka, Z. Zhang, R. Noppens, M. R. Grafe, D. W. Koh, V. L. Dawson, J. M. de Murcia, P. D. Hurn and R. J. Traystman (2006). "Differential effect of PARP-2 deletion on brain injury after focal and global cerebral ischemia." J Cereb Blood Flow Metab **26**(1): 135-141.

Kostulas, N., P. Kivisakk, Y. Huang, D. Matusevicius, V. Kostulas and H. Link (1998). "Ischemic stroke is associated with a systemic increase of blood mononuclear cells expressing interleukin-8 mRNA." Stroke **29**(2): 462-466.

Kostulas, N., S. H. Pelidou, P. Kivisakk, V. Kostulas and H. Link (1999). "Increased IL-1beta, IL-8, and IL-17 mRNA expression in blood mononuclear cells observed in a prospective ischemic stroke study." Stroke **30**(10): 2174-2179.

Kouwenhoven, M., C. Carlstrom, V. Ozenci and H. Link (2001). "Matrix metalloproteinase and cytokine profiles in monocytes over the course of stroke." J Clin Immunol **21**(5): 365-375.

Kratsovnik, E., Y. Bromberg, O. Sperling and E. Zoref-Shani (2005). "Oxidative stress activates transcription factor NF-kB-mediated protective signaling in primary rat neuronal cultures." J Mol Neurosci **26**(1): 27-32.

Kretschmer, D., A. K. Gleske, M. Rautenberg, R. Wang, M. Koberle, E. Bohn, T. Schoneberg, M. J. Rabiet, F. Boulay, S. J. Klebanoff, K. A. van Kessel, J. A. van Strijp, M. Otto and A. Peschel (2010). "Human formyl peptide receptor 2 senses highly pathogenic Staphylococcus aureus." Cell Host Microbe **7**(6): 463-473.

Kukulski, F., F. Ben Yebdri, J. Lecka, G. Kauffenstein, S. A. Levesque, M. Martin-Satue and J. Sevigny (2009). "Extracellular ATP and P2 receptors are required for IL-8 to induce neutrophil migration." Cytokine **46**(2): 166-170.

Kumari, R., L. B. Willing, S. D. Patel, J. K. Krady, W. J. Zavadoski, E. M. Gibbs, S. J. Vannucci and I. A. Simpson (2010). "The PPAR-gamma agonist, darglitazone, restores acute inflammatory responses to cerebral hypoxia-ischemia in the diabetic ob/ob mouse." J Cereb Blood Flow Metab **30**(2): 352-360.

La, M., M. D'Amico, S. Bandiera, C. Di Filippo, S. M. Oliani, F. N. Gavins, R. J. Flower and M. Perretti (2001). "Annexin 1 peptides protect against experimental myocardial ischemia-reperfusion: analysis of their mechanism of action." FASEB J **15**(12): 2247-2256.

Landau, W. M. (1992). "Causes of stroke." Ann Neurol **32**(4): 596-597.

Latchaw, R. E., M. J. Alberts, M. H. Lev, J. J. Connors, R. E. Harbaugh, R. T. Higashida, R. Hobson, C. S. Kidwell, W. J. Koroshetz, V. Mathews, P. Villablanca, S. Warach and B. Walters (2009). "Recommendations for imaging of acute ischemic stroke: a scientific statement from the American Heart Association." Stroke **40**(11): 3646-3678.

Lavine, S. D., F. M. Hofman and B. V. Zlokovic (1998). "Circulating antibody against tumor necrosis factor-alpha protects rat brain from reperfusion injury." J Cereb Blood Flow Metab **18**(1): 52-58.

Lee, H. Y., M. K. Kim, K. S. Park, E. H. Shin, S. H. Jo, S. D. Kim, E. J. Jo, Y. N. Lee, C. Lee, S. H. Baek and Y. S. Bae (2006). "Serum amyloid A induces contrary immune responses via formyl peptide receptor-like 1 in human monocytes." Mol Pharmacol **70**(1): 241-248.

Lee, H. Y., S. D. Kim, J. W. Shim, H. J. Kim, J. Y. Kwon, J. M. Kim, S. H. Baek, J. S. Park and Y. S. Bae (2010). "Activation of human monocytes by a formyl peptide receptor 2-derived pepducin." FEBS Lett **584**(18): 4102-4108.

Lee, H. Y., S. D. Kim, J. W. Shim, H. J. Kim, J. Yun, S. H. Baek, K. Kim and Y. S. Bae (2010). "A pertussis toxin sensitive G-protein-independent pathway is involved in serum amyloid A-induced formyl peptide receptor 2-mediated CCL2 production." Exp Mol Med **42**(4): 302-309.

Lee, H. Y., S. D. Kim, J. W. Shim, S. Y. Lee, H. Lee, K. H. Cho, J. Yun and Y. S. Bae (2008). "Serum amyloid A induces CCL2 production via formyl peptide receptor-like 1-mediated signaling in human monocytes." J Immunol **181**(6): 4332-4339.

Lees, K. R., G. A. Ford, K. W. Muir, N. Ahmed, A. G. Dyker, S. Atula, L. Kalra, E. A. Warburton, J. C. Baron, D. F. Jenkinson, N. G. Wahlgren and M. R. Walters (2008). "Thrombolytic therapy for acute stroke in the United Kingdom: experience from the safe implementation of thrombolysis in stroke (SITS) register." QJM **101**(11): 863-869.

Legos, J. J., R. G. Whitmore, J. A. Erhardt, A. A. Parsons, R. F. Tuma and F. C. Barone (2000). "Quantitative changes in interleukin proteins following focal stroke in the rat." Neurosci Lett **282**(3): 189-192.

Leoni, G., H. B. Patel, A. L. F. Sampaio, F. N. E. Gavins, J. F. Murray, P. Grieco, S. J. Getting and M. Perretti (2008). "Inflamed phenotype of the mesenteric microcirculation of melanocortin type 3 receptor-null mice after ischemia-reperfusion." Faseb Journal **22**(12): 4228-4238.

Levasseur, J. E., E. P. Wei, A. J. Raper, A. A. Kontos and J. L. Patterson (1975). "Detailed description of a cranial window technique for acute and chronic experiments." Stroke **6**(3): 308-317.

Levy, B. D., C. B. Clish, B. Schmidt, K. Gronert and C. N. Serhan (2001). "Lipid mediator class switching during acute inflammation: signals in resolution." Nat Immunol **2**(7): 612-619.

Levy, B. D., N. W. Lukacs, A. A. Berlin, B. Schmidt, W. J. Guilford, C. N. Serhan and J. F. Parkinson (2007). "Lipoxin A4 stable analogs reduce allergic airway responses via mechanisms distinct from CysLT1 receptor antagonism." FASEB J **21**(14): 3877-3884.

Levy, B. D., M. Romano, H. A. Chapman, J. J. Reilly, J. Drazen and C. N. Serhan (1993). "Human alveolar macrophages have 15-lipoxygenase and generate 15(S)-hydroxy-5,8,11-cis-13-trans-eicosatetraenoic acid and lipoxins." J Clin Invest **92**(3): 1572-1579.

Ley, K. and P. Gaehtgens (1991). "Endothelial, not hemodynamic, differences are responsible for preferential leukocyte rolling in rat mesenteric venules." Circ Res **69**(4): 1034-1041.

Li, F., T. Omae and M. Fisher (1999). "Spontaneous hyperthermia and its mechanism in the intraluminal suture middle cerebral artery occlusion model of rats." Stroke **30**(11): 2464-2470; discussion 2470-2461.

Li, X., K. K. Blizzard, Z. Zeng, A. C. DeVries, P. D. Hurn and L. D. McCullough (2004). "Chronic behavioral testing after focal ischemia in the mouse: functional recovery and the effects of gender." Exp Neurol **187**(1): 94-104.

Li, X., J. A. Klaus, J. Zhang, Z. Xu, K. K. Kibler, S. A. Andrabi, K. Rao, Z. J. Yang, T. M. Dawson, V. L. Dawson and R. C. Koehler (2010). "Contributions of poly(ADP-ribose) polymerase-1 and -2 to nuclear translocation of apoptosis-inducing factor and injury from focal cerebral ischemia." J Neurochem.

Liesz, A., S. Hagmann, C. Zschoche, J. Adamek, W. Zhou, L. Sun, A. Hug, M. Zorn, A. Dalpke, P. Nawroth and R. Veltkamp (2009). "The spectrum of systemic immune alterations after murine focal ischemia: immunodepression versus immunomodulation." Stroke **40**(8): 2849-2858.

Lim, L. H. and S. Pervaiz (2007). "Annexin 1: the new face of an old molecule." FASEB J **21**(4): 968-975.

Lima-Garcia, J. F., R. C. Dutra, K. da Silva, E. M. Motta, M. M. Campos and J. B. Calixto (2011). "The precursor of resolvin D series and aspirin-triggered resolvin D1 display anti-hyperalgesic properties in adjuvant-induced arthritis in rats." Br J Pharmacol **164**(2): 278-293.

Locke, L. W., M. D. Chordia, Y. Zhang, B. Kundu, D. Kennedy, J. Landseadel, L. Xiao, K. D. Fairchild, S. S. Berr, J. Linden and D. Pan (2009). "A novel neutrophil-specific PET imaging agent: cFLFLFK-PEG-64Cu." J Nucl Med **50**(5): 790-797.

Longa, E. Z., P. R. Weinstein, S. Carlson and R. Cummins (1989). "Reversible middle cerebral artery occlusion without craniectomy in rats." Stroke **20**(1): 84-91.

Loscalzo, J. and D. E. Vaughan (1987). "Tissue plasminogen activator promotes platelet disaggregation in plasma." J Clin Invest **79**(6): 1749-1755.

Lozano, J. D., D. P. Abulafia, G. H. Danton, B. D. Watson and W. D. Dietrich (2007). "Characterization of a thromboembolic photochemical model of repeated stroke in mice." J Neurosci Methods **162**(1-2): 244-254.

Lyden, P., A. Shuaib, K. Ng, K. Levin, R. P. Atkinson, A. Rajput, L. Wechsler, T. Ashwood, L. Claesson, T. Odergren and E. Salazar-Grueso (2002). "Clomethiazole Acute Stroke Study in ischemic stroke (CLASS-I): final results." Stroke **33**(1): 122-128.

Machado, F. S., J. E. Johndrow, L. Esper, A. Dias, A. Bafica, C. N. Serhan and J. Aliberti (2006). "Anti-inflammatory actions of lipoxin A4 and aspirin-triggered lipoxin are SOCS-2 dependent." Nat Med **12**(3): 330-334.

Maddox, J. F., M. Hachicha, T. Takano, N. A. Petasis, V. V. Fokin and C. N. Serhan (1997). "Lipoxin A4 stable analogs are potent mimetics that stimulate human monocytes and THP-1 cells via a G-protein-linked lipoxin A4 receptor." J Biol Chem **272**(11): 6972-6978.

Maddox, J. F. and C. N. Serhan (1996). "Lipoxin A4 and B4 are potent stimuli for human monocyte migration and adhesion: selective inactivation by dehydrogenation and reduction." J Exp Med **183**(1): 137-146.

Maderna, P., D. C. Cottell, T. Toivonen, N. Dufton, J. Dalli, M. Perretti and C. Godson (2010). "FPR2/ALX receptor expression and internalization are critical for lipoxin A4 and annexin-derived peptide-stimulated phagocytosis." FASEB J **24**(11): 4240-4249.

Maderna, P., D. C. Cottell, T. Toivonen, N. Dufton, J. Dalli, M. Perretti and C. Godson (2010). "FPR2/ALX receptor expression and internalization are critical for lipoxin A4 and annexin-derived peptide-stimulated phagocytosis." FASEB J.

Mamdouh, Z., A. Mikhailov and W. A. Muller (2009). "Transcellular migration of leukocytes is mediated by the endothelial lateral border recycling compartment." Journal of Experimental Medicine **206**(12): 2795-2808.

Mandal, P., M. Novotny and T. A. Hamilton (2005). "Lipopolysaccharide induces formyl peptide receptor 1 gene expression in macrophages and neutrophils via transcriptional and posttranscriptional mechanisms." J Immunol **175**(9): 6085-6091.

Marcheselli, V. L., S. Hong, W. J. Lukiw, X. H. Tian, K. Gronert, A. Musto, M. Hardy, J. M. Gimenez, N. Chiang, C. N. Serhan and N. G. Bazan (2003). "Novel docosanoids inhibit brain ischemia-reperfusion-mediated leukocyte infiltration and pro-inflammatory gene expression." J Biol Chem **278**(44): 43807-43817.

Matsuo, Y., H. Onodera, Y. Shiga, H. Shozuhara, M. Ninomiya, T. Kihara, T. Tamatani, M. Miyasaka and K. Kogure (1994). "Role of cell adhesion molecules in brain injury after transient middle cerebral artery occlusion in the rat." Brain Res **656**(2): 344-352.

Mattson, M. P., C. Culmsee and Z. F. Yu (2000). "Apoptotic and antiapoptotic mechanisms in stroke." Cell Tissue Res **301**(1): 173-187.

Mayzel-Oreg, O., T. Omae, M. Kazemi, F. Li, M. Fisher, Y. Cohen and C. H. Sotak (2004). "Microsphere-induced embolic stroke: an MRI study." Magn Reson Med **51**(6): 1232-1238.

McArthur, S., C. Reutlingsperger, R. Flower and M. Perretti (2012). "Monocyte recruitment during inflammation: a novel role for the annexin A1/Fpr2 pathway." British Pharmacological Society Winter Meeting.

McCarty, J. H. (2005). "Cell biology of the neurovascular unit: implications for drug delivery across the blood-brain barrier." Assay Drug Dev Technol **3**(1): 89-95.

Mewis, R. E. and S. J. Archibald (2010). "Biomedical applications of macrocyclic ligand complexes." Coordination Chemistry Reviews **254**(15-16): 1686-1712.

Migeotte, I., D. Communi and M. Parmentier (2006). "Formyl peptide receptors: a promiscuous subfamily of G protein-coupled receptors controlling immune responses." Cytokine Growth Factor Rev **17**(6): 501-519.

Minamisawa, H., P. Mellergard, M. L. Smith, F. Bengtsson, S. Theander, F. Boris-Moller and B. K. Siesjo (1990). "Preservation of brain temperature during ischemia in rats." Stroke **21**(5): 758-764.

Modo, M., D. Cash, K. Mellodew, S. C. Williams, S. E. Fraser, T. J. Meade, J. Price and H. Hodges (2002). "Tracking transplanted stem cell migration using bifunctional, contrast agent-enhanced, magnetic resonance imaging." Neuroimage **17**(2): 803-811.

Morris, G. F., R. Bullock, S. B. Marshall, A. Marmarou, A. Maas and L. F. Marshall (1999). "Failure of the competitive N-methyl-D-aspartate antagonist Selfotel (CGS 19755) in the treatment of severe head injury: results of two phase III clinical trials. The Selfotel Investigators." J Neurosurg **91**(5): 737-743.

Munger, K. A., A. Montero, M. Fukunaga, S. Uda, T. Yura, E. Imai, Y. Kaneda, J. M. Valdivielso and K. F. Badr (1999). "Transfection of rat kidney with human 15-lipoxygenase suppresses inflammation and preserves function in experimental glomerulonephritis." Proc Natl Acad Sci U S A **96**(23): 13375-13380.

Murakami, K., T. Kondo, M. Kawase and P. H. Chan (1998). "The development of a new mouse model of global ischemia: focus on the relationships between ischemia duration, anesthesia, cerebral vasculature, and neuronal injury following global ischemia in mice." Brain Res **780**(2): 304-310.

Murakami, Y., K. Saito, A. Hara, Y. Zhu, K. Sudo, M. Niwa, H. Fujii, H. Wada, H. Ishiguro, H. Mori and M. Seishima (2005). "Increases in tumor necrosis factor-alpha following transient global cerebral ischemia do not contribute to neuron death in mouse hippocampus." J Neurochem **93**(6): 1616-1622.

Murdoch, C. and A. Finn (2000). "Chemokine receptors and their role in inflammation and infectious diseases." Blood **95**(10): 3032-3043.

Murray, P. J. (2005). "The primary mechanism of the IL-10-regulated antiinflammatory response is to selectively inhibit transcription." Proc Natl Acad Sci U S A **102**(24): 8686-8691.

NCBI (2010a). "http://www.ncbi.nlm.nih.gov/protein/NP_032065.1 fpr2 mus musculus."

NCBI (2010b). "http://www.ncbi.nlm.nih.gov/protein/NP_032068.2 fpr 3 mus musculus."

NCBI (2010c). "http://www.ncbi.nlm.nih.gov/protein/AAC53198.1 LXA4R mus musculus."

Neigh, G. N., K. Karelina, E. R. Glasper, S. L. Bowers, N. Zhang, P. G. Popovich and A. C. DeVries (2009). "Anxiety after cardiac arrest/cardiopulmonary resuscitation: exacerbated by stress and prevented by minocycline." Stroke **40**(11): 3601-3607.

Ng, Y. Y., C. C. Hou, W. Wang, X. R. Huang and H. Y. Lan (2005). "Blockade of NFkappaB activation and renal inflammation by ultrasound-mediated gene transfer of Smad7 in rat remnant kidney." Kidney Int Suppl(94): S83-91.

Niedel, J., S. Wilkinson and P. Cuatrecasas (1979). "Receptor-mediated uptake and degradation of 125I-chemotactic peptide by human neutrophils." J Biol Chem **254**(21): 10700-10706.

Niedel, J. E., I. Kahane and P. Cuatrecasas (1979). "Receptor-mediated internalization of fluorescent chemotactic peptide by human neutrophils." Science **205**(4413): 1412-1414.

NINDS (1995). "Tissue plasminogen activator for acute ischemic stroke. The National Institute of Neurological Disorders and Stroke rt-PA Stroke Study Group." N Engl J Med **333**(24): 1581-1587.

OED (2012). "Oxford English Dictionary."

Offner, H., S. Subramanian, S. M. Parker, M. E. Afentoulis, A. A. Vandenbark and P. D. Hurn (2006). "Experimental stroke induces massive, rapid activation of the peripheral immune system." J Cereb Blood Flow Metab **26**(5): 654-665.

Okada, Y., B. R. Copeland, E. Mori, M. M. Tung, W. S. Thomas and G. J. del Zoppo (1994). "P-selectin and intercellular adhesion molecule-1 expression after focal brain ischemia and reperfusion." Stroke **25**(1): 202-211.

Olmez, I. and H. Ozyurt (2012). "Reactive oxygen species and ischemic cerebrovascular disease." Neurochem Int **60**(2): 208-212.

Olsson, S. B. (2003). "Stroke prevention with the oral direct thrombin inhibitor ximelagatran compared with warfarin in patients with non-valvular atrial fibrillation (SPORTIF III): randomised controlled trial." Lancet **362**(9397): 1691-1698.

ONS, O. f. N. S. (2008). Mortality statistics: Deaths registered in 2008. Chapter IX Diseases of the circulatory system.

Ormstad, H., H. C. Aass, N. Lund-Sorensen, K. F. Amthor and L. Sandvik (2011). "Serum levels of cytokines and C-reactive protein in acute ischemic stroke patients, and their relationship to stroke lateralization, type, and infarct volume." J Neurol **258**(4): 677-685.

Padden, M., S. Leech, B. Craig, J. Kirk, B. Brankin and S. McQuaid (2007). "Differences in expression of junctional adhesion molecule-A and beta-catenin in multiple sclerosis brain tissue: increasing evidence for the role of tight junction pathology." Acta Neuropathol **113**(2): 177-186.

Pei, L., J. Zhang, F. Zhao, T. Su, H. Wei, J. Tian, M. Li and J. Shi (2011). "Annexin 1 exerts anti-nociceptive effects after peripheral inflammatory pain through formyl-peptide-receptor-like 1 in rat dorsal root ganglion." Br J Anaesth **107**(6): 948-958.

Penn, C. L. (2009). "Time is brain. Stroke--like trauma--demands immediate, definitive treatment." J Ark Med Soc **105**(11): 252-255.

Perretti, M., N. Chiang, M. La, I. M. Fierro, S. Marullo, S. J. Getting, E. Solito and C. N. Serhan (2002). "Endogenous lipid- and peptide-derived anti-inflammatory pathways generated with glucocorticoid and aspirin treatment activate the lipoxin A4 receptor." Nat Med **8**(11): 1296-1302.

Perretti, M., H. Christian, S. K. Wheller, I. Aiello, K. G. Mugridge, J. F. Morris, R. J. Flower and N. J. Goulding (2000). "Annexin I is stored within gelatinase granules of human neutrophil and mobilized on the cell surface upon adhesion but not phagocytosis." Cell Biol Int **24**(3): 163-174.

Perretti, M. and R. J. Flower (2004). "Annexin 1 and the biology of the neutrophil." J Leukoc Biol **76**(1): 25-29.

Perretti, M., S. J. Getting, E. Solito, P. M. Murphy and J. L. Gao (2001). "Involvement of the receptor for formylated peptides in the in vivo anti-migratory actions of annexin 1 and its mimetics." Am J Pathol **158**(6): 1969-1973.

Perretti, M., F. Ingegnoli, S. K. Wheller, M. C. Blades, E. Solito and C. Pitzalis (2002). "Annexin 1 modulates monocyte-endothelial cell interaction in vitro and cell migration in vivo in the human SCID mouse transplantation model." J Immunol **169**(4): 2085-2092.

Prestigiacomo, C. J., S. C. Kim, E. S. Connolly, Jr., H. Liao, S. F. Yan and D. J. Pinsky (1999). "CD18-mediated neutrophil recruitment contributes to the pathogenesis of reperfused but not nonreperfused stroke." Stroke **30**(5): 1110-1117.

Prossnitz, E. R. and R. D. Ye (1997). "The N-formyl peptide receptor: a model for the study of chemoattractant receptor structure and function." Pharmacol Ther **74**(1): 73-102.

Pulsinelli, W. A. and J. B. Brierley (1979). "A new model of bilateral hemispheric ischemia in the unanesthetized rat." Stroke **10**(3): 267-272.

Rabiet, M. J., E. Huet and F. Boulay (2005). "Human mitochondria-derived N-formylated peptides are novel agonists equally active on FPR and FPRL1, while Listeria monocytogenes-derived peptides preferentially activate FPR." Eur J Immunol **35**(8): 2486-2495.

Rabiet, M. J., L. Macari, C. Dahlgren and F. Boulay (2011). "N-formyl peptide receptor 3 (FPR3) departs from the homologous FPR2/ALX receptor with regard to the major processes governing chemoattractant receptor regulation, expression at the cell surface, and phosphorylation." J Biol Chem **286**(30): 26718-26731.

Radovsky, A., P. Safar, F. Sterz, Y. Leonov, H. Reich and K. Kuboyama (1995). "Regional prevalence and distribution of ischemic neurons in dog brains 96 hours after cardiac arrest of 0 to 20 minutes." Stroke **26**(11): 2127-2133; discussion 2133-2124.

Relton, J. K., P. J. Strijbos, C. T. O'Shaughnessy, F. Carey, R. A. Forder, F. J. Tilders and N. J. Rothwell (1991). "Lipocortin-1 is an endogenous inhibitor of ischemic damage in the rat brain." J Exp Med **174**(2): 305-310.

Resnati, M., I. Pallavicini, J. M. Wang, J. Oppenheim, C. N. Serhan, M. Romano and F. Blasi (2002). "The fibrinolytic receptor for urokinase activates the G protein-coupled chemotactic receptor FPRL1/LXA4R." Proc Natl Acad Sci U S A **99**(3): 1359-1364.

Reynolds, K., B. Lewis, J. D. Nolen, G. L. Kinney, B. Sathya and J. He (2003). "Alcohol consumption and risk of stroke: a meta-analysis." JAMA **289**(5): 579-588.

Richard Green, A., T. Odergren and T. Ashwood (2003). "Animal models of stroke: do they have value for discovering neuroprotective agents?" Trends Pharmacol Sci **24**(8): 402-408.

Rohl, L., L. Ostergaard, C. Z. Simonsen, P. Vestergaard-Poulsen, G. Andersen, M. Sakoh, D. Le Bihan and C. Gyldensted (2001). "Viability thresholds of ischemic penumbra of hyperacute stroke defined by perfusion-weighted MRI and apparent diffusion coefficient." Stroke **32**(5): 1140-1146.

Romisch, J., E. Schuler, B. Bastian, T. Burger, F. G. Dunkel, A. Schwinn, A. A. Hartmann and E. P. Paques (1992). "Annexins I to VI: quantitative determination in different human cell types and in plasma after myocardial infarction." Blood Coagul Fibrinolysis **3**(1): 11-17.

Rubin, L. L. and J. M. Staddon (1999). "The cell biology of the blood-brain barrier." Annu Rev Neurosci **22**: 11-28.

Sacquegna, T., P. De Carolis, A. Andreoli, R. Ferrara, P. Limoni, C. Testa and E. Lugaresi (1984). "Long term prognosis after occlusion of middle cerebral artery." Br Med J (Clin Res Ed) **288**(6429): 1490-1491.

Saito, K., K. Suyama, K. Nishida, Y. Sei and A. S. Basile (1996). "Early increases in TNF-alpha, IL-6 and IL-1 beta levels following transient cerebral ischemia in gerbil brain." Neurosci Lett **206**(2-3): 149-152.

Saka, O., A. McGuire and C. Wolfe (2009). "Cost of stroke in the United Kingdom." Age Ageing **38**(1): 27-32.

Saver, J. L. (2006). "Time is brain--quantified." Stroke **37**(1): 263-266.

Schaar, K. L., M. M. Brenneman and S. I. Savitz (2010). "Functional assessments in the rodent stroke model." Exp Transl Stroke Med **2**(1): 13.

Schaff, U. Y., I. Yamayoshi, T. Tse, D. Griffin, L. Kibathi and S. I. Simon (2008). "Calcium flux in neutrophils synchronizes beta2 integrin adhesive and signaling events that guide inflammatory recruitment." Ann Biomed Eng **36**(4): 632-646.

Schiffmann, E., H. V. Showell, B. A. Corcoran, P. A. Ward, E. Smith and E. L. Becker (1975). "The isolation and partial characterization of neutrophil chemotactic factors from Escherichia coli." J Immunol **114**(6): 1831-1837.

Schneider, A., B. W. Bottiger and E. Popp (2009). "Cerebral resuscitation after cardiocirculatory arrest." Anesth Analg **108**(3): 971-979.

Schwab, J. M., N. Chiang, M. Arita and C. N. Serhan (2007). "Resolvin E1 and protectin D1 activate inflammation-resolution programmes." Nature **447**(7146): 869-874.

Serhan, C. N., N. Chiang and T. E. Van Dyke (2008). "Resolving inflammation: dual anti-inflammatory and pro-resolution lipid mediators." Nat Rev Immunol **8**(5): 349-361.

Serhan, C. N., M. Hamberg and B. Samuelsson (1984). "Lipoxins: novel series of biologically active compounds formed from arachidonic acid in human leukocytes." Proc Natl Acad Sci U S A **81**(17): 5335-5339.

Serhan, C. N., S. Hong, K. Gronert, S. P. Colgan, P. R. Devchand, G. Mirick and R. L. Moussignac (2002). "Resolvins: a family of bioactive products of omega-3 fatty acid transformation circuits initiated by aspirin treatment that counter proinflammation signals." J Exp Med **196**(8): 1025-1037.

Serhan, C. N., T. Takano, C. B. Clish, K. Gronert and N. Petasis (1999). "Aspirin-triggered 15-epi-lipoxin A4 and novel lipoxin B4 stable analogs inhibit neutrophil-mediated changes in vascular permeability." Adv Exp Med Biol **469**: 287-293.

Simmons, K. M., K. A. Brown, A. P. Kirk, J. D. Perry and D. C. Dumonde (1987). "Enhanced chemotaxis of monocytes in rheumatoid arthritis." Br J Rheumatol **26**(4): 245-250.

Sims, N. R. and H. Muyderman (2010). "Mitochondria, oxidative metabolism and cell death in stroke." Biochim Biophys Acta **1802**(1): 80-91.

Smith, H. K. (Unpublished). "Illustrations of stroke and inflammatory processes."

Smith, H. K. and F. N. Gavins (2012). "The potential of stem cell therapy for stroke: is PISCES the sign?" FASEB J.

Smith, M. L., G. Bendek, N. Dahlgren, I. Rosen, T. Wieloch and B. K. Siesjo (1984). "Models for studying long-term recovery following forebrain ischemia in the rat. 2. A 2-vessel occlusion model." Acta Neurol Scand **69**(6): 385-401.

Smith, W. S., G. Sung, J. Saver, R. Budzik, G. Duckwiler, D. S. Liebeskind, H. L. Lutsep, M. M. Rymer, R. T. Higashida, S. Starkman, Y. P. Gobin, D. Frei, T. Grobelny, F. Hellinger, D. Huddle, C. Kidwell, W. Koroshetz, M. Marks, G. Nesbit and I. E. Silverman (2008). "Mechanical thrombectomy for acute ischemic stroke: final results of the Multi MERCI trial." Stroke **39**(4): 1205-1212.

Soleman, S., P. K. Yip, D. A. Duricki and L. D. Moon (2012). "Delayed treatment with chondroitinase ABC promotes sensorimotor recovery and plasticity after stroke in aged rats." Brain **135**(Pt 4): 1210-1223.

Solito, E., I. A. Romero, S. Marullo, F. Russo-Marie and B. B. Weksler (2000). "Annexin 1 binds to U937 monocytic cells and inhibits their adhesion to microvascular endothelium: involvement of the alpha 4 beta 1 integrin." J Immunol **165**(3): 1573-1581.

Somers, W. S., J. Tang, G. D. Shaw and R. T. Camphausen (2000). "Insights into the molecular basis of leukocyte tethering and rolling revealed by structures of P- and E-selectin bound to SLe(X) and PSGL-1." Cell **103**(3): 467-479.

Sonobe, Y., H. Takeuchi, K. Kataoka, H. Li, S. Jin, M. Mimuro, Y. Hashizume, Y. Sano, T. Kanda, T. Mizuno and A. Suzumura (2009). "Interleukin-25 expressed by brain capillary endothelial cells maintains blood-brain barrier function in a protein kinase Cepsilon-dependent manner." J Biol Chem **284**(46): 31834-31842.

Stasiuk, G. J., H. Smith, M. Wylezinska-Arridge, J. L. Tremoleda, W. Trigg, S. K. Luthra, V. M. Iveson, F. N. Gavins and N. J. Long (2013). "Gd(3+) cFLFLFK conjugate for MRI: a targeted contrast agent for FPR1 in inflammation." Chem Commun (Camb) **49**(6): 564-566.

Steensberg, A., C. P. Fischer, C. Keller, K. Moller and B. K. Pedersen (2003). "IL-6 enhances plasma IL-1ra, IL-10, and cortisol in humans." Am J Physiol Endocrinol Metab **285**(2): E433-437.

Stenfeldt, A. L., J. Karlsson, C. Wenneras, J. Bylund, H. Fu and C. Dahlgren (2007). "Cyclosporin H, Boc-MLF and Boc-FLFLF are antagonists that preferentially inhibit activity triggered through the formyl peptide receptor." Inflammation **30**(6): 224-229.

Strausbaugh, H. J. and S. D. Rosen (2001). "A potential role for annexin 1 as a physiologic mediator of glucocorticoid-induced L-selectin shedding from myeloid cells." J Immunol **166**(10): 6294-6300.

Su, S. B., W. Gong, J. L. Gao, W. Shen, P. M. Murphy, J. J. Oppenheim and J. M. Wang (1999). "A seven-transmembrane, G protein-coupled receptor, FPRL1, mediates the chemotactic activity of serum amyloid A for human phagocytic cells." J Exp Med **189**(2): 395-402.

Sukerkar, P. A., K. W. MacRenaris, T. R. Townsend, R. A. Ahmed, J. E. Burdette and T. J. Meade (2011). "Synthesis and biological evaluation of water-soluble progesterone-conjugated probes for magnetic resonance imaging of hormone related cancers." Bioconjug Chem **22**(11): 2304-2316.

Ternowitz, T., T. Herlin and K. Fogh (1987). "Human monocyte and polymorphonuclear leukocyte chemotactic and chemokinetic responses to leukotriene B4 and FMLP." Acta Pathol Microbiol Immunol Scand C **95**(2): 47-54.

Tiffany, H. L., J. L. Gao, E. Roffe, J. M. Sechler and P. M. Murphy (2011). "Characterization of Fpr-rs8, an atypical member of the mouse formyl peptide receptor gene family." J Innate Immun **3**(5): 519-529.

Tilg, H., E. Trehu, M. B. Atkins, C. A. Dinarello and J. W. Mier (1994). "Interleukin-6 (IL-6) as an anti-inflammatory cytokine: induction of circulating IL-1 receptor antagonist and soluble tumor necrosis factor receptor p55." Blood **83**(1): 113-118.

Utgaard, J. O., F. L. Jahnsen, A. Bakka, P. Brandtzaeg and G. Haraldsen (1998). "Rapid secretion of prestored interleukin 8 from Weibel-Palade bodies of microvascular endothelial cells." J Exp Med **188**(9): 1751-1756.

Valente, A. J., D. T. Graves, C. E. Vialle-Valentin, R. Delgado and C. J. Schwartz (1988). "Purification of a monocyte chemotactic factor secreted by nonhuman primate vascular cells in culture." Biochemistry **27**(11): 4162-4168.

van Lookeren Campagne, M., G. R. Thomas, H. Thibodeaux, J. T. Palmer, S. P. Williams, D. G. Lowe and N. van Bruggen (1999). "Secondary reduction in the apparent diffusion coefficient of water, increase in cerebral blood volume, and delayed neuronal death after middle cerebral artery occlusion and early reperfusion in the rat." J Cereb Blood Flow Metab **19**(12): 1354-1364.

Vannucci, S. J., L. B. Willing, S. Goto, N. J. Alkayed, R. M. Brucklacher, T. L. Wood, J. Towfighi, P. D. Hurn and I. A. Simpson (2001). "Experimental stroke in the female diabetic, db/db, mouse." J Cereb Blood Flow Metab **21**(1): 52-60.

Vergnolle, N., C. Comera, J. More, M. Alvinerie and L. Bueno (1997). "Expression and secretion of lipocortin 1 in gut inflammation are not regulated by pituitary-adrenal axis." Am J Physiol **273**(2 Pt 2): R623-629.

Vila, N., J. Castillo, A. Davalos, A. Esteve, A. M. Planas and A. Chamorro (2003). "Levels of anti-inflammatory cytokines and neurological worsening in acute ischemic stroke." Stroke **34**(3): 671-675.

Vora, N. A., S. J. Shook, H. C. Schumacher, A. L. Tievsky, G. W. Albers, L. R. Wechsler and R. Gupta (2011). "A 5-item scale to predict stroke outcome after cortical middle cerebral artery territory infarction: validation from results of the Diffusion and Perfusion Imaging Evaluation for Understanding Stroke Evolution (DEFUSE) Study." Stroke **42**(3): 645-649.

Waje-Andreassen, U., J. Krakenes, E. Ulvestad, L. Thomassen, K. M. Myhr, J. Aarseth and C. A. Vedeler (2005). "IL-6: an early marker for outcome in acute ischemic stroke." Acta Neurol Scand **111**(6): 360-365.

Walther, A., K. Riehemann and V. Gerke (2000). "A novel ligand of the formyl peptide receptor: annexin I regulates neutrophil extravasation by interacting with the FPR." Mol Cell **5**(5): 831-840.

Wang, F., Y. Wang, X. Geng, K. Asmaro, C. Peng, J. M. Sullivan, J. Y. Ding, X. Ji and Y. Ding (2012). "Neuroprotective effect of acute ethanol administration in a rat with transient cerebral ischemia." Stroke **43**(1): 205-210.

Wang, Q., X. N. Tang and M. A. Yenari (2007). "The inflammatory response in stroke." J Neuroimmunol **184**(1-2): 53-68.

Wang, Y. F., S. E. Tsirka, S. Strickland, P. E. Stieg, S. G. Soriano and S. A. Lipton (1998). "Tissue plasminogen activator (tPA) increases neuronal damage after focal cerebral ischemia in wild-type and tPA-deficient mice." Nat Med **4**(2): 228-231.

Wang, Z. G. and R. D. Ye (2002). "Characterization of two new members of the formyl peptide receptor gene family from 129S6 mice." Gene **299**(1-2): 57-63.

Wellons, J. C., 3rd, H. Sheng, D. T. Laskowitz, G. Burkhard Mackensen, R. D. Pearlstein and D. S. Warner (2000). "A comparison of strain-related susceptibility in two murine recovery models of global cerebral ischemia." Brain Res **868**(1): 14-21.

Wenzel-Seifert, K., C. M. Hurt and R. Seifert (1998). "High constitutive activity of the human formyl peptide receptor." J Biol Chem **273**(37): 24181-24189.

Willems, J., M. Joniau, S. Cinque and J. van Damme (1989). "Human granulocyte chemotactic peptide (IL-8) as a specific neutrophil degranulator: comparison with other monokines." Immunology **67**(4): 540-542.

Williams, G. R., Jr. and F. C. Spencer (1958). "The clinical use of hypothermia following cardiac arrest." Ann Surg **148**(3): 462-468.

Williams, L. A., I. Martin-Padura, E. Dejana, N. Hogg and D. L. Simmons (1999). "Identification and characterisation of human Junctional Adhesion Molecule (JAM)." Mol Immunol **36**(17): 1175-1188.

Williams, R. N., C. A. Paterson, K. E. Eakins and P. Bhattacherjee (1982). "Quantification of ocular inflammation: evaluation of polymorphonuclear leucocyte infiltration by measuring myeloperoxidase activity." Curr Eye Res **2**(7): 465-470.

Williams, S. L., I. R. Milne, C. J. Bagley, J. R. Gamble, M. A. Vadas, S. M. Pitson and Y. Khew-Goodall (2010). "A proinflammatory role for proteolytically cleaved annexin A1 in neutrophil transendothelial migration." J Immunol **185**(5): 3057-3063.

Wolfensohn, S. and M. Lloyd (2006). "Handbook of Laboratory Animal Managment and Welfare, Third Edition." Blackwell Publishing.

Wolfensohn, S. and M. Lloyd (2007). "Handbook of Laboratory Animal Management and Welfare, Third Edition." Blackwell Publishing.

Worthmann, H., R. Dengler, H. Schumacher, A. Schwartz, W. G. Eisert, R. Lichtinghagen and K. Weissenborn (2012). "Monocyte chemotactic protein-1 as a potential biomarker for early anti-thrombotic therapy after ischemic stroke." Int J Mol Sci **13**(7): 8670-8678.

Xiao, L., Y. Zhang, S. S. Berr, M. D. Chordia, P. Pramoonjago, L. Pu and D. Pan (2012). "A novel near-infrared fluorescence imaging probe for in vivo neutrophil tracking." Mol Imaging **11**(5): 372-382.

Xing, Z., J. Gauldie, G. Cox, H. Baumann, M. Jordana, X. F. Lei and M. K. Achong (1998). "IL-6 is an antiinflammatory cytokine required for controlling local or systemic acute inflammatory responses." J Clin Invest **101**(2): 311-320.

Yago, T., B. J. Shao, J. J. Miner, L. B. Yao, A. G. Klopocki, K. Maeda, K. M. Coggeshall and R. P. McEver (2010). "E-selectin engages PSGL-1 and CD44 through a common signaling pathway to induce integrin alpha(L)beta(2)-mediated slow leukocyte rolling." Blood **116**(3): 485-494.

Yamasaki, Y., N. Matsuura, H. Shozuhara, H. Onodera, Y. Itoyama and K. Kogure (1995). "Interleukin-1 as a pathogenetic mediator of ischemic brain damage in rats." Stroke **26**(4): 676-680; discussion 681.

Yang, D., Q. Chen, B. Gertz, R. He, M. Phulsuksombati, R. D. Ye and J. J. Oppenheim (2002). "Human dendritic cells express functional formyl peptide receptor-like-2 (FPRL2) throughout maturation." J Leukoc Biol **72**(3): 598-607.

Yang, D., Q. Chen, Y. Le, J. M. Wang and J. J. Oppenheim (2001). "Differential regulation of formyl peptide receptor-like 1 expression during the differentiation of monocytes to dendritic cells and macrophages." J Immunol **166**(6): 4092-4098.

Yang, G., K. Kitagawa, K. Matsushita, T. Mabuchi, Y. Yagita, T. Yanagihara and M. Matsumoto (1997). "C57BL/6 strain is most susceptible to cerebral ischemia following bilateral common carotid occlusion among seven mouse strains: selective neuronal death in the murine transient forebrain ischemia." Brain Res **752**(1-2): 209-218.

Yazid, S., L. V. Norling and R. J. Flower (2011). "Anti-inflammatory drugs, eicosanoids and the annexin A1/FPR2 anti-inflammatory system." Prostaglandins Other Lipid Mediat.

Ye, R. D., F. Boulay, J. M. Wang, C. Dahlgren, C. Gerard, M. Parmentier, C. N. Serhan and P. M. Murphy (2009). "International Union of Basic and Clinical Pharmacology. LXXIII. Nomenclature for the formyl peptide receptor (FPR) family." Pharmacol Rev **61**(2): 119-161.

Ye, X. H., Y. Wu, P. P. Guo, J. Wang, S. Y. Yuan, Y. Shang and S. L. Yao (2010). "Lipoxin A4 analogue protects brain and reduces inflammation in a rat model of focal cerebral ischemia reperfusion." Brain Res **1323**: 174-183.

Ye, X. H., Y. Wu, P. P. Guo, J. Wang, S. Y. Yuan, Y. Shang and S. L. Yao (2010). "Lipoxin A(4) analogue protects brain and reduces inflammation in a rat model of focal cerebral ischemia reperfusion." Brain Res.

Yepes, M., M. Sandkvist, M. K. Wong, T. A. Coleman, E. Smith, S. L. Cohan and D. A. Lawrence (2000). "Neuroserpin reduces cerebral infarct volume and protects neurons from ischemia-induced apoptosis." Blood **96**(2): 569-576.

Yoshioka, H., K. Niizuma, M. Katsu, H. Sakata, N. Okami and P. H. Chan (2011). "Consistent injury to medium spiny neurons and white matter in the mouse striatum after prolonged transient global cerebral ischemia." J Neurotrauma **28**(4): 649-660.

Zhang, J., Y. Li, X. Zheng, Q. Gao, Z. Liu, R. Qu, J. Borneman, S. B. Elias and M. Chopp (2008). "Bone marrow stromal cells protect oligodendrocytes from oxygen-glucose deprivation injury." J Neurosci Res **86**(7): 1501-1510.

Zhang, L., A. Nair, K. Krady, C. Corpe, R. H. Bonneau, I. A. Simpson and S. J. Vannucci (2004). "Estrogen stimulates microglia and brain recovery from hypoxia-ischemia in normoglycemic but not diabetic female mice." J Clin Invest **113**(1): 85-95.

Zhang, L., Z. G. Zhang, R. L. Zhang, M. Lu, M. Krams and M. Chopp (2003). "Effects of a selective CD11b/CD18 antagonist and recombinant human tissue plasminogen activator treatment alone and in combination in a rat embolic model of stroke." Stroke **34**(7): 1790-1795.

Zhang, R. L., M. Chopp, C. Zaloga, Z. G. Zhang, N. Jiang, S. C. Gautam, W. X. Tang, W. Tsang, D. C. Anderson and A. M. Manning (1995). "The temporal profiles of ICAM-1 protein and mRNA expression after transient MCA occlusion in the rat." Brain Res **682**(1-2): 182-188.

Zhang, R. L., M. Chopp, Z. G. Zhang, M. L. Phillips, C. L. Rosenbloom, R. Cruz and A. Manning (1996). "E-selectin in focal cerebral ischemia and reperfusion in the rat." J Cereb Blood Flow Metab **16**(6): 1126-1136.

Zhou, Y., T. Lekic, N. Fathali, R. P. Ostrowski, R. D. Martin, J. Tang and J. H. Zhang (2010). "Isoflurane posttreatment reduces neonatal hypoxic-ischemic brain injury in rats by the sphingosine-1-phosphate/phosphatidylinositol-3-kinase/Akt pathway." Stroke **41**(7): 1521-1527.

Zivin, J. A. and D. R. Waud (1992). "Quantal bioassay and stroke." Stroke **23**(5): 767-773.